NISTIR 6162

A Modeling Study of Ventilation, IAQ and Energy Impacts of Residential Mechanical Ventilation

Andrew K. Persily

Building and Fire Research Laboratory
Gaithersburg, MD 20899

United States Department of Commerce
Technology Administration
National Institute of Standards and Technology

NISTIR 6162

A Modeling Study of Ventilation, IAQ and Energy Impacts of Residential Mechanical Ventilation

Andrew K. Persily

May 1998
Building and Fire Research Laboratory
National Institute of Standards and Technology
Gaithersburg, MD 20899

U. S. Department of Commerce
William M. Daley, *Secretary*

Technology Administration
Gary R. Bachula, *Acting Under Secretary for Technology*

National Institute of Standards and Technology
Raymond G. Kammer, *Director*

Prepared for:
Electric Power Research Institute
Palo Alto, CA

ABSTRACT

Based on concerns about indoor air quality and trends towards tighter envelope construction, there has been increasing interest in mechanical ventilation in residential buildings. A variety of ventilation approaches have been examined through both field measurements and computer simulation studies. This paper reports on a simulation study of indoor air quality, ventilation and energy impacts of several mechanical ventilation approaches in a single-family residential building. The study focused on a fictitious two-story house in Spokane, Washington and employed the multizone airflow and contaminant dispersal model CONTAM. The model of the house included a number of factors related to airflow including exhaust fan and forced-air system operation, duct leakage and weather effects, as well as factors related to contaminant dispersal including adsorption/desorption of water vapor and volatile organic compounds, surface losses of particles and nitrogen dioxide, outdoor contaminant concentrations, and occupant activities. The contaminants studied include carbon monoxide, carbon dioxide, nitrogen dioxide, water vapor, fine and coarse particles, and volatile organic compounds. One-year simulations were performed for four different ventilation approaches: a base case of envelope infiltration only, passive inlet vents in combination with exhaust fan operation, an outdoor intake duct connected to the forced-air system return balanced by exhaust fan operation, and a continuously-operated exhaust fan. Results discussed include whole building air change rates, air distribution within the house, heating and cooling loads, contaminants concentrations, and occupant exposure to contaminants.

Keywords: building performance, exposure, indoor air quality, modeling, residential, ventilation

BLANK PAGE

TABLE OF CONTENTS

BLANK PAGE

LIST OF TABLES

LIST OF FIGURES

INTRODUCTION

While existing data are limited, there appears to be a trend towards tighter envelope construction in single-family buildings in North America (Sherman and Dickeroff 1994). This trend, along with specific energy-efficient construction programs in which special attention is given to building airtightness and increasing awareness of indoor air quality issues, has led to the realization that mechanical ventilation may be needed in some residential buildings. A variety of mechanical ventilation strategies have been developed to provide effective ventilation, with the additional objective of minimizing situations in which the building is overventilated and unnecessary energy consumption results. A number of investigations of particular ventilation approaches have been performed; however, questions remain about the effectiveness of these different systems in terms of indoor contaminant control, the actual ventilation rates provided, ventilation air distribution, and energy impacts. This paper reports on a study in which computer simulations were used to examine these issues in a house intended to represent recent energy-efficient construction in the Pacific Northwest region of the U.S. These simulations employed the multizone airflow and contaminant dispersal model CONTAM96 (Walton 1997).

A number of previous studies have employed computer modeling to evaluate the impacts and effectiveness of mechanical ventilation in residential buildings (Blomsterberg 1991; Carlsson and Blomsterberg 1995; Hamlin and Cooper 1991; Hamlin and Cooper 1993; Hekmat et al. 1986; Matson and Feustel 1997; Sibbit and Hamlin 1991; Yuill and Jeanson 1990; Yuill et al. 1991). Some of these studies have predicted only building ventilation rates, while others have also studied indoor contaminant concentrations and energy consumption associated with different system types, climatic conditions, and levels of building envelope airtightness. Some of these studies have employed single-zone modeling approaches, while others have used multizone building models. Of particular relevance to this study is an earlier effort involving multizone modeling of ventilation and indoor air quality in a number of single-family residential buildings (Emmerich and Persily 1996). This previous study serves as a basis for much of the work presented in this report, in particular the house airflow and contaminant model.

Another key activity related to the work presented here is International Energy Agency Annex 27 (Mansson 1995; Millet et al. 1996). IEA Annex 27 is an international research effort intended to develop methods for evaluating residential ventilation systems in terms of ventilation rates, contaminant levels, acoustics, energy consumption and economics, to validate these methods with experimental data, and to demonstrate the performance of these systems in different climates and building types. Ventilation and contaminant modeling is an important aspect of this effort (Millet et al. 1996), and some of the modeling approaches and assumptions used in Annex 27 were utilized in this effort.

DESCRIPTION OF HOUSE MODEL

The house that was modeled is intended to be representative of recent residential construction in the Pacific Northwest region of the U.S. This region of the country is somewhat unique because of several energy efficient residential construction programs. Therefore, recently constructed houses in the Pacific Northwest, constructed as part of these programs, are generally more efficient and more airtight than other houses (Palmiter et al. 1991). This study is focused on a two-story house, with a crawl space and attached garage, that is based on a house used in a previous ventilation and indoor air quality simulation study (Emmerich and Persily 1996). A schematic floor plan of the house is shown in Figure 1, and a schematic elevation (showing the air distribution system discussed later) in shown is Figure 2. Each room or zone is identified in Figure 1 with a short zone code in parentheses, e.g. LR for living room, that was used within the CONTAM96 model to identify the zone. There is a crawl space (CS) beneath the first floor living-area zones, with the garage (GAR) and crawl space floors at the same elevation. There is an attic (ATC) with the same floor area as the second floor. Both the crawl space and attic are vented to the outdoors as described in the section on airflow characteristics. The house has a central air-conditioning system and is heated with an electric heat pump. A forced-air distribution system is located in the garage, with some of the ductwork located in the crawl space and attic. The details of the system and ductwork are described in the section on ventilation systems.

The floor areas and volumes of the zones are shown in Table 1, along with the totals for each floor and the whole building. The zones in the living area (first and second floors) have ceiling heights of 2.4 m (7.9 ft). The crawl space has a height of 1.0 m (3.3 ft), and the garage has a height of 3.4 m (11.2 ft). The attic has a peaked roof, and the height in its center is 2.0 m (6.6 ft).

This section describes the details of the house model as represented in CONTAM96. Figures 3 through 6 show the individual floors of the house as they appear on the CONTAM96 sketchpad.

Airflow Characteristics

The airflow characteristics of the house, that is, the location and magnitude of the various air leakage paths in the exterior walls and interior partitions, are based on those of the two-story house studied previously (Emmerich and Persily 1996). The leakage values used in the reference and in this study are based on Table 3 in Chapter 25, Ventilation and Infiltration, of the ASHRAE Fundamentals Handbook (1997) and on information in Klote and Milke (1992). A general description of the airflow elements in the house model is presented here, along with key differences between it and the model used previously. All airflow elements or paths are described in terms of their effective leakage areas (ELA) at 4 Pa (0.016 in. w.g.). The effective leakage area of an opening is the area of an orifice with a discharge coefficient of 1.0 that would result in the same airflow rate as that across the opening at a pressure difference of 4 Pa (0.016 in. w.g.).

Exterior Envelope. A number of different exterior wall airflow paths are used in the house model. These, expressed as ELA per unit wall area or per unit interface length, include the following:

Exterior wall: 0.1 cm^2 per m^2 of wall area (1.4 x 10^{-3} in^2/ft^2)
Floor-wall interface: 0.8 cm^2 per m of interface (3.8 x 10^{-2} in^2/ft)
Ceiling-wall interface: 0.5 cm^2 per m of interface (2.4 x 10^{-2} in^2/ft)
Corner interface: 0.5 cm^2 per m of interface (2.4 x 10^{-2} in^2/ft)
Window: 2 cm^2 each (0.3 in^2)

The floor-wall and ceiling-wall interfaces are intended to represent the combined effect of all the leaks located low in the wall and high in the wall, and not necessarily specific leaks at these locations. Other exterior envelope leaks include a sliding glass door and door frame in the KFA zone, the front door and door frame in the ENTR zone, and the exterior door and door frame from the KFA zone to the GAR zone. All the door frames have an ELA of 0.3 cm^2/m^2 (4.3 x 10^{-3} in^2/ft^2) of door area. The sliding glass door has an ELA of 3 cm^2 (0.47 in^2), and the other two exterior doors each have an ELA of 6 cm^2 (0.93 in^2). The garage has an exterior wall leakage of 0.4 cm^2/m^2 of wall area (5.8 x 10^{-3} in^2/ft^2). In addition, the wall-floor and wall-ceiling interfaces of the garage have a leakage area of 2 cm^2/m (9.4 x 10^{-2} in^2/ft) of interface length. Air leakage paths are also included in the crawl space ceiling to the zone above. The values of ELA for these paths are obtained by multiplying the floor area of the zone above by 0.5 cm^2/m^2 (7.2 x 10^{-3} in^2/ft^2). Air leakage paths from the attic to the zones below are also included in the house model. These are also based on a value of 0.5 cm^2/m^2 (7.2 x 10^{-3} in^2/ft^2). At any location where a duct passes through the crawl space ceiling or the attic floor, an additional leakage path of 1 cm^2 (0.16 in^2) is included.

The wind pressure coefficients for the exterior wall openings employ the same correlation with wind direction that was employed in the previous study (Emmerich and Persily 1996). This correlation is based on Equation 27 in Chapter 25, Ventilation and Infiltration, of the ASHRAE Fundamentals Handbook (1997), with separate expressions used for the long and short walls of the house. In converting weather station wind speeds to site wind speeds, the house is assumed to be located in suburban terrain.

The attic venting to the outdoors is based on the requirements of the BPA Super Good Cents program, that is 1 m^2 of free vent area per 300 m^2 of attic "floor area" for vents at both the ridge and eaves (BPA 1995). Based on the attic floor area of 94.4 m^2 (1016 ft^2), this corresponds to 0.315 m^2 (3.39 ft^2) of vent area. Half of the vent area is located at the eaves and half at the ridge. Specifically, four ridge vents are included, each with an area of 325 cm^2 (50 in^2), along with two vents of the same area on each of the eaves. The total vent area is actually somewhat less than that derived from the 1-to-300 requirement. The wind pressure coefficients for the ridge vents are based on the values used in the Annex 27 simulations, while the values for the eave vents use the long-wall pressure profile used for the other openings in the exterior walls.

The venting of the crawl space is also based on the requirements of the BPA Super Good Cents program, that is 1 m^2 of free vent area per 150 m^2 of crawl space floor area (BPA 1995). Given the crawl space floor area of 90.5 m^2 (974 ft^2), this corresponds to 0.603 m^2 (6.49 ft^2) of vent area. Eight individual vents are installed in the three crawl space walls exposed to the outdoors; one of the crawl space walls is adjacent to the garage. Each vent has an effective leakage area at 4 Pa (0.016 in. w.g.) of 700 cm^2 (110 in^2), which is somewhat less than the total required

vent area divided by eight. Each vent is at an elevation of 0.25 m (0.8 ft) above ground level, which is 0.75 m (2.5 ft) above the crawl space floor. In addition to the vents, the crawl space walls have a leakage area of 2 cm^2/m^2 (2.9 x 10^{-2} in^2/ft^2).

Adding the effective leakage areas of all the airflow paths from the occupied zones of the building to the outdoors and to the unoccupied zones (crawl space, attic and garage) yields a total effective leakage area for the building of 290 cm^2 (45 in^2). Later in the paper, this value is compared to the results of a simulated pressurization test of the house.

Interior Partitions. Similar to the exterior wall airflow paths, the paths between the interior zones are based on the previous study (Emmerich and Persily 1996). These interior openings consist of wall leakage at 2 cm^2/m^2 (2.9 x 10^{-2} in^2/ft^2) and ceiling leakage at the first floor ceiling of 0.79 cm^2/m^2 (1.1 x 10^{-2} in^2/ft^2). The interior doors are open and closed based on individual schedules based on the assumed occupancy patterns. For example, all bedroom doors are assumed to be closed at night. Each interior door is associated with a leakage area of 250 cm^2 (39 in^2) to account for frame leakage and undercutting.

Ventilation Systems

This section describes the ventilation systems included in the simulated house. These include the forced-air system and the local exhaust systems that serve the kitchen area and the bathrooms. In addition, there are the ventilation systems that are the subject of this study. These include an approach in which air inlet vents are installed in the bedrooms and first floor living areas and an exhaust fan operates to induce outdoor air intake through these vents. The other approach studied is one in which an outdoor air intake duct is connected to the forced-air return with a damper that opens whenever the forced-air fan is operating. In this approach, an exhaust fan operates to balance the outdoor air intake through this duct. Finally, a ventilation approach is examined in which an exhaust fan operates continuously.

Forced-Air System. The house has a forced-air heating and cooling system intended to represent a system that is typical of the Pacific Northwest region of the U.S. A schematic of the air distribution system is shown in Figure 2. The air handler itself is located in the attached garage. The supply ductwork serving the first floor runs through the crawl space, while the supply ductwork serving the second floor runs through the joist space between the first and second floors. A single, centrally-located return serves each floor, with the return ductwork for both floors running through the attic before entering the garage.

The duct system modeling capabilities of CONTAM96 were used to model airflow through the forced-air system. This duct model requires the user to input lengths of ductwork, junctions, transitions and terminals, with each element accounting for friction losses, leakage and dynamic losses as appropriate. It is up to the user to determine the input values for the parameters that account for these losses. Dynamic losses at junctions and transitions in the duct system were determined using the values in the ACCA residential duct system manual (ACCA 1995). This manual provides equivalent length of ductwork for a wide range of fittings based on fitting

geometry, friction loss rate and air velocity.

Once the duct model was entered into CONTAM96, a number of simulations were performed with the forced-air system operating to assess the airflow rates through the various branches in the system. "Dampers" were installed at each supply grille in the duct model to provide a means of "balancing" the system. These dampers were CONTAM96 airflow paths based on an orifice model, in which the orifice area could be adjusted individually. These orifice dampers were adjusted until simulated supply airflow rates of approximately 50 L/s (100 cfm) were achieved at the supply air vents to the bedrooms (BR2, BR3, BR4 and MBR), the living room (LR), the dining room (DR) and the kitchen/family area (KFA). The target values for the supply airflow rates were 25 L/s (50 cfm) in the bathrooms (BA2, BA3 and MBA) and front entrance (ENTR). While residential air distribution systems are not typically balanced at this level of detail, this process was needed in the simulations to insure that the intended levels of supply airflow were actually being provided to the individual rooms.

The forced-air fan operated for a constant fraction of on-time during each month of the year, with the monthly on-time fraction based on the mean outdoor temperature for the month. The system on-time is assumed to be 60% at design conditions, and the relationship between monthly on-time and monthly mean outdoor temperature is assumed to be linear. The on-time fractions determined in this manner were rounded off to the nearest 5 minutes, such that the forced-air fan is assumed to operate for 25 min per hour in January, for 20 min per hour in February, July and December, for 15 min per hour in March, August and November, for 10 min per hour in April, May, June and October, and for 5 min per hour in September. A schedule was created for each month in CONTAM96 such that the forced-air fan is on for the specified duration for each hour of the month.

Duct Leakage. Leakage in air distribution ductwork to and from unconditioned spaces has been shown to have significant impacts on residential building airtightness and infiltration rates, particularly when the forced-air fan is operating (Cummings and Tooley 1989; Lambert and Robison 1989; Modera 1989; Olson et al. 1993; Parker 1989; Robison and Lambert 1989). In order to account for the impacts of duct leakage, openings in the duct system are included on the return side of the air handler in the garage, in the return duct passing through the attic, in the return duct in the first floor ceiling from the outdoors, and in the supply duct passing through the crawl space. The values of these leaks, expressed as orifice areas with a flow exponent of 0.5 and a discharge coefficient of 0.6, are as follows:

Garage return: 75.0 cm^2 (11.6 in^2)
Attic return: 37.5 cm^2 (5.8 in^2)
First-floor ceiling return: 37.5 cm^2 (5.8 in^2)
Crawl space supply: 100.0 cm^2 (15.5 in^2)

These values are based on a recent survey of homes in the Pacific Northwest, which showed a mean value of duct leakage expressed in orifice areas as above of about 260 cm^2 (40 in^2) (Haskell 1995).

Local Exhaust Systems. The simulated house has exhaust fans in the kitchen and in each of the three bathrooms. The kitchen exhaust fan is based on a commercially-available model with a capacity of 47 L/s (100 cfm) at a pressure of 25 Pa (0.1 in. w.g.). It is modeled with the duct model in CONTAM96, using a fan curve relating airflow rate to pressure difference and including a short length of ductwork in the outside wall. The fan and ductwork are shown in the CONTAM96 sketchpad schematic of the first floor (described in more detail later) in Figure 4. For simulations in which the kitchen fan operates, the fan is on from 6:30 to 7:30 a.m. and from 5 to 6 p.m. on weekdays. On weekends, the fan is on from 9:30 to 10 a.m., from 11:30 a.m. to 12:30 p.m., and from 5 to 6 p.m.

The three bathroom exhaust fans are based on a commercially-available fan with a capacity of 22 L/s (47 cfm) at a pressure of 25 Pa (0.1 in w.g.). These fans are also modeled with the duct model in CONTAM96, using a fan curve relating airflow rate to pressure difference and including ductwork from the fan location to the attic and then horizontally out of the attic gable wall. The bathroom fan from the first floor bathroom (BA3) is connected to a vertical duct that runs through the second floor to the attic. The bathroom fans in the second floor hall bath (BA2) and in the master bath (MBA) are each connected to a short vertical duct to the attic. In these simulations, the first floor bath fan never operates. The bath fan in BA2 is operated from 7 to 7:30 a.m. on weekdays. On weekends, the fan is on from 9 to 9:10 a.m., from 10 to 10:10 a.m., and from 11 to 11:10 a.m. The bath fan in MBA is operated from 6 to 6:10 a.m. and from 6:30 to 6:40 a.m. on weekdays. On weekends, the MBA fan is on from 7 to 7:30 a.m. In two cases of the simulations, the MBA exhaust fan is used to induce outdoor airflow into the building through passive inlet vents or through an outdoor air intake duct on the forced-air system return. In these cases, the MBA fan curve was modified to induce a higher airflow rate. Specifically, the fan capacity was doubled to 44 L/s (94 cfm) at a pressure of 25 Pa (0.1 in. w.g.). In another ventilation approach, the MBA exhaust fan operated continuously. In these simulations, the fan capacity was 32 L/s (68 cfm). The exhaust airflow rate for this case was selected based on a target air change rate of 0.35 h^{-1} and a nominal air change rate of 0.22 h^{-1} from envelope leakage alone. Based on the house volume, an additional ventilation rate of 16 L/s (34 cfm) is required to achieve 0.35 h^{-1}, which is then doubled to 32 L/s (68 cfm) to account for the nonlinear addition of ventilation and infiltration airflow rates. The operation of the MBA fan in conjunction with these outdoor air ventilation strategies is discussed in the following sections.

Passive Vents And Exhaust. One of the ventilation approaches studied in the simulations is the use of passive inlet vents in the exterior walls in combination with exhaust fan operation. The vents installed in the house are based on commercially-available devices. Measured data from a product sheet on the airflow rate through one of these vents as a function of pressure difference were used to determine that each vent is associated with an effective leakage area of 15 cm^2 (2.3 in^2) at 4 Pa (0.016 in. w.g.). These vents are relatively large compared with those typically used in the Pacific Northwest (Lubliner 1998). Each vent is modeled in CONTAM96 using the orifice airflow path model with this leakage area, a discharge coefficient of 1.0 and a flow exponent of 0.5. Each vent is placed at a height of 1.2 m (3.9 ft) above the floor, with one in each of the three

small bedrooms and the dining room, two in the master bedroom, and three in the living room.

In the simulations performed to evaluate this ventilation approach, these vents are always open. In addition, the exhaust fan in the master bathroom operates on an 8-h schedule each day. This exhaust fan is the higher capacity fan referred to earlier with a capacity of 44 L/s (94 cfm). During these simulations, this fan runs from 6 to 10, both a.m. and p.m.

Outdoor Air Intake Duct. Another ventilation approach studied is an outdoor air intake duct attached to the forced-air system return. This duct is seen in the CONTAM96 sketchpad schematic in Figure 4 and runs through the garage to the air handler. This duct was modeled such that roughly 43 L/s (91 cfm) of outdoor air is drawn into the forced-air system when the fan operates. Based on the living space volume this outdoor airflow rate corresponds to about 0.35 air changes per hour, which is the outdoor air requirement for residential buildings in ASHRAE Standard 62-1989.

In the simulations performed to evaluate this ventilation approach, this duct is open on an 8-h schedule each day, at which time the forced-air fan and the high-capacity exhaust fan in the master bathroom operate. This 8-h schedule is the same as that used for the passive vent approach, that is from 6 to 10, both a.m. and p.m. In addition, the intake duct is open at other times that the forced-air fan operates on the previously-discussed schedule based on space conditioning needs. At these other times, the master bathroom exhaust fan does not operate.

Continuous Exhaust Fan. The last ventilation approach studied involves an exhaust fan that operates continuously in the master bathroom. In these simulations, the fan capacity is 32 L/s (68 cfm). As discussed later, the air distribution system duct leakage is reduced to 10% of its original value in these simulations.

Occupants

In order to account for occupant-generated contaminants and to determine the exposure of building occupants to indoor contaminants, a family of five is assumed to occupy this house. These occupants are based on assumptions made in the IEA Annex 27 simulations and other reasonable expectations for a modern family in the U.S. However, no attempt was made to make this family truly representative based on an analysis of census data, residential occupancy patterns or other information. The five family members are as follows: an adult male working full-time, an adult female working part-time, a 16 year-old child (Child #1), a 13-year old child (Child #2), and a 10-year old child (Child #3).

Each individual is associated with an occupancy schedule that specifies the time spent in each room of the house, as well as out of the house. Based on these schedules, CONTAM96 accounts for the contaminants generated by each individual (as discussed below) in the room where they are located at each point in time. In addition, CONTAM96 keeps track of the contaminant concentrations to which they are exposed as they move through the building and determines the mean concentration over the simulation period as a measure of exposure.

Each individual is associated with a unique occupancy schedule which is based on their work schedule for the adults and on their age for the children. The schedules are different during the

daytime on weekdays and weekends, and for evenings before weekdays and weekends. While CONTAM96 allows for unique schedules on holidays or other atypical days, these are not used in these simulations.

Contaminants

Seven contaminants were considered in these simulations: carbon dioxide (CO_2), carbon monoxide (CO), nitrogen dioxide (NO_2), water vapor (H_2O), fine particles (diameters less than 2.5 μm), coarse particles (diameters greater than 2.5 μm), and volatile organic compounds (VOC). The sources of CO_2 included occupant respiration and outdoor air. Gas cooking was simulated as a source of CO, NO_2, water vapor and fine particles; the entry of these contaminants from the outdoor air was also considered. While the analysis of gas cooking in a house heated with an electric heat pump may appear somewhat unusual, gas cooking was studied as an example of a localized, episodic contaminant source. The generation of CO_2 from gas cooking was not included, in part, because the behavior of this source was captured by the contaminants other than CO_2. Also, since not all homes have gas cooking as a source of CO_2, the simulations of CO_2 focused on the CO_2 generated by the occupants. In addition, the entry of CO_2 with the outdoor air was considered. The sources of water vapor included occupant respiration, bathing, dishwashing and outdoor air. Volatile organic compounds were emitted by a generic source in each room, scaled by floor area, and entered with the outdoor air. A single VOC was simulated, which was intended to account for the combined emissions of VOCs from building materials and furnishings. While indoor VOCs include a broad class of compounds with varied physical and chemical properties and health impacts, the inclusion of multiple compounds would have greatly complicated the study and would have required input data that are currently unavailable. Therefore, only a single, generic compound was modeled, with full recognition of the limitations in doing so. This section describes how each contaminant was modeled, including source strengths and non-ventilation transport mechanisms.

Sources and Emission Rates. This section describes the sources of each of the contaminants in the simulations and the emission rates associated with these sources. Only indoor sources are accounted for in this section. The entry of contaminants with outdoor air, via infiltration and mechanical ventilation, are dealt with in the following section on outdoor concentration.

The only indoor source of CO_2 in these simulations is the respiration of the occupants. The generation rate of CO_2 from a person is a function of their body size and level of physical activity (Persily 1997). In these simulations, the rate of CO_2 generation for the adult male and female are assumed to equal 9.1 mg/s (0.072 lb/h) and 8.0 mg/s (0.064 lb/h) respectively when they are awake. The generation rates for the children, when awake, are 7.8 mg/s (0.062 lb/h) for Child #1, 6.9 mg/s (0.055 lb/h) for Child #2, and 5.5 mg/s (0.043 lb/h) for Child #3. These generation rates are equal to 0.0050 L/s, 0.0044 L/s, 0.0043 L/s, 0.0038 L/s and 0.0030 L/s in somewhat more familiar units. All of these generation rates are based on sedentary activity levels. When the occupants are asleep, their CO_2 generation rates are reduced to 0.66 of the values when awake, with this reduction based on the assumptions used in IEA Annex 27. The CO_2 generation of each

individual occurs in the room in which they are located according to the occupancy schedules.

The indoor sources of water vapor include the respiration and perspiration of the occupants, bathing, cooking and dishwashing. Similar to CO_2, the generation rate of H_2O is a function of body size and level of physical activity. In these simulations, the rate of H_2O generation due to respiration and perspiration for the adult male and female are both assumed to equal 15.3 mg/s (0.121 lb/h) when awake. The generation rates, when awake, for the children are 13.9 mg/s (0.110 lb/h) for Child #1, 12.5 mg/s (0.099 lb/h) for Child #2, and 11.1 mg/s (0.088 lb/h) for Child #3. When the occupants are asleep, their H_2O generation rates are reduced to 0.55 of the values when awake. These generation rates, and the reduction when sleeping, are based on the assumptions used in IEA Annex 27. They are also consistent with other values in the literature (Christian 1993 and 1994).

The generation rate of water vapor associated with bathing, actually showering, is assumed to equal 0.67 g/s (5.29 lb/h). This value is based on the assumptions used in IEA Annex 27 and values presented in Christian (1994). Each shower is assumed to last 10 min and to occur on a fixed schedule for each occupant. The adult male is assumed to shower every weekday at 6 a.m. and during the weekend at 9 a.m. The adult female is assumed to shower at 6:30 a.m. on weekdays and 9:10 a.m. on weekends. These showers are assumed to occur in the master bathroom (MBA). All three children are assumed to shower for 10 min successively between 7 and 7:30 a.m. during the week in the second floor hall bathroom (BA2). During the weekend, Child #3 is assumed to shower at 9 a.m., Child #2 at 10 a.m. and Child #1 at 11 a.m.

The other sources of water vapor in the house are cooking and dishwashing, both of which occur in the kitchen-family area (KFA) zone. The cooking of breakfast, lunch and dinner generates 0.25 kg (0.11 lb), 0.75 kg (0.34 lb) and 1 kg (0.45 lb) of water vapor respectively. During the week, the 0.25 kg (0.11 lb) associated with breakfast is generated between 6:30 and 7 a.m.; on weekends it is generated between 9:30 and 10 a.m. During the week, no moisture generation is associated with lunch, but on the weekends 0.75 kg (0.34 lb) is generated between 11:30 a.m. and 12:30 p.m. The 1 kg (0.45 lb) of water vapor associated with dinner is generated between 5 and 6 p.m. everyday of the week. In addition, 0.30 kg (0.14 lb) of water vapor is generated by dishwashing between 7 and 7:30 p.m. everyday. This value is based on Christian (1994).

The only indoor source of CO, NO_2 and fine particles (diameters less than 2.5 μm) is gas cooking, which occurs in the KFA zone. The generation rates of these three contaminants from cooking are all based on data contained in Mueller (1989), which is a review of contaminant sources due to indoor combustion. These generation rates are shown in Table 2. Note that there is no generation of these contaminants due to lunch on weekdays.

The generation of VOC occurs in each zone of the house. The generation rate in each room depends on its floor area and is based on a value of 0.21 $\mu g/s\text{-}m^2$ (1.5×10^{-7} $lb/h\text{-}ft^2$), which corresponds to a value of 0.75 $mg/h\text{-}m^2$ in somewhat more familiar units. The only exceptions are the crawl space and attic where no VOC generation occurs, the bathrooms where the rate is based on a value of 0.14 $\mu g/s\text{-}m^2$ (1.0×10^{-7} $lb/h\text{-}ft^2$), and the garage where the generation rate is based on 0.28 $\mu g/s\text{-}m^2$ (2.1×10^{-7} $lb/h\text{-}ft^2$).

While coarse particles (diameters greater than 2.5 μm) were modeled, no indoor sources are

included in these simulations.

Outdoor Concentrations. In addition to the indoor sources, the simulations account for the entry of the seven contaminants from outdoors. Whenever outdoor air enters the building, whether it is via an air leakage path, an intentional opening or an intake duct, contaminants are brought in at the outdoor air concentration. The outdoor concentrations are assumed to vary with the time of day and are presented for all contaminants other than water vapor in Table 3. These values are used for every day of the simulations, and are based on those used in Emmerich and Persily (1996). The outdoor concentration of water vapor is calculated hourly based on the temperature and relative humidity data contained in the weather file, which is discussed later. Note that coarse particles have no indoor source and a constant outdoor concentration. Therefore, the simulation results for coarse particles are not particularly interesting and are not discussed further in this paper.

Removal of NO_2 and Fine Particles. The removal of NO_2 and fine particles is accounted for using a first order loss coefficient in which the rate of contaminant removal is given by

$$k\rho VC_i \tag{1}$$

where

k = first order rate constant, s^{-1}
ρ = density of air, kg/m^3 (lb/ft^3)
V = zone volume, m^3 (ft^3)
C_i = contaminant concentration in zone air, kg-contaminant/kg-air (lb/lb).

The first order rate constants used in the simulations are 2.2×10^{-5} s^{-1} (0.08 h^{-1}) for fine particles and 2.4×10^{-4} s^{-1} (0.87 h^{-1}) for NO_2. These values are based on those used in Emmerich and Persily (1996), which were in turn based on consideration of values in the literature. The removal of these contaminants is modeled in CONTAM96 using the "constant coefficient" sink model in which contaminant loss is expressed as $-DC_i$, where D is equal to $k\rho V$ in Equation 1. Therefore, a separate value of D is used for each zone.

VOC Storage. The effects of absorption and desorption of VOCs on interior surfaces in the building are accounted for using a boundary layer diffusion controlled (BLDC) model with a linear adsorption isotherm. This model is described by Axley (1991) and was used in the previous IAQ modeling project (Emmerich and Persily 1996). In this model, the rate at which a contaminant is transferred to, or from, a "sink" is as follows:

$$h\rho A\left(C_i - \frac{C_s}{K}\right) \tag{2}$$

where

h = film mass transfer coefficient, m/h (ft/h)
ρ = density of air, kg/m^3 (lb/ft^3)
A = area of sorbent surface, m^2 (ft^2)
C_i = contaminant concentration in zone air, kg-contaminant/kg-air (lb/lb)
C_s = contaminant concentration in sorbent, kg-contaminant/kg-sorbent (lb/lb)
K = partition coefficient, kg-air/kg-sorbent (lb/lb).

In addition to the parameters listed above, use of this model also requires a value for the mass of sorbent per unit surface area. In these simulations, the values used for the film mass transfer coefficient, the sorbent mass per area, and the partition coefficient are 0.126 m/h (0.413 ft/h), 6 kg/m^2 (1.2 lb/ft^2) and 0.5 kg-air/kg-sorbent (0.5 lb/lb) respectively, based on the values used in Emmerich and Persily (1996). The surface area available for absorption and desorption is assumed to equal the zone interior surface area. A BLDC element exists within CONTAM96 that implements this model and requires the user to input the relevant parameters for each BLDC "sink." One BLDC sink element is included in each zone of the house model.

Water Vapor Storage. The effects of water vapor absorption and desorption by building materials are addressed using a model developed at CSTB (Jones 1995). This model relates the mass of water absorbed in a material to the relative humidity in the room air, using the following expression:

$$\frac{dm}{dt} = \alpha RH - \beta m \tag{3}$$

where

m = mass of water absorbed in the material, kg
t = time, h
RH = relative humidity of the room air
α = constant, suggested equal to 1.75 in Jones (1995)
β = constant, suggested equal to 0.018 in Jones (1995).

It turns out that Equation (3) is of the same mathematical form as Equation (2) used to implement the BLDC sink element in CONTAM96. While several other models are available to account for moisture storage in buildings (Jones 1995; Keresteciogl u et al. 1990; TenWolde 1994), they would have required modifications to the CONTAM96 program. However, the CSTB model could be used without making any changes to CONTAM96. In order to use the BLDC element to account for water vapor storage using the CSTB model, the values of the coefficients of the CONTAM96 BLDC element had to be related to the values of α and β in Equation (3). These values are determined for each room using the suggested value of β in Jones (1995) and the values of α used in IEA Annex 27, which also employed the CSTB moisture storage model. In the Annex 27 effort, the value of α is set equal to 0.035 times a value that can be approximated by the zone floor area. By relating the CSTB model and the CONTAM96 BLDC element, the critical coefficients in Equation (2), that is film mass transfer coefficient h and the mass of sorbent per unit surface area, are determined for each zone of the house to create a BLDC sink to account for moisture storage. In doing so, the air density is assumed to equal 1.2 kg/m^3 (0.075 lb/ft^3) and the partition coefficient for moisture storage is assumed to equal 5 based on data presented in Thomas and Burch (1990).

Based on these assumptions, the values of h and sorbent mass per unit area varied from room to room. In general, the values of h ranged from about 0.2 m/h (0.7 ft/h) to 0.4 m/h (1.3 ft/h). The values of sorbent mass per unit area varied from about 4 kg/m^2 (0.8 lb/ft^2) to 8 kg/m^2 (1.6 lb/ft^2). These ranges are reasonably close to the values used in the BLDC elements accounting for VOC

absorption and desorption. Using this model of humidity storage and these particular parameters are admittedly approximations, but such is the state of the art. The alternatives included ignoring water vapor storage altogether or using another storage model, which would have involved the need to imperfectly estimate another set of model parameters.

Water Vapor Removal by Cooling Equipment. CONTAM96 does not include models for space conditioning equipment, therefore the filter element of CONTAM96 is employed to approximate the removal of water vapor by the air conditioning equipment. This "water vapor filter" is placed in the forced-air system ductwork just upstream of the system fan. The filter efficiency of 17% is based on an analysis of an "ideal" cooling coil which would remove no water vapor when the humidity ratio of the airstream is below 7.82 g/kg. This value corresponds to a relative humidity of 50% and an air temperature of 21 °C (70 °F). At higher humidity ratios in the airstream, this ideal coil would reduce the humidity ratio to 7.82 g/kg. The water vapor filter is only assumed to operate during the months of June, July and August, and only acts when the forced-air system is on.

SIMULATION APPROACH

As discussed earlier, the simulations employed the multizone airflow and contaminant dispersal model CONTAM96 (Walton 1997). CONTAM96 enables one to represent a building as a system of interconnected zones, each at a uniform temperature and contaminant concentration. Airflow paths between zones, and between zones and the outdoors, are specified in the building model along with other information relevant to airflow such as ventilation system parameters, outdoor weather, and wind pressure coefficients on exterior surfaces. Based on these inputs, CONTAM96 calculates airflow rates between each zone under steady-state or transient conditions based on a simultaneous mass balance of air in each of the zones. In addition, given information on contaminant sources and removal mechanisms and on outdoor contaminant concentrations, CONTAM96 calculates contaminant concentrations in the zones based on the calculated airflow rates and contaminant-specific information.

The simulations in this study cover an entire year using outdoor weather based on the TMY2 weather file for Spokane, Washington (Marion and Urban 1995). Table 4 presents a summary of the climate for Spokane, including mean monthly values of outdoor temperature, wind speed, humidity ratio and relative humidity. While the house, specifically the locations of the air handler and ductwork, is more typical of a coastal location in the Pacific Northwest, Spokane weather was used in order to "challenge" the house with more severe winter weather. The simulations for each case were performed a month at a time to allow the use of monthly schedules of forced-air system on-time and to extract monthly summaries of CONTAM96 outputs. The contaminant concentrations at the end of each month served as the initial conditions for the next month's simulations. Since the concentrations at the end of December were not available for the simulations at the beginning of the year, the months of January and February were simulated again after running through the year. The simulations employed a 5-min time step, resulting in airflow rates through each path and contaminant concentrations in each zone at 5-min intervals for an entire year.

Cases Analyzed

Year-long simulations were performed for the following six cases:

Case #1: All fans off; all interior doors open.
Case #2: Forced-air fan, exhaust fans and interior doors on schedules.
Case #3: Passive inlet vents open with 8-h exhaust fan.
Case #4: Intake duct on forced-air fan with 8-h exhaust fan.
Case #5: Reduced duct leakage and constant exhaust fan.
Case #6: Constant air change rate of 0.35 h^{-1}.

Case #1 was analyzed to assess the building ventilation rates due to envelope leakage alone; no contaminant analysis was included. Case #2 includes the effects of exhaust and forced-air fan operation, duct leakage, and interior door opening, and serves as a baseline for comparing the other ventilation approaches. Contaminant concentrations were simulated and analyzed for this and all subsequent cases.

The next two cases, #3 and #4, involve two ventilation approaches, passive inlet vents and an outdoor air intake duct on the return side of the forced-air fan. In Case #3, passive inlet vents are installed in the bedrooms, living and dining rooms, and kitchen/family area as discussed previously. In addition, a high-capacity exhaust fan operates in the master bathroom (MBA) for 8 h each day. This fan has a capacity of 44 L/s (94 cfm) and runs from 6 to 10, both a.m. and p.m. In Case #4, an outdoor air intake duct is attached to the return side of the forced-air system. This duct is sized to provide outdoor air at a rate of about 0.35 air changes per hour, which is the outdoor air requirement for residential buildings in ASHRAE Standard 62-1989. During the simulations, this duct is open on an 8-h schedule each day, at which time the forced-air fan and the same high-capacity exhaust fan used in Case #3 operate. This 8-h schedule is from 6 to 10, both a.m. and p.m. In addition, the intake duct is open at other times that the forced-air fan operates according to the monthly schedule based on space conditioning loads. At these other times, the master bathroom exhaust fan does not operate.

Case #5 involves another approach to residential mechanical ventilation, which is expected to result in better performance than Cases #3 and #4. In this case, a more carefully sized exhaust fan is operated in the master bathroom (MBA) 24 h each day. Its fan capacity of 32 L/s (68 cfm) is based on a target air change rate of 0.35 h^{-1} and a nominal air change rate of 0.22 h^{-1} from envelope leakage alone. In addition, all four of the duct leaks are reduced to 10% of their values in the other cases. The constant exhaust fan is intended to provide more consistent ventilation to the building, while the reduced duct leakage is intended to limit overventilation.

The last case, #6, is another baseline case in which the house has a constant air change rate of 0.35 h^{-1} for every hour of the year. This reference case is of interest since it represents an idealized situation in which the house always complies with the outdoor air requirement in ASHRAE Standard 62-1989, with no situations of either underventilation or overventilation. In this case, all exterior envelope leaks are eliminated except for one opening for air intake and another for an exhaust fan with a constant airflow rate. The forced-air fan operates continuously at an elevated airflow rate to achieve uniform contaminant concentrations throughout the house.

Airtightness and Ventilation

The airflow simulations were focused on the building ventilation rates throughout the year as they compared with the requirements of ASHRAE Standard 62-1989. However, additional simulations and analyses were performed to better understand the airflow characteristics of the simulated house. These simulations included pressurization tests to determine the airtightness of the building envelope, analyses of airflow patterns between the major volumes of the house, and determinations of the age of air to characterize outdoor air distribution to the different zones of the house.

Building ventilation rates were calculated for each hour of the year based on the airflow rates calculated in the simulations. These air change rates were based on the total airflow rate into the conditioned space of the building and forced-air system (via duct leakage) from the outdoors as well as from the unconditioned spaces, that is, the attic, crawl space and garage. This total airflow rate was then divided by the building volume of the conditioned space to yield the air change rate in units of h^{-1}. The mean ventilation rate and the percentages of hours below 0.35 h^{-1} and above 0.70 h^{-1} were calculated for each month.

Pressurization tests of the house were simulated with CONTAM96, mimicking the measurement of envelope airtightness in real buildings using ASTM test methods E779 (ASTM 1987) or E1827 (ASTM 1996). In these tests, a fan is installed in a doorway of a house and is used to pressurize (or depressurize) the interior of the building relative to the outdoors. The airflow rates required to maintain the house at a series of indoor-outdoor pressure differences are measured and used to determine a measure of the building airtightness. Pressurization tests were simulated at indoor-outdoor pressures of 4 Pa (0.016 in. w.g.) and 50 Pa (0.20 in. w.g.). This was done in CONTAM96 by setting the pressure in the Entry zone on the first floor at the reference pressure and running a steady-state airflow simulation with no indoor-outdoor temperature difference and zero wind speed. All interior doors (except the door to the garage) and the garage door to the outside were opened during the simulation. After the simulation, all of the airflows from the building to the outdoors, crawl space, attic and garage were added together. The total airflow rate at 4 Pa (0.016 in. w.g.) was converted to an effective leakage area, and the total airflow rate at 50 Pa (0.20 in.w.g.) was divided by the building volume to determine the air change rate.

Airflow patterns in the house were examined by summing all the airflow rates between the major volumes of the building including the first and second floors, attic, crawl space and garage. These sums were determined for several conditions including forced-air fan off and on, passive vents open, outdoor air intake duct open, and various combinations of exhaust fan operation. The net airflow rates through the envelope, into and out of the air handling system, and into and out of the duct leaks are presented in schematic diagrams.

The ventilation analysis also includes the determination of the age of air in each of the living space zones, that is, the bedrooms, living and dining rooms, and kitchen/family area. Given that the CONTAM96 simulations are based on an assumption of uniform contaminant concentration in each individual zone, the ages of air are discussed on a zonal basis rather than at specific locations within zones. The age of air in a zone is the length of time since the air in a zone entered the building from outdoors and is a measure of outdoor air distribution (Roulet and Vandaele 1991; Sandberg 1983). In a building with complete mixing between zones, the age of air will be the same

in each zone and equal to the inverse of the building air change rate. Otherwise, zones with low ages of air correspond to higher outdoor airflow rates into the zones than zones with higher ages. The age of air in each zone was calculated directly from the airflow matrix used by CONTAM96 in the airflow calculation. Monthly means of the age of air in each zone were determined and are presented in the section on results.

Energy

The energy loads associated with outdoor air ventilation were estimated in order to compare the energy impacts of the different ventilation approaches examined in the study. These estimates employed an approximate technique based on the hourly mean air change rates determined from the CONTAM96 simulations. The sensible heating load for each hour was based on the following expression:

$$\rho C_p I V \Delta T \times 1\ h \tag{4}$$

where

ρ = air density, 1.2 kg/m^3 (0.075 lb/ft^3)
C_p = specific heat of air, 1000 J/kg-°C (0.239 Btu/lb-°F)
I = house air change rate, h^{-1}
V = house volume, 445 m^3 (15,700 ft^3)
ΔT = indoor-outdoor air temperature difference, °C (°F)

Equation (4) was applied to all hours of the year for which the outdoor air temperature was below 15.6 °C (60 °F). The sensible cooling load for each hour was also based on Equation (4), but was applied to only those hours for which the outdoor air temperature was above 26.7 °C (80 °F). In these calculations, the indoor air temperature was assumed to be constant at 21.0 °C (69.8 °F) under heating and 24.4 °C (75.9 °F) under cooling. The sensible heating and sensible cooling energy calculated with Equation (4) was summed over each hour for each month of the year.

The latent cooling load for each hour was based on the following expression:

$$\rho h_{fg} I V \Delta W \times 1\ h \tag{5}$$

where

h_{fg} = latent heat of water vapor, 2.34 x 10^6 J/kg (1010 Btu/lb)
ΔW = indoor-outdoor air humidity ratio difference, kg water vapor/kg dry air (lb/lb)

Equation (5) was also applied to all hours of the year for which the outdoor air temperature was above 26.7 °C (80 °F). In these calculations, the indoor relative humidity was assumed to be constant at 50%, which corresponds to 9.64 kg/kg at an air temperature of 24.4 °C (75.9 °F). It turned out that the outdoor humidity ratio was never greater than 9.64 kg/kg for Spokane, resulting in no additional latent cooling loads for the houses associated with the outdoor air.

The energy consumed by the fans in the house, forced-air and exhaust, was computed by multiplying the hours that each fan operated, based on the assumed operating schedules, by the power consumed by each fan. The fans are assumed to consume energy at the following rates:

forced-air fan 560 W; kitchen exhaust fan 55 W; typical bathroom fan (used in BA2 in all cases and in MBA in Case #2) 27 W; upgraded bathroom fan (used in MBA in Cases #3 and #4) 54W; and, continuous bathroom fan (used in MBA in Case #5) 37 W.

Contaminants

The calculated contaminant concentrations were analyzed in two ways: mean concentrations and occupant exposure. The CONTAM96 simulations determined contaminant concentrations at each 5-min time step in each zone of the house. Mean concentrations were then calculated separately for each contaminant in the zone(s) of interest and over a specific time period, with both the zones and averaging time selected based on the contaminant. The predicted VOC concentrations were converted into hourly mean concentrations and averaged over the so-called "living area" zones. These living area zones include the bedrooms, the living and dining room, and the kitchen/family area. These zones were selected to avoid the high concentrations in closets and other small zones where the occupants would be expected to spend very little time. For CO and NO_2, hourly mean concentrations were calculated for the kitchen/family area, the living room and the four bedrooms averaged together. In the case of NO_2, only the daily peak hourly mean for each of these three locations is reported. For water vapor, the hourly mean value of the relative humidity, averaged over all of the conditioned zones of the house, was calculated. In addition, the percentage of hours for which the indoor relative humidity was below 30% and the percentage for which the relative humidity was above 60% were calculated for each month. For CO_2, the mean concentration in the four bedrooms was calculated on an hourly basis, and the daily peak of these hourly means is reported. No fine particle concentrations are reported, as these were consistently quite low, that is, less than the outdoor concentration of 13 $\mu g/m^3$. In addition to these summaries of mean contaminant concentrations, the occupant exposures to VOC, CO, CO_2 and NO_2 were calculated for each of the five occupants. These values are the mean concentration to which each occupant is exposed during their time in the house.

RESULTS

This section contains the results of the simulations in the model house. The airflow-related results address building airtightness, airflow patterns, ventilation rates and air distribution. In addition, the energy consumption associated with the ventilation rates are presented. Mean contaminant concentrations and occupant exposure are also presented.

Airtightness

As discussed earlier, pressurization tests were simulated in the model house using CONTAM96 to evaluate the airtightness of the envelope. These simulations resulted in an effective leakage area at 4 Pa (0.016 in.w.g.) of 291 cm^2 (45.1 in^2) with the duct leaks closed and 435 cm^2 (67.4 in^2) with the duct leaks open. The air change rate at 50 Pa (0.2 in. w.g.) was 3.1 h^{-1} without the duct leaks and 4.2 h^{-1} with the duct leakage included. Therefore, the duct leakage increased the overall leakage of the building by about 50% in terms of effective leakage area and 34% in terms of air changes at 50 Pa (0.2 in. w.g.), which is similar in magnitude to increases seen in field tests. For example, Lambert and Robison (1989) found an increase of about 25% in effective leakage area due to duct leakage in a field study.

The airtightness results, expressed as normalized leakage, are 0.19 with no duct leakage and 0.29 with duct leakage. Normalized leakage (NL) is a non-dimensional measure of airtightness based on the effective leakage area at 4 Pa (0.016 in. w.g.) normalized by building floor area and building height, and is used in ASHRAE Standard 119 on air leakage in single-family residential buildings (ASHRAE 1988). This standard establishes performance requirements for air leakage in the form of classes from A to J, with each class comprising a range of normalized leakage values and Class A being the tightest. The more severe the climate, the lower the class required by the standard. For Spokane, the air leakage is required to be Class F or below, which corresponds to normalized leakage below 0.57. For coastal Washington state, the air leakage is required to be Class G or less, which corresponds to normalized leakage below 0.80. The results of the simulated pressurization tests correspond to class C for no duct leakage and Class E with the duct leakage included. Therefore, the model house complies with the requirements of ASHRAE Standard 119.

The simulated airtightness values are comparable to measured values in recently-constructed homes in the Pacific Northwest. In a group of these homes constructed with goals of energy-efficiency and innovation, the mean air change rate at 50 Pa (0.2 in. w.g.) was 5.6 h^{-1}, and the mean value of the effective leakage area at 4 Pa (0.016 in.w.g.) was 450 cm^2 (70 in^2) (Palmiter et al. 1991). These values should be compared with the model house value with the duct leaks open, that is 4.2 h^{-1} and 435 cm^2 (67.4 in^2). Another group of homes representing more typical construction had a mean value of the air change rate at 50 Pa (0.2 in. w.g.) of 9.3 h^{-1}, and a mean value of the effective leakage area at 4 Pa (0.016 in.w.g.) of 806 cm^2 (125 in^2). Therefore the airtightness of the simulated house is similar to that seen in recently constructed homes with a goal of energy efficiency, as intended.

As mentioned earlier, the sum of the effective leakage areas of all the openings in the exterior envelope that were included in the house model was 290 cm^2 (45 in^2). As noted above, the

effective leakage area was 291 cm^2 (45.1 in^2) in the simulated pressurization test. Such good agreement between the input values and those obtained from a simulated pressurization test is expected and serves only as a check on the accuracy of the house model as it was represented within CONTAM96.

The airtightness evaluation was repeated after the inlet vents were installed for the simulations in Case #3. With the inlet vents, the effective leakage area at 4 Pa (0.016 in.w.g.) increased to 569 cm^2 (88.2 in^2), an increase of 134 cm^2 (20.8 in^2) or 31% over the leakage without the vents. The air change rate at 50 Pa (0.2 in. w.g.) increased to 5.2 h^{-1}, an increase of 24%. The increase of 134 cm^2 (20.8 in^2) in effective leakage area compares to the combined leakage area of the nine passive vents of 135 cm^2 (2.3 in^2), based on 15 cm^2 (2.3 in^2) per vent. For Case #5, with the duct leakage reduced, the effective leakage area at 4 Pa (0.016 in. w.g.) was 305 cm^2 (47.3 in^2), a reduction of 130 cm^2 (20.2 in^2) or 30% relative to the effective leakage area with the original duct leakage values. The air change rate at 50 Pa (0.2 in. w.g.) decreased to 3.2 h^{-1}, a change of 24%.

Airflow Patterns

In order to understand the air movement patterns in the house, steady-state airflow simulations were performed and analyzed for selected cases. Figure 7 is a schematic of the airflow patterns for four different cases of fan operation. In the first case, the forced-air fan and all other fans are off. In addition, all interior doors are open. For this case, and subsequent cases discussed in this section, the indoor-outdoor air temperature difference is 20 °C (36 °F) and the wind speed is zero. With the fans off, outdoor air tends to enter the conditioned space at lower elevations such as openings in the crawl space and in the exterior walls of the first floor, and then to move up within the building. Indoor air tends to exit the building from the upper floors to the outdoors and to the attic. Air also flows up in the supply and return ductwork. Note that air flows into the supply ductwork through the crawl space supply leak and out of the first and second floor supply vents. Air flows into the return ductwork via the garage return leak and the first floor return vent, and out of the first floor and attic return leaks. The air change rate with all the fans off and the interior doors open is 0.25 h^{-1}. Another fans-off simulation (not shown) was performed with the bedroom doors closed, but the airflow pattern changed very little. The second case in Figure 7 is with the kitchen exhaust fan on. With this exhaust airflow rate of 49.9 L/s (105.7 cfm), all of the airflows out of the building via envelope leakage are reduced and the airflows into the building are increased. Air no longer flows upward from the first floor to the second floor, but instead flows down to the first floor to "feed" the kitchen exhaust fan. The building air change rate with the kitchen exhaust fan on is 0.51 h^{-1}, compared to 0.25 h^{-1} with the fan off. The increased air change rate corresponds to 32.3 L/s (68.4 cfm), which is 65% of the exhaust fan airflow rate. The exhaust airflow rate does not convert directly into an increase in air change rate because some of the exhaust airflow simply "replaces" exfiltration that exists without the exhaust fan operating.

In the third case in Figure 7, the upstairs bathroom exhaust fans are operating and these bathroom doors are closed. Similar to the previous case, the exhaust airflow increases leakage into the building and reduces leakage out relative to the case with no fan operation. The airflows into and out of the building are similar to those with the kitchen exhaust fan operating. However, there

is a significant increase in the airflow from the first floor to the second floor. The building air change rate with the exhaust fans operating is 0.48 h^{-1}. The increase in the air change rate, relative to the fans-off situation, corresponds to 63% of the total exhaust fan airflow rate. The last case in Figure 7 shows the airflow rates with just the forced-air fan on. Due to the predominance of leakage in the return ductwork (in the attic, first floor and garage), the conditioned space becomes pressurized relative to the outdoors. This duct leakage also tends to pressurize the crawl space and depressurize the garage and attic. Under these conditions, little air enters the conditioned space due to infiltration from outdoors, the garage or the crawl space. However, significant quantities of outdoor air enter the return side of the duct system due to leakage, both directly from the outdoors as well as indirectly via the attic and garage. The air change rate with the forced-air fan on is 0.52 h^{-1}, twice that of the fan-off case, even though the airflow rate directly from outdoors to the conditioned space due to envelope leakage decreases from 6.5 L/s (13.8 cfm) to 0.4 L/s (0.8 cfm).

Figure 8 shows four cases with the forced-air fan on. The first case is the same as the last case in Figure 7, that is with the forced-air fan on and all interior doors open. In the second case, the forced-air fan is on and the bedroom doors are closed. With these doors closed, the airflow out of the second floor envelope leaks increases because the bedrooms are at a higher pressure. Note that there is only a single return vent on the second floor in the hall, causing the closed bedroom doors to restrict the return flow out of the bedrooms. Air also flows from the bedrooms, through openings in the floor, to the first floor of the house. The net airflow from the first floor to the second increases to "feed" the second floor return. The air change rate with the bedroom doors closed increases slightly relative to the doors-open case, from 0.52 h^{-1} to 0.54 h^{-1}. The third and fourth cases in Figure 8 correspond to the kitchen exhaust fan and the upstairs bathroom exhaust fans operating, similar to the second and third cases in Figure 7. Both cases increase the leakage airflows into the building, as expected. The building air change rates for these two cases increase to 0.69 h^{-1} and 0.68 h^{-1}. These increases in air change rate correspond to 43% and 42% of the exhaust airflow rates respectively.

Figure 9 shows the airflow patterns with the passive inlet vents installed (Case #3). In the first case, the forced-air fan is off and all interior doors are open. With the forced-air fan off, the airflow pattern and airflow rates are similar to those without the inlets installed (first case in Figure 7), except that the vents provide additional paths for infiltration and exfiltration on the first and second floors. These extra airflows increase the building air change rate to 0.32 h^{-1} from 0.25 h^{-1} without the inlet vents. Note that indoor air flows out of the second floor inlets due to the stack-driven, upward airflow pattern. Therefore, under these and similar conditions (cold outdoor air and low wind speed), the inlets do not provide outdoor air directly to these second floor spaces. They do result in increased outdoor air entry into the building, which presumably results in the building, including the second floor, being better ventilated. Of course, under some conditions of nonzero wind speed, outdoor air will flow into the building through the inlet vents. In the second case in Figure 9, the forced-air fan is still off, but the master bathroom exhaust fan is on. Recall that in Case #3, the airflow rate associated with this exhaust fan is increased to 45.0 L/s (95.3 cfm) to meet the whole house ventilation requirements of ASHRAE Standard 62-1989. The operation of this fan increases infiltration and inflow as expected, but air still flows out of the second floor inlet vents. However, some infiltration does occur on the second floor, through envelope leaks at floor

level. The whole building air change rate for this case is 0.51 h^{-1}, with the increase corresponding to 52% of the exhaust fan airflow rate. In the third case in Figure 9, the forced-air fan is on. Again, due to duct leakage, the building is pressurized, which reduces the incoming airflows and increases the outflows. The airflow pattern is similar to that seen without the inlets, with the only difference being the additional flows through the inlets themselves. In this case, indoor air flows out of the building through all the inlets. The building air change rate is 0.57 h^{-1} for this case. In the last case in the figure, the forced-air and the master bathroom exhaust fans are both on. The exhaust fan operation works against the pressurization induced by the forced-air fan, causing outdoor air to enter the building through the first floor inlets and causing a small amount of infiltration on the second floor. The whole building air change rate increases to 0.74 h^{-1} for this last case.

Figure 10 shows the impact of the other two ventilation approaches, the outdoor air intake duct on the forced-air return (Case #4) and the continous exhaust fan with the tightened duct work (Case #5). The first case in the figure repeats the case with the forced-air fan on and all interior doors open. In the second case, the forced-air fan is on, the intake duct on the forced-air return is open, and the master bathroom exhaust fan is on. The airflow pattern in the second case is similar to that in the first, with the pressurization of the building and the dominance of outgoing leakage reduced due to the exhaust fan. Also, there is a significant airflow from the first floor to the second floor to provide "make-up" air for the exhaust fan. The whole building air change rate increases to 0.85 h^{-1}. The increase in the air change rate relative to the case with no intake duct or exhaust fan operation corresponds to 95% of the airflow through the intake duct. This high percentage is due to the balanced nature of this ventilation approach, that is, a mechanical exhaust airflow exists to match the supply airflow. The last case in Figure 10 is that of reduced duct leakage and a continous exhaust fan in the master bathroom. The reduced duct leakage obviously decreases the airflow rates into and out of the duct leaks, thereby decreasing the pressurization of the building with the forced-air fan operating. This decrease, in combination with the exhaust fan operation, leads to infiltration flows on both floors, which are now the largest airflows into the building. The air change rate for this last case is 0.35 h^{-1}, which is consistent with the exhaust fan being sized to meet the ventilation requirement of ASHRAE Standard 62-1989.

Figures 7 through 10 reveal a few key aspects of the airflow patterns in this building. First, an upward airflow pattern dominates under these conditions of low wind speed and a higher indoor air temperature than outdoor. This pattern leads, in general, to most of the air entering the building on the first floor and very little entering on the second floor. The only conditions that induce outdoor airflow into the building on the second floor is the operation of exhaust fans. Due to the levels of duct leakage in this building and the dominance of return-side leaks, the operation of the forced-air fan tends to pressurize the building, reducing infiltration through the envelope. However, outdoor airflow into the building through the return leaks more than compensates for the reduction in infiltration, leading to roughly a doubling of the whole building air change rate. Installation of the inlet vents simply adds more envelope leakage and has very little impact on the overall airflow pattern. Due to the stack-dominated airflow pattern, air flows out of the building through the second floor inlets under the conditions presented, that is, zero wind speed. As expected, the balanced mechanical ventilation approach, that is, the outdoor air intake duct in

combination with an exhaust fan, is most effective in supplementing the building ventilation rate. Finally, reducing the duct leakage decreases the building pressurization with the forced-air fan running, and leads to infiltration into the second floor with the fan running. Obviously these airflow patterns will differ for nonzero wind speeds and will depend on wind direction. While the impact of wind speed and direction was not considered in this discussion, their influences are reflected in the airflow and contaminant concentration results presented in the sections that follow.

Ventilation Rates

This section presents the predicted whole building air change rates. These rates are presented as hourly means based on the airflow rates calculated at each 5-min time step. The air change rates are based on the sum of the airflow rates into the living area from the outdoors, crawl space, garage and attic (including the airflows into the duct system via duct leakage), divided by the volume of the living area.

Airflow simulations were performed for Case #1, all fans off and all interior doors open, to evaluate the ventilation characteristics of the building due to envelope leakage alone. Figure 11 is a plot of the the hourly mean air change rate over one year versus the indoor-outdoor air temperature difference. The data all lie above an envelope of minimum air change rates, which corresponds to stack-dominated ventilation of the building. The spread in the direction of higher air change rates is due to wind effects. Figure 12 is a plot of the same data restricted to those hours for which the wind speed is less than 2 m/s (4.5 mph), and shows the expected dependence of the air change rate on temperature difference. Figure 13 is a frequency distribution of the hourly air change rates for Case #1. There is a predominance of values in the 0.1 h^{-1} to 0.3 h^{-1} range, based on the distribution of weather conditions. The mean air change rate over the entire year is 0.22 h^{-1}, and 88% of the hourly values are below the outdoor air ventilation requirement in ASHRAE Standard 62-1989 for residential buildings of 0.35 h^{-1}. Therefore, envelope leakage alone, in this building, will not provide adequate ventilation as defined by the ASHRAE standard. However, this building and real houses, are subject to other driving forces for ventilation including exhaust fan operation, airflow into the building due to duct leakage, and occupant activities such as window and door openings. The other cases studied in this effort include the influences of the first two factors, but do not consider the effects of window or door opening.

The simulations in Case #2 include the effects of forced-air and exhaust fan operation, as well as interior door position, and serves as a base case for comparison of the alternative ventilation approaches. Figure 14 is a plot of the hourly mean air change rates for this case, restricted to wind speeds less than 2 m/s (4.5 mph). These air change rates are higher than in the infiltration-only Case #1, due to the operation of the forced-air fan in conjunction with duct leakage and due to the exhaust fans. These data show more scatter than that seen in Case #1 due to the differences in fan operating time for the different months. The data fall into two main groups, with the upper group associated with the operation of the kitchen and bathroom exhaust fans. The variation in the lower group of points is due primarily to differences in the fraction of forced-air on-time for the different months. Figure 15 is a frequency distribution of the hourly air change rates for Case #2. The shape of this distribution is smoother than that seen for Case #1,

presumably due to the variation in air change rates induced by fan operation and door openings. The mean air change rate over the year is 0.31 h^{-1}, and 71% of the hourly air change rates are below 0.35 h^{-1}. Therefore, for this case, air leakage as impacted by duct leakage and exhaust fan operation does not meet the requirements of ASHRAE Standard 62 for most of the year.

Tracer gas measurement of building air change rates were performed on the group of homes in the Pacific Northwest mentioned earlier (Palmiter et al. 1991). Based on these measurements, the mean air change rate over the heating season was 0.33 h^{-1} for the houses constructed under the energy efficiency program and 0.40 h^{-1} for the more typical houses. The mean for Case #2 over the heating season (November through April) is 0.42 h^{-1}; however, the indoor-outdoor air temperature difference over the heating season in Spokane is larger than the weather encountered in the field study. Therefore, the predicted air change rates for Case #2 appear reasonable relative to the values obtained in this field study.

Figure 16 is a plot of the hourly mean air change rates for Case #3, with the air inlet vents open, again restricted to low wind speeds. These data fall into three groups. The lowest group corresponds to hours with no exhaust fans running. The middle group corresponds to the operation of the master bathroom exhaust fan during its 8-hour schedule, or the operation of the kitchen exhaust fan alone. The upper group of points corresponds to hours where the master bathroom exhaust fan operates in conjunction with the kitchen exhaust fan or the second floor hall bathroom fan. Figure 17 is a frequency distribution of the hourly air change rates for Case #3. This distribution is broadened relative to Case #2, due to the variation induced by the extended exhaust fan operation. The mean air change rate for this Case #3 over the year is 0.44 h^{-1}, and only 30% of the hourly values are below 0.35 h^{-1}. This case exhibits better compliance with the ASHRAE Standard 62 than the previous cases, but there are significant number of hours of over ventilation relative to the standard and there is an energy penalty associated with this overventilation. In fact, the air change rate exceeds 0.70 h^{-1} for 11% of the hours of the year.

The hourly mean air change rates for Case #4, with the outdoor air intake duct on the forced-air system return, are plotted in Figure 18. These data fall into two major groups. The upper group of points corresponds to hours when the intake duct is open and the master bathroom exhaust fan is running, resulting in relatively high air change rates. This upper group is also divided into two collections of points, one corresponding to no other exhaust fans running (lower air change rates) and another with the kitchen exhaust fan or the second floor hall bathroom exhaust fan running (higher air change rates). The other major group of points, with air change rates between about 0.1 h^{-1} and 0.6 h^{-1}, occurs when the master bathroom exhaust fan is not running. This lower group exhibits some higher air change rates during hours when the kitchen or other bathroom exhaust fans are running. Figure 19 is a frequency distribution of the hourly air change rates for Case #4. This distribution is bimodal, corresponding to the master bath exhaust fan being on or off. The mean air change rate for this case over the year is 0.51 h^{-1}, and 36% of the hourly values are below 0.35 h^{-1}. Even though the mean air change rate for this case is higher than for Case #3, the distribution of air change rates for Case #4 results in the percentage of hours below the 0.35 h^{-1} requirement being greater. In addition, there are a large number of hours for which the air change rate is well above the Standard 62 requirement. Specifically, the air change rate exceeds 0.70 h^{-1} for 34% of the hours of the year.

Figure 20 is a plot of the hourly mean air change rates for Case #5, with the reduced duct leakage and a continuously-operating exhaust fan in the master bathroom. The lower group of points corresponds to hours with no other exhaust fans operating, while the upper group of points corresponds to various combinations of other exhaust fans operating. There is much less scatter in the lower group of points than seen in previous cases because the monthly differences in forced-air fan on-time have less of an impact on the air change rate, given the reduced duct leakage. The air change rate is never above about 0.6 h^{-1}, which occurs when multiple exhaust fans are running and outdoor air is infiltrating into the building over the entire envelope. Figure 21 is a frequency distribution of the hourly air change rates for Case #5. This distribution exhibits a strong peak between 0.25 h^{-1} and 0.35 h^{-1}, due to the stability induced by the continuous fan operation and the reduced duct leakage. The mean air change rate for this case over the year is 0.34 h^{-1}, and 71% of the hourly values are below 0.35 h^{-1}. However, the air change rates that are below 0.35 h^{-1} are never less than about 0.25 h^{-1}. The other cases have minimum air change rates as low as 0.1 h^{-1}.

Table 5 summarizes the air change rates for the five cases, presenting the mean air change rate and the percentage of hours below the ASHRAE requirement of 0.35 h^{-1} for each case by month. In addition, the table contains the annual values of the mean air change rate, standard deviation, ratio of the standard deviation to the mean, median air change rate, and the percentages of hourly air change rates below 0.35 h^{-1} and above 0.70 h^{-1}, twice the ASHRAE requirement. As expected, the air change rates are higher during the colder months when the driving forces for infiltration are larger and the forced-air system on-times are longer, which increases the air change due to duct leakage. Note that Case #5 exhibits less variation in the monthly mean air change rates than the other cases. This stability exists because the reduced duct leakage lessens the impact of the variability in the forced-air on-time. Also, the continous exhaust fan increases the air change rates in the milder months. While most of the hours in this case are below 0.35 h^{-1}, this is a function of the sizing of the exhaust fan. A higher capacity fan would have reduced the number of hours with air change rates below the ASHRAE requirement. The median of all cases, except Case #4, is just under the mean air change rate, reflecting the distributions being skewed towards lower air change rates. For Case #4, the median is much lower than the mean, due to the bimodal distribution of the air change rates. Note that the two cases involving the higher capacity exhaust fan in the master bathroom, Cases #3 and #4, have a significant number of hours with air change rates greater than twice the requirement in ASHRAE Standard 62. For Case #4, the air change rate exceeds 0.7 h^{-1} for about one-third of the year. Case #5 has essentially no hours at this high rate, reflecting the attempt to control over-ventilation by reducing the duct leakage and using a more carefully sized exhaust fan.

Air Distribution

The age of air was calculated in each room as part of the airflow simulations. As mentioned earlier, the age of air for a room is the mean amount of time that has passed since the air in that room entered the building, and is an indicator of the distribution of ventilation air. Low values of the age of air in a zone, relative to the building mean value, indicate that a larger proportion of outdoor air is flowing directly into that zone relative to zones with higher ages of air. High values

indicate that little, or even no, outdoor air is entering the zone directly. And while little or no outdoor air might enter a zone, this zone can still have a low age of air if the ventilation air reaches the zone from another building zone with a high airflow rate from outdoors. Also, if the air within the building is well-mixed by the forced-air distribution system, zones that are served by that system will not necessarily have low ages, even if there is no air flowing directly from the outdoors into the zones. In these simulations, outdoor air tends to enter this house at lower levels and flow up to the second floor. Consideration of the airflow patterns presented earlier indicate no outdoor air entry into the second floor for many cases. However, the mean age of air on the second floor is at most twice the mean age on the first floor, since the age of air takes into account the outdoor air that reaches the second-floor rooms via the first floor.

The 0.35 h^{-1} ventilation requirement in ASHRAE Standard 62-1989 corresponds to an age of air of 2.86 h in a single-zone, well-mixed building. If the house was meeting the requirement in the ASHRAE standard, and the outdoor air was uniformly distributed among the zones, then the age of air would be 2.86 h in all the zones. Such a uniform distribution of ventilation air can be achieved by providing outdoor air to each room in proportion to its volume, or by having a high degree of mixing between the rooms.

Table 6 shows the mean monthly values for the age of air for Cases #2, #3, #4 and #5 for each of the major living area zones, as well as the volume-weighted means for the first and second floors. The mean ages in the table are based on the ages calculated at each 5-min time step of the simulations, which results in the values being higher than if they had been calculated based on hourly average ages. The age at 5-min time steps can be quite high when the weather and fan operation are such that the air change rate is very low. Hourly average ages are lower than the 5-min ages, as there is always some fan operation during each hour, which results in the hourly air change rate being higher than the 5-min values. All the values in the table for which the age is 3.0 h or greater are in bold type, based on the value of 2.86 h corresponding to the ventilation requirement in ASHRAE Standard 62-1989. Most of the values are above 3.0 h, indicating outdoor air delivery to these zones that is inconsistent with the 0.35 h^{-1} ventilation requirement in ASHRAE Standard 62. The upward airflow pattern in the building is evident by the lower ages on the first floor than on the second. Also, the age of air tends to be higher in the non-winter months when weather-driven infiltration rates and forced-air system on-times are lower. The occurrence of mean ages of air below 3 h is less common in the envelope leakage case, #2, than in the three cases with mechanical ventilation, #3, #4 and #5. Of the mechanically ventilated cases, Case #3 has the highest number of months with mean ages of air below 3 h. Note that the monthly mean age of air is rarely below 3 h in any of the bedrooms.

Note that the ages for Case #4 are greater than those for Case #3, despite the fact that the mean air change rate for Case #4 (0.51 h^{-1}) is greater than the mean for Case #3 (0.44 h^{-1}). At first glance, this difference is not expected because higher air change rates generally correspond to lower ages of air. This discrepancy occurs because the ages in Table 6 are based on the 5-min time step used in the simulations and because of the distribution of air change rates for Case #4. In both Cases #3 and #4, the short time step results in some very low air change rates and very high ages, when no fans are on. Due to the existence of the inlet vents in Case #3, Case #4 actually has lower air change rates, and higher ages, under these no-fan conditions even though it has a higher mean

air change rate. Furthermore, the distribution of air change rates for Case #4 results in these lower air change rates dominating the ages presented in Table 6.

The results in Table 6 indicate that the outdoor air ventilation to the individual rooms does not on average meet the requirements of the ASHRAE standard. This is consistent with the large number of hours with air change rates below 0.35 h^{-1} discussed in the previous section. However, high ages of air in individual rooms do not necessarily mean that the air quality is unacceptable. The acceptability of the air quality in these rooms depends on the pollutant sources in the rooms and the concentration of pollutants of the air that enters these rooms, regardless of whether this air comes from within the building or from outdoors. The age of air of a room, and its comparison to 3 h or any other value, simply provides an indication of the outdoor air ventilation of that room.

Energy

The energy consumption associated with each of the ventilation approaches was calculated as described earlier and is shown in Table 7. This table presents the energy associated with heating, cooling and fan operation, as well as the percentage of the total energy consumption attributable to heating, cooling and fans. The heating load, as discussed earlier, is determined from the hourly building air change rates times the heat capacity of air and the indoor-outdoor air temperature differences for each hour. These loads are then summed over the year. The heating load is converted to energy consumption by assuming that the house is heated by a heat pump with a COP of 2.2 W/W (7.5 Btu/h per W). The cooling load consists entirely of the sensible load, which is determined similarly to the heating load. The latent cooling load, based on the indoor-outdoor humidity ratio difference, was also calculated, but as mentioned earlier no latent cooling load due to ventilation existed for this climate. The conversion of the cooling loads to energy consumption is based on an air conditioner with a SEER of 3.5 W/W (12 Btu/h per W). The fan energy calculations in Table 7 are based on the operating schedules of the various fans in each case. The fans are assumed to consume energy at the following rates: forced-air fan 560 W; kitchen exhaust fan 55 W; typical bathroom fan (used in BA2 in all cases and in MBA in Case #2) 27 W; upgraded bathroom fan (used in MBA in Cases #3 and #4) 54W; and, continuous bathroom fan (used in MBA in Case #5) 37 W. During heating, some of the energy consumed by the forced-air fan will reduce the heating load, though at a lower efficiency than the heat pump. Under cooling, this fan energy will increase the cooling load. Because the heating and cooling impacts are in opposite direction and to the first order are similar in magnitude, and because detailed analysis of these impacts was beyond the scope of this effort, these effects were ignored.

The energy loads presented for Case #1 include only the heating and cooling loads, and not the fan loads, as this is the case of envelope leakage only. Case #2 is another baseline case with the forced-air fan operating on a schedule that varies by month and with the exhaust fans operating on schedules. The heating and cooling loads of Case #2 increase relative to Case #1 by 37% and 80% respectively, due to the airflows induced by duct leakage and exhaust fan operation. The total energy consumption, due to these increases and the energy consumed by the fans, roughly doubles from 6800 MJ (1890 kWh) to 13790 MJ (3830 kWh), an increase of 103%. The first mechanical ventilation option, i.e., the use of passive air inlets in combination with an exhaust fan (Case #3),

increases the energy consumption as expected. The increases in heating, cooling, fan and total energy relative to Case #2 are 42%, 22%, 12% and 32% respectively. The use of an outdoor air intake duct in Case #4, again with an exhaust fan operating, increases the energy consumption even more. Relative to Case #2, the increases in heating, cooling, fan and total energy are 58%, 33%, 112% and 75% respectively. The increase in fan energy is so large for Case #4 due to the operation of the forced-air fan for 8 h each day to induce ventilation through the intake duct.

In Case #5, the duct leakage was reduced and an exhaust fan was operated continuously. The decreased duct leakage reduces the heating and cooling energy consumption relative to the other two cases with mechanical ventilation, particularly during the months requiring the most heating and cooling. The exhaust fan operation tends to increase energy consumption during periods of mild weather by increasing the air change rate at these times. The net effect is an increase in the heating and cooling energy consumption relative to Case #2 of 6% and 11% respectively, which is relatively small compared to increases seen for Cases #3 and #4. The fan energy for Case #5 is still significant, but the total energy consumed is well below that of Cases #3 and #4. Case #6 is another reference case corresponding to a constant air change rate of 0.35 h^{-1}. Fan energy is not included in this case, as it is not meant to represent any particular system.

It turns out that the total energy consumption for heating and cooling for each case exhibits an approximately linear relationship with the annual mean air change rates shown in Table 5. The total energy consumption also exhibits this linear relationship, with the exception of Case #6 for which no fan energy is included.

Contaminants

The contaminant concentrations for Case #2 are summarized in Table 8. For each month, and for the year, this table shows the following monthly mean concentrations: hourly mean VOC concentration in the living area zones (bedrooms, living and dining room, and kitchen/family area); hourly mean CO concentration in the kitchen/family area, living room and averaged over the four bedrooms; daily peak value of the hourly mean NO_2 concentration for the kitchen/family area, living room and bedroom mean; hourly mean relative humidity averaged over all conditioned zones of the house (excluding the crawl space, attic and garage); and, daily peak value of the hourly mean CO_2 concentration averaged over the four bedrooms. In addition, the percent of hours for which the relative humidity averaged over the house is less than 30% is shown in the table. The annual values for each contaminant are the mean and standard deviation of each hourly concentration value over the whole year, except in the cases of NO_2 and CO_2 in which the annual values are based on the peaks of the daily hourly mean. The ratios of the standard deviation to the mean annual values are also given for each contaminant.

As expected, the VOC concentrations are lower in months with higher air change rates and higher in months with lower rates. The relationship between concentration and air change rate follows the expected theoretical relationship fairly closely, that is, the concentration depends on the inverse of the air change rate. This theoretical relationship is based on a single-zone, steady-state contaminant mass balance with constant values for the contaminant source strength, ventilation rate and outdoor contaminant concentration. A close correspondence with theory is expected since the

VOC source strength is constant over time and uniformly distributed throughout the house. Figure 22 is a plot of the monthly mean VOC concentration versus air change rate for Case #2 and shows the inverse relationship between concentration and air change rate. Each point is labeled with the month. Some deviations occur from July through September, due to VOC storage effects.

The monthly mean CO concentrations in the KFA zone do not exhibit as much variation from month to month as the VOC concentrations, and are less dependent on air change rate. While the standard deviation of all the hourly values is 64% of the mean CO concentration for the year, the standard deviation of the monthly means is only 9% compared with 18% for VOCs. The fact that the indoor CO source is localized in the kitchen and occurs only during specific time periods (during cooking), leads to less dependence on air change rate. In fact, the extent of mixing in the house, as determined by the forced-air system on-time, is an important determinant of the CO concentration in the KFA zone. Less mixing, that is, lower values of forced-air system on-time, result in higher concentrations in the KFA zone. Figure 23 is a plot of the KFA CO concentration versus air change rate for Case #2, with each point labeled by month and number of minutes per hour of forced-air system on-time. While there is some suggestion of an inverse relationship between concentration and air change rate, the dependence on air change rate is not as strong as in the case of VOCs in Figure 22. And the months with lower values of forced-air system on-time tend to have higher concentrations in the KFA zone. In particular, the September value is much higher than the others, due in part to the low forced-air system on-time, which results in less mixing of the CO generated by cooking with the rest of the house. The CO concentrations in the rest of the house, as exhibited by the concentrations in the LR and bedroom zones, show little variation from month to month. The variation that does exist includes the inverse relationship with air change rate, combined with a tendency to lower concentrations during months with lower forced-air system on-times due to mixing effects.

The daily peaks of the hourly mean NO_2 concentrations depend primarily on the monthly forced-air system on-time. The highest concentrations in the KFA zone occur during months with low on-times, which in turn correspond to the lowest concentrations in the other zones. The strong dependence on mixing, relative to CO, occurs for NO_2 because these are peak concentrations during the day as opposed to mean concentrations over the entire day. Figure 24 is a plot of the KFA NO_2 concentration versus air change rate for Case #2, with each point labeled by month and number of minutes per hour of forced-air system on-time. There is no evidence of an inverse relationship between concentration and air change rate. Instead, the months with the same on-time values have the same NO_2 concentrations, with lower on-times corresponding to higher concentrations.

The monthly means of relative humidity depend on outdoor humidity level, air change rate and operation of the air conditioning system. The indoor relative humidity levels are fairly low, due to a combination of the low outdoor humidity levels for Spokane and the low indoor source strengths. Figure 25 is a plot of the whole house relative humidity versus air change rate for Case #2, with each point labeled by month, minutes per hour of forced-air system on-time, and monthly mean of the outdoor absolute humidity. There is some suggestion of an inverse relationship between concentration and air change rate, but other factors are important in the variation in indoor humidity. From January to May, the air change rate decreases and the outdoor humidity level

increases. Since the indoor humidity ratio is higher than outdoors during these months, both of these factors contribute to an increase in the indoor humidity over these five months. The air conditioner operates in June, July and August, leading to lower indoor humidity levels, with higher values of AC on-time corresponding to lower values of indoor humidity. In September, the AC is off and the indoor humidity increases. However, the September value is somewhat below the January through May curve, presumably due to water vapor storage elements in the house being depleted during the summer months and being "refilled" during September. The indoor levels from October through December decrease as the air change rate increases and the outdoor humidity levels drop. However, the indoor levels during these three months are above those seen from January through May, due in part to water vapor being released from the storage elements as the indoor humidity drops. The values from January through May are lower because these storage elements are being filled as the humidity levels rise during these months. Examining the percentages of hours with the indoor relative humidity below 30% in Table 8, these percentages are largest during the cold weather and during July when the air conditioner operates the most. The percentages of hours for which the humidity was above 60% were also determined, as an indicator of the potential for condensation and perhaps microbial growth. However, almost no hours had these high humidity values, again due to the climate and the strength of the indoor moisture sources. Houses in this climate with higher indoor source strengths would have higher indoor moisture levels, perhaps leading to significant numbers of hours with the indoor relative humidity greater than 60%.

The daily peaks of the hourly mean CO_2 concentrations in the bedrooms depend primarily on the air change rate, with a secondary impact of forced-air system on-time. Figure 26 is a plot of the bedroom CO_2 concentration versus air change rate for Case #2, with each point labeled by month and minutes per hour of forced-air system on-time. The inverse relationship between concentration and air change rate is evident in the data. However, the months with lower on-times tend to have higher CO_2 concentrations in the bedrooms due to the lower level of mixing with the rest of the house. In fact, months with the same on-time values tend to lie on a unique line relating concentration to air change rate. Also, note that all of the mean peak values are in excess of the 1800 mg/m^3 (1000 ppm(v)) guideline value for CO_2 in ASHRAE Standard 62-1989. However, this guideline value is based on the correlation between CO_2 concentrations and the perception of body odor from human bioeffluents, and not on any health impacts of the CO_2 itself.

The contaminant concentrations for Case #3 (inlet vents and exhaust fan operation) are summarized in Table 9. Relative to the results for Case #2 in Table 8, the most significant differences are seen in the VOC and CO_2 concentrations, as those two contaminants are most dependent on air change rate. The annual mean air change rate increases from 0.31 h^{-1} for Case #2 to 0.44 h^{-1} for Case #3, an increase of 42%, due to the installation of the inlet vents and the extended exhaust fan operation. Correspondingly, the annual mean VOC concentration decreases from 1.40 mg/m^3 to 0.95 mg/m^3 and the annual mean bedroom CO_2 concentrations decreases from 3330 mg/m^3 to 2660 mg/m^3, decreases of 32% and 20% respectively. The CO concentrations and the relative humidity levels decrease for Case #3, but only slightly. The NO_2 levels change very little. The relationships between the contaminant concentrations, air change rates and forced-air fan

on-time for Case #3 are similar to those seen for Case #2 in Figures 22 through 26.

The contaminant concentrations for Case #4 (air intake on forced-air return) are summarized in Table 10. The annual mean air change rate for Case #4 is 65% higher than that for Case #2, 0.51 h^{-1} compared with 0.31 h^{-1}, due to the installation of the outdoor air intake in combination with the extended exhaust fan operation. The contaminant concentrations are almost identical for Cases #4 and #3, despite the fact that the annual mean air change rate is 0.07 h^{-1}, or 16%, higher for Case #4. The reason for the lack of change in concentration has to do with differences in the distribution of air change rates for the two cases and the inadequacy of mean contaminant concentrations in characterizing non-normal concentration distributions. As discussed earlier, the tighter envelope for Case #4 (no inlet vents) results in more frequent occurrences of low air change rates than for Case #3. These lower air change rates elevate the mean contaminant concentrations for Case #4 due to the higher concentrations that occur at the lower rates.

The contaminant concentrations for Case #5 (reduced duct leakage and continuous exhaust fan operation) are summarized in Table 11. Relative to the results for Case #2 in Table 8, all of the contaminant concentrations are reduced, with the exception of NO_2. The most significant differences are seen in the VOC and CO_2 concentrations, as those two contaminants are most dependent on air change rate. The annual mean air change rate increases from 0.31 h^{-1} for Case #2 to 0.34 h^{-1} for Case #5, an increase of only 10%. The annual mean VOC concentration decreases from 1.40 mg/m^3 to 1.08 mg/m^3 and the annual mean bedroom CO_2 concentration decreases from 3330 mg/m^3 to 3080 mg/m^3, decreases of 23% and 8% respectively. The relationships between the contaminant concentrations, air change rates and forced-air fan on-time for Case #5 are similar to those seen for Case #2 in Figures 22 through 26.

Finally, the contaminant concentrations for Case #6 (constant air change rate of 0.35 h^{-1}) are summarized in Table 12. Monthly values are presented only for relative humidity, as this is the only contaminant that varies by month for this case. Relative to Case #2 in Table 8, all of the contaminant concentrations are reduced, with the exception of CO in the living room and bedrooms and the whole house level of H_2O. The reductions are primarily due to the increase in the air change rate from 0.31 h^{-1} for Case #2 to 0.35 h^{-1} for Case #6, an increase of 11%. The concentrations are also impacted by the high rate of internal mixing for this case. The annual mean VOC concentration decreases from 1.40 mg/m^3 to 0.97 mg/m^3 and the annual mean bedroom CO_2 concentration decreases from 3330 mg/m^3 to 2240 mg/m^3, decreases of 31% and 33% respectively. The change in the CO concentrations in Case #6 relative to Case #2 are due to the higher air change rates and the higher rate of mixing. The increased mixing distributes the CO more completely within the house, reducing the concentration in the KFA zone and increasing it elsewhere. The increased mixing is also responsible for the decreases in the peak NO_2 concentrations in the KFA zone and the increases in the LR and bedroom zones. The indoor humidity levels increase in the colder months because the air change rate decreases, thereby reducing the entry of drier outdoor air. During the summer, the air change rates are higher for Case #6, increasing the entry of humid outdoor air and contributing to the increase in the indoor humidity levels. The relationships between the contaminant concentrations and air change rates for Case #6 are similar to those seen for Case #2.

Exposure

Table 13 contains the annual mean exposure levels for CO, NO_2, VOC and CO_2 for each occupant of the house, as well as the mean for all the occupants. As mentioned earlier, these values are the mean concentrations to which each occupant is exposed while they are in the house. Exposure that occurs while they are outside of the house is neglected. Exposure is not presented for fine or coarse particles, since the concentrations of these contaminants did not exhibit much variation over time and were close to the outdoor levels. The exposure to water vapor is not reported either since it is not a contaminant of concern in terms of human exposure. These exposures are not presented as indicators of any expected health impacts, nor are health impacts necessarily expected to be linearly related to the average exposures presented.

Considering Case #2 and the contaminants associated with gas cooking, it is seen that CO and NO_2 exposure is lowest for the adult male. This is because his full-time work schedule keeps him out of the house during some of the time that cooking occurs. The adult female and Child #3 experience the highest levels of exposure to these two contaminants, since they are together in the KFA zone during many of the hours when cooking occurs. There is little variation among the occupants in their VOC exposure. The adult male experiences the highest CO_2 exposure, since he spends more time in the house during times of high occupancy. Child #1 experiences the lowest CO_2 exposure, since he/she spends less time in the house, and because much of that time is spent alone in his/her bedroom. Comparing Case #3 (inlet vents) to Case #2, there is little reduction in the CO exposure and the NO_2 exposure is almost identical despite the increase in air change rate. This similarity occurs because the concentrations of these contaminants are not particularly sensitive to air change rate. The mean VOC exposure is reduced by 44% from 1.44 mg/m^3 to 1.00 mg/m^3. The mean CO_2 exposure decreases from 2890 mg/m^3 to 2290 mg/m^3, a reduction of 21%.

The exposure values for Case #4 (air intake on forced-air return) are similar to those for Case #3. The CO exposure is essentially identical, and the NO_2 exposure is reduced slightly on average. The mean VOC exposure is reduced by 3%, and the CO_2 exposure is reduced by 7%. Earlier it was seen that the contaminant concentrations changed very little between Case #3 and Case #4, despite the fact that the air change rate for Case #4 was higher. This lack of change in concentration was attributed to differences in the distribution of air change rates for the two cases. With respect to exposure, the higher mean air change rate for Case #4 is reflected in lower exposure for those contaminants most closely related to ventilation rates, VOC (for three of the five occupants), and CO_2. Case #5 (reduced duct leakage and continuous exhaust fan operation) exhibits reduced exposure levels relative to Case #2, but higher than for Cases #3 and #4. As seen earlier, the contaminant concentrations for Case #5 are higher than for these other two cases. Nonetheless, the mean VOC exposure is reduced by 22% relative to Case #2, from 1.44 mg/m^3 to 1.13 mg/m^3. The mean CO_2 exposure is reduced from 2890 mg/m^3 to 2580 mg/m^3, a reduction of 11%.

The contaminant concentrations for Case #6 (constant air change rate of 0.35 h^{-1}) are similar to the other cases for CO and NO_2. The NO_2 exposures are reduced somewhat because of the increased internal mixing for this case. The VOC exposure is 0.98 mg/m^3, a 32% reduction relative to Case #2. The CO_2 exposure is less than any other case, 1990 mg/m^3, again because of the increase in mixing which reduces the bedroom CO_2 concentrations.

SUMMARY AND DISCUSSION

Trends towards tighter envelope construction in single-family buildings in North America, along with increasing awareness of indoor air quality issues, has led to the realization that mechanical ventilation may be needed in some residential buildings. While a variety of mechanical ventilation strategies have been developed and applied in residential buildings, many questions remain about the effectiveness of these systems in terms of indoor contaminant control, the actual ventilation rates provided, ventilation air distribution, and energy impacts. This paper reports on a study in which computer simulations were used to examine these issues in a house intended to represent recent energy-efficient construction in the Pacific Northwest region of the U.S.

While a number of previous studies have employed computer modeling to evaluate the impacts and effectiveness of mechanical ventilation in residential buildings, some of these efforts have been limited in the extent of their analysis. Some have predicted only building ventilation rates and have not examined indoor contaminant concentrations and energy impacts. Some of these studies have employed single-zone modeling approaches, rather than using multizone building models. This study builds on previous work at NIST (Emmerich and Persily 1996) and analyzes ventilation rates, airflow patterns, energy consumption, contaminant concentrations and occupant exposure for a single-family residential building exposed to the climate of Spokane, Washington. This work was done using the multizone airflow and indoor air quality model CONTAM96 (Walton 1997).

This section summarizes the results of this study and discusses them relative to the analysis approach employed and different options for ventilating residential buildings. In discussing these results, it is important to note that only one house in one climate was studied, with very specific inputs related to the house, weather, contaminants, and sources. While some of the results can be generalized to other buildings, it is important that similar analyses be conducted in other buildings in other climates subject to different indoor pollutant challenges. Also, other ventilation options, in addition to those studied here, merit consideration.

Airtightness and Ventilation

The model house was intended to be representative of recent energy-efficient construction in the Pacific Northwest region of the U.S. Based on a simulated pressurization test of the house that was conducted using CONTAM96, the air change rate at 50 Pa (0.2 in. w.g.) is 4.2 h^{-1}, including duct leakage. While this is tighter than most homes in the U.S., it is not exceptionally airtight compared to what is currently feasible (Sherman and Dickeroff 1994). It is, however, close to airtightness levels achieved in energy-efficient homes in the Pacific Northwest, therefore the airtightness goal of the house model was achieved.

Without any mechanical ventilation, the simulation results showed that even this level of airtightness led to a significant number of hours of overventilation during the year, particularly in colder and windier weather. On the other hand, during milder weather the air change rate was often below 0.35 h^{-1}, corresponding to underventilation relative to the outdoor air ventilation requirement in ASHRAE Standard 62-1989 for residential buildings. Therefore, ventilation based

on infiltration and local exhaust ventilation resulted in both energy and potential indoor air quality penalties from overventilation and underventilation respectively. The occurrence of overventilation, and the associated heating and cooling loads, can be addressed by a tighter envelope and reduced duct leakage. However, these changes would increase the level of some indoor contaminants, potentially compromising indoor air quality further. The occurrence of underventilation can be addressed by mechanical ventilation, but overventilation can still occur depending on the sizing of the mechanical ventilation system airflows and on the level of duct leakage. Based on the ventilation rates simulations, this study points to the effectiveness of tighter building envelopes, reduced duct leakage and mechanical ventilation to reduce the occurrence of over- and underventilation.

These simulations point out the difficulty in characterizing ventilation and air movement in buildings. In the case of ventilation rates, this study predicted hourly air change rates over an entire year. These were presented in terms of the mean and median values, the percentage of hours for which the air change rates were less than 0.35 h^{-1}, and the percentage of hours above 0.70 h^{-1}. While these measures are useful, they do not necessarily capture the details of the ventilation characteristics of a building, particularly in those cases where the air change rates are not normally distributed. For example, Case #4 had a bimodal distribution of air change rates, which limits the usefulness of mean values for characterizing ventilation.

Similarly these multizone airflow simulations provided a great deal of information on the airflow patterns in the house, specifically the airflow rate between every zone at each time step. These airflow patterns are affected by weather conditions, equipment operation, and door opening patterns, and given even a modest number of zones and situations of interest, the interpretation of these airflow patterns is difficult. In this study, airflow patterns were examined for a select number of cases, which showed the basic features of the building airflows. However, many more cases could have been examined, for example different conditions of wind speed and direction.

The airflow patterns presented in this report do reveal some key features of the airflows in this building. First, an upward airflow pattern dominates under conditions of low wind speed and a higher indoor air temperature than outdoor. This pattern leads, in general, to most of the outdoor air entering the building on the first floor and very little entering on the second floor. Due to the levels of duct leakage in this building and the dominance of return-side leaks, the operation of the forced-air fan tends to pressurize the building, reducing the infiltration through the envelope. However, the airflow into the building through the return leaks more than compensates for the reduced envelope infiltration, leading to roughly a doubling of the whole building air change rate when the forced-air fan operates. Installation of the inlet vents simply adds another envelope leak and has very little impact on the overall airflow pattern. Due to the stack-dominated airflow pattern, air flows out of the building through the second floor inlet vents under low wind speeds. As expected, the balanced mechanical ventilation approach, that is, the outdoor air intake duct in combination with an exhaust fan, is most effective in increasing the building ventilation rate. Finally, reducing the duct leakage decreases the building pressurization with the forced-air fan running, and leads to infiltration into the second floor with the fan running.

Energy

The energy consumption associated with ventilation was determined for the house, and for all cases the heating load dominated the total energy consumption, comprising 60% to almost 100% of the total load due to heating, cooling and fans combined. Cooling loads contributed only about 1% of the total. Fan energy was also found to be significant, especially when the forced-air fan was used to ventilate the building. In Case #4, in which the forced-air fan operated for 8 h each day, the fan energy consumption was roughly twice that seen in the other cases. Continuous exhaust fan operation (Case #5), also increased fan energy consumption, but the availability of low energy fans (Lubliner et al. 1997) makes this approach potentially more attractive.

Contaminants

As was discussed for ventilation and interzone airflow rates, it is difficult to characterize predicted contaminant concentrations in a multizone building over an entire year. In this study, seven contaminants were analyzed, and the concentrations were predicted at each 5-min time step in each zone of the building. For each case, it is desirable to summarize these concentrations for comparison to both "absolute" measures and for comparison to other cases. Most of the results were presented in terms of mean concentrations, with the zones on which the mean was based and the averaging period based on the contaminant and source characteristics. Based on these analyses, a number of conclusions were drawn.

For contaminants whose emissions are well distributed throughout a building and whose source strengths are constant over time, with VOC being the best example in this study, the concentration depends primarily on the inverse of the air change rate. This dependence is expected from a single-zone, steady-state mass balance analysis. The contaminants in this study that were most dependent on air change rate, relative to other independent variables (e.g. mixing), are VOC and CO_2. While the emissions of the latter contaminant are not as well distributed as for VOCs, the sources of CO_2, namely the occupants, do occupy all the major zones of the building. The concentrations of contaminants with localized sources (CO and NO_2), especially the peak concentrations, depend less on the air change rates. These peaks are impacted more significantly by mixing within the building, which is induced by forced-air fan operation in this study. Circumstances in which this fan operates more frequently lower concentrations in the room with the source and increase them elsewhere. The variation in indoor relative humidity depends on several factors, including outdoor humidity levels, air change rate, water vapor storage within the building, and air conditioner operation.

Comparison of Ventilation Approaches

Figures 27 through 29 summarize the results of the predictions for the different cases analyzed, with Figure 27 focusing on ventilation and energy consumption. This figure contains the mean air change rate, the percentage of hours with air change rates below 0.35 h^{-1} and above 0.70 h^{-1}, and the energy consumption associated with heating and cooling and with fan operation. Cases #1 and #2 are seen to result in many hours of underventilation, relative to the residential

requirement in ASHRAE Standard 62-1989 of 0.35 h^{-1}. This result demonstrates the inability of infiltration to provide "adequate" ventilation. One could argue that window opening by occupants would address this concern, but windows may not necessarily be opened during all times of underventilation in all houses. Cases #3 and #4, inlet vents and forced-air intake respectively, are "overventilated," as seen by the percentage of hours above 0.70 h^{-1}, mostly due to envelope and duct leakage. However, there are still significant percentages of hours during the year when the air change rate is below 0.35 h^{-1} for these two cases. Case #5 (continuous exhaust and reduced duct leakage) is also slightly "underventilated", but this underventilation is mostly a function of the sizing of the continuous exhaust fan. It could have been "remedied" with a slightly higher fan capacity. Figure 27 also shows the energy penalty of forced-air fan operation for Case #4, along with the increased heating and cooling loads due to overventilation for Cases #3 and #4. The heating and cooling energy consumption of Case #5 is closest to Case #6 (constant air change rate of 0.35 h^{-1}), showing good "control" of loads for this case. With a more efficient exhaust fan, one could further reduce the energy cost of mechanical ventilation for Case #5.

Figure 28 summarizes the contaminant concentration results for the different ventilation approaches. Case #2, corresponding to envelope infiltration alone, consistently results in the highest contaminant concentrations. In considering these results, it is important to note that absolute concentrations for a given case are of less interest than relative concentrations between cases for two important reasons. First, no concentration standards exist for residential environments. Second, the absolute concentration values depend on the specific input values used in the simulations, and many of these are not known particularly well. The VOC and relative humidity concentrations are fairly similar for all the mechanical ventilation options, that is, Cases #3, #4 and #5. The reference case of a fixed air change rate of 0.35 h^{-1}, Case #6, yields mean contaminant concentrations that are less than or equal to those in the other cases. The concentration of CO_2 is higher for Case #5, compared with Cases #3, #4 and #6, due to the lower air change rate.

Figure 29 summarizes the occupant exposure results for the different ventilation approaches. Case #2 has the highest exposure for ventilation-dependent contaminants, that is, VOC and CO_2. Less difference between cases is seen for the other contaminants, with Case #5 exhibiting the highest exposure levels. The exposure to CO and NO_2 is less variable among the cases, with the exception of lower CO exposure for Cases #3 and #4 due to the higher air change rates.

The simulations presented in this report have shown the impacts on ventilation, energy consumption, indoor contaminant concentration and occupant exposure of selected mechanical ventilation approaches in a specific residential building. The results have shown that envelope leakage, even in a relatively tight house, results in overventilation (relative to the residential ventilation requirement in ASHRAE Standard 62-1989) during severe weather. However, the same house can be underventilated during mild weather conditions. The existence of typical levels of duct leakage makes the overventilation situation, and the energy consumption associated with this leakage, even more significant. Incorporating a mechanical ventilation system increases the air change rate during mild weather, thereby reducing contaminant concentrations and occupant exposure, but the issue of overventilation remains. In order to deal with the overventilation issue, a

tighter building envelope and reduced duct leakage appear to be required.

In terms of the different ventilation approaches that were investigated, the reductions in contaminant concentration and exposure are to the first order related to the increase in air change rate. Deviations in that relationship do exist for contaminants with emissions that are episodic or localized, such as those associated with cooking and presumably other occupant activities. The relationship between concentration and air change rate is also more complicated for contaminants, such as water vapor, where the outdoor concentration varies with time. A major difference among the mechanical ventilation approaches is between balanced systems, such as the forced-air intake in combination with exhaust fan operation, and exhaust-dominated systems. The balanced systems result in more significant increases in air change rate, but the forced-air intake system investigated here has a significant energy penalty associated with fan operation. Other balanced approaches with smaller, more efficient fans that are dedicated to ventilation merit closer examination. Also, exhaust-only systems with more efficient fans may prove advantageous. Finally, in addition to these other system types, analysis is needed for other contaminants and sources, as well as other housing types and climates.

ACKNOWLEDGEMENTS

This work was performed for the Electric Power Research Institute under CRADA CN-1309/WO3512-27. The author acknowledges the support of John Kesselring of EPRI, as well as Mark Jackson of the Bonneville Power Administration. The assistance of Mike Lubliner of Washington State University, and of Steven Emmerich, Michael Pantiuk and George Walton of NIST is also acknowledged.

REFERENCES

ACCA. 1995. Residential Duct Systems Manual D. Air Conditioning Contractors of America.

ASHRAE. 1988. ANSI/ASHRAE Standard 119-1988, Air leakage performance for detached single-family residential buildings. American Society of Heating, Refrigerating and Air-Conditioning Engineers, Inc.

ASHRAE. 1989. ANSI/ASHRAE Standard 62-1989, Ventilation for acceptable indoor air quality. American Society of Heating, Refrigerating and Air-Conditioning Engineers, Inc.

ASHRAE. 1997. ASHRAE Handbook Fundamentals, Chapter 25 Ventilation and Infiltration. American Society of Heating, Refrigerating and Air-Conditioning Engineers, Inc.

ASTM. 1987. E779-87, Standard test method for determining air leakage rate by fan pressurization. American Society for Testing and Materials.

ASTM. 1996. E1827-96, Standard test method for determining airtightness of buildings using an orifice blower door. American Society for Testing and Materials.

Axley, J.W. 1991. Adsorption modeling for building contaminant dispersal analysis. Indoor Air, 1 (2): 147-171.

BPA. 1995. Super Good Cents Builder's Field Guide to Energy Efficient Construction. Bonneville Power Administration, DOE/BP-2651.

Blomsterberg, A. 1991. Ventilation control within exhaust fan ventilated houses. Proceedings of 12th Air Infiltration and Ventilation Centre Conference, Air Movement & Ventilation Control within Buildings, 2: 285-305.

Carlsson, T.; and A. Blomsterberg. 1995. Improvement of mechanical ventilation systems regarding utilization of outdoor air. Proceedings of 16th Air Infiltration and Ventilation Centre Conference, Implementing the Results of Ventilation Research, 2: 315-326.

Christian, J.E. 1993. A search for moisture sources. Proceedings of Bugs, Mold & Rot II, 71-81. National Institute of Building Sciences.

Christian, J.E. 1994. Moisture Sources. Manual on Moisture Control in Buildings, MNL 18, 176-182. American Society for Testing and Materials.

Cummings, J.B.; and J.J. Tooley, Jr. 1989. Infiltration and pressure differences induced by forced air systems in Florida residences. ASHRAE Transactions, 95 (2): 551-560.

Emmerich, S.J.; and A.K. Persily. 1996. Multizone Modeling of Three Residential Indoor Air Quality Control Options. National Institute of Standards and Technology, NISTIR 5801.

Hamlin, T.; and K. Cooper. 1991. The potential for residential demand controlled ventilation. Proceedings of 12th AIVC Conference, Air Movement & Ventilation Control within Buildings, 2: 235-243.

Hamlin, T.; and K. Cooper. 1993. CMHC residential indoor air quality - parametric study. Proceedings of 13th AIVC Conference, Ventilation for Energy Efficiency and Optimum Indoor Air Quality, 207-216.

Haskell, T. 1995. RCDP IV Final Report: Improved Air Distribution Systems for Forced-Air Heating. Bonneville Power Administration, Contract #DE-B179-94BP31124.

Hekmat, D.; H.E. Feustel; and M.P. Modera. 1986. Impacts of ventilation strategies on energy consumption and indoor air quality in single-family residences. Energy and Buildings, 9 (3): 239-251.

Jones, R. 1995. Indoor humidity calculation procedures. Building Services Engineering Research and Technology, 16 (3): 119-126.

Kerestecioglu, A.; M. Swami; and A. Kamel. 1990. Theoretical and computational investigation of simultaneous heat and moisture transfer in buildings: "effective penetration depth" theory. ASHRAE Transactions, 96 (1): 447-454.

Klote, J.H. and J.A. Milke. 1992. Design of Smoke Management Systems. American Society of Heating, Refrigerating and Air-Conditioning Engineers, Inc.

Lambert, L.A.; and D.H. Robison. 1989. Effects of ducted forced-air heating systems on residential air leakage and heating energy use. ASHRAE Transactions, 95 (2): 534-541.

Lubliner, M.; D.T. Stevens; and B. Davis. 1997. Mechanical ventilation in HUD-code manufactured housing in the Pacific northwest. ASHRAE Transactions, 103 (1): 693-705.

Lubliner, M. 1998. Personal communication.

Mansson, L.-G. 1995. Evaluation and Demonstration of Domestic Ventilation. State of the Art. Swedish Council for Building Research, Report A12:1995.

Marion, W.; and K. Urban. 1995. User's Manual for TMY2s, Typical Meteorological Years, Derived from the 1961-1990 National Solar Radiation Data Base. National Renewable Energy Laboratory, NREL/SP-463-7668, E95004064.

Matson, N.E.; and H.E. Feustel. 1997. Residential Ventilation Systems. Lawrence Berkeley National Laboratory, LBL-40859.

Millet, J.-R.; J.G. Villenave; and J. Riberon. 1996. French ventilation system performances in residential buildings. Proceedings of 17th Air Infiltration and Ventilation Centre Conference, Optimum Ventilation and Air Flow Control in Buildings, 1: 167-173.

Modera, M.P. 1989. Residential duct system leakage: magnitude, impacts, and potential for reduction. ASHRAE Transactions, 95 (2): 561-569.

Mueller, E.A. 1989. Indoor Air Quality Environmental Information Handbook: Combustion Sources. 1989 Update. U.S. Department of Energy, DOE/EH/79079-H1.

Olson, J.R.; L. Palmiter; B. Davis; M. Geffon; and T. Bond. 1993. Field Measurements of the Heating Efficiency of Electric Forced-Air Systems in 24 Homes. Ecotope, Inc.

Palmiter, L.S.; I.A. Brown; and T.C. Bond. 1991. Measured infiltration and ventilation in 472 all-electric homes. ASHRAE Transactions, 97 (2): 979-987.

Parker, D.S. 1989. Evidence of increased levels of space heat consumption and air leakage associated with forced air heating systems in houses in the Pacific northwest. ASHRAE Transactions, 95 (2): 527-533.

Persily, A.K. 1997. Evaluating building IAQ and ventilation with indoor carbon dioxide. ASHRAE Transactions, 103 (2): 193-204.

Robison, D.H.; and L.A. Lambert. 1989. Field investigation of residential infiltration and heating duct leakage. ASHRAE Transactions, 95 (2): 542-543.

Roulet, C.-A.; and L. Vandaele. 1991. Air flow patterns within buildings measurement techniques. Air Infiltration and Ventilation Centre, Technical Note AIVC 34.

Sandberg, M. 1983. Ventilation efficiency as a guide to design. ASHRAE Transactions, 89 (2B): 455-477.

Sherman, M.; and D. Dickeroff. 1994. Air-tightness of U.S. dwellings. Proceedings of 15th AIVC Conference, The Role of Ventilation, 225-234.

Sibbitt, B.E.; and T.L. Hamlin. 1991. Meeting Canadian residential ventilation standard requirements with low-cost systems. ASHRAE Transactions, 97 (2): 969-978.

TenWolde, A. 1994. Ventilation, humidity, and condensation in manufactured houses during winter. ASHRAE Transactions, 100 (1): 103-115.

Thomas, W.C.; and D.M. Burch. 1990. Experimental validation of a mathematical model for predicting water vapor sorption at interior building surfaces. ASHRAE Transactions, 96 (1): 487-496.

Walton, G.N. 1997. CONTAM96 users manual. National Institute of Standards and Technology, NISTIR 6056.

Yuill, G.K.; and M.R. Jeanson. 1990. An analysis of several strategies for four ventilation systems. Proceedings of 5th International Conference on Indoor Air Quality and Climate, 4: 341-346.

Yuill, G.K.; M.R. Jeanson; and C.P. Wray. 1991. Simulated performance of demand-controlled ventilation systems using carbon dioxide as an occupancy indicator. ASHRAE Transactions, 97 (2): 963-968.

TABLE 1.
Floor Areas and Volumes of House Zones

	Floor area m^2 (ft^2)	Volume m^3 (ft^3)
Ground Level		
Crawl Space (CS)	90.5 (974)	90.5 (3200)
Garage (GAR)	54.3 (584)	184.6 (6520)
First Floor		
Kitchen/family area (KFA)	30.8 (332)	73.9 (2610)
Dining room (DR)	17.0 (183)	40.8 (1440)
Living room (LR)	25.0 (269)	60.0 (2120)
Utility closet (UCL)	2.2 (24)	5.3 (190)
Bathroom #3 (BA3)	3.6 (39)	8.6 (300)
Closet (CLO)	4.7 (51)	11.3 (400)
Entrance (ENTR)	7.9 (85)	19.0 (670)
Second Floor		
Bedroom #2 (BR2)	13.5 (145)	32.4 (1140)
Bedroom #3 (BR3)	11.8 (127)	28.3 (1000)
Bedroom #4 (BR4)	11.8 (127)	28.3 (1000)
Master bedroom (MBR)	27.4 (295)	65.8 (2330)
Hallway (HAL)	12.8 (138)	30.7 (1080)
Master bathroom (MBA)	4.3 (46)	10.3 (360)
Bathroom #2 (BA2)	4.1 (44)	9.8 (350)
Master bedroom closet (MCLO)	8.7 (94)	20.9 (740)
Attic Level		
Attic (ATC)	94.4 (1016)	92.5 (3269)
Totals		
First Floor	91.2 (982)	218.9 (7730)
Second Floor	94.4 (1016)	226.5 (8000)
Living area	185.6 (1998)	445.4 (15740)
Living area, plus crawl space, attic and garage	424.8 (4573)	813.0 (28,730)

TABLE 2.
Contaminant Generation Rates Associated with Cooking

Time of day	Carbon monoxide (CO)	Nitrogen dioxide (NO_2)	Fine particles (Diameter < 2.5 μm)
Weekdays			
6:30-7:30 a.m.	210 (1.7×10^{-3})	28 (2.2×10^{-4})	0.028 (2.2×10^{-7})
17-17:30 p.m.	420 (3.3×10^{-3})	56 (4.4×10^{-4})	0.056 (4.4×10^{-7})
17:30-18 p.m.	830 (6.6×10^{-3})	111 (8.8×10^{-4})	0.111 (8.8×10^{-7})
Weekends			
9:30-10 a.m.	210 (1.7×10^{-3})	28 (2.2×10^{-4})	0.028 (2.2×10^{-7})
11:30 a.m.-12:30 p.m.	420 (3.3×10^{-3})	56 (4.4×10^{-4})	0.056 (4.4×10^{-7})
17-17:30 p.m.	420 (3.3×10^{-3})	56 (4.4×10^{-4})	0.056 (4.4×10^{-7})
17:30-18 p.m.	830 (6.6×10^{-3})	111 (8.8×10^{-4})	0.111 (8.8×10^{-7})

All generation rates are expressed in μg/s, with lb/h in parentheses.

TABLE 3.
Outdoor Contaminant Concentrations

Carbon monoxide and nitrogen dioxide

Time of day	CO	NO_2
Midnight - 7 a.m.	1.14 mg/m^3 (1.0 ppm(v))	37.6 µg/m^3 (20 ppb(v))
7-9 a.m.	2.28 mg/m^3 (2.0 ppm(v))	75.2 µg/m^3 (40 ppb(v))
9 a.m. - 5 p.m.	1.71 mg/m^3 (1.5 ppm(v))	37.6 µg/m^3 (20 ppb(v))
5 p.m. - 7 p.m.	3.42 mg/m^3 (3.0 ppm(v))	75.2 µg/m^3 (40 ppb(v)))
7 p.m. - midnight.	1.71 mg/m^3 (1.5 ppm(v))	37.6 µg/m^3 (20 ppb(v))

Carbon dioxide
Constant value of 630 mg/m^3 (350 ppm(v)).

Fine particles
Constant value of 13 µg/m^3.

Coarse particles
Constant value of 75 µg/m^3.

Volatile organic compounds
Constant value of 100 µg/m^3.

TABLE 4.
Summary of Climatic Variables for Spokane, Washington

Month	Outdoor temperature °C (°F)	Wind speed m/s (mph)	Humidity ratio (g/kg)	Relative humidity (%)
January	-2.8 (26.9)	4.6 (10.3)	2.9	87
February	0.6 (33.0)	4.6 (10.3)	3.2	77
March	4.3 (39.7)	4.6 (10.3)	3.6	70
April	7.2 (44.9)	4.5 (10.1)	4.4	70
May	11.7 (53.0)	4.0 (8.9)	5.3	65
June	16.3 (61.3)	4.7 (10.5)	6.1	56
July	21.8 (71.2)	3.9 (8.7)	6.4	43
August	19.3 (66.7)	3.9 (8.7)	6.6	52
September	14.9 (58.9)	4.5 (10.1)	5.5	58
October	8.0 (46.5)	4.2 (9.4)	5.0	76
November	1.7 (35.1)	4.7 (10.5)	4.0	90
December	-1.0 (30.2)	3.9 (8.7)	3.4	91
Annual	8.5 (47.4)	4.3 (9.6)	4.7	70

TABLE 5.
Summary of Monthly Air Change Rates

Month	Air change rates, h^{-1} (Percentage of rates < 0.35 h^{-1})				
	Case #1	Case #2	Case #3	Case #4	Case #5
January	0.31 (64)	0.43 (15)	0.58 (0)	0.62 (0)	0.41 (44)
February	0.27 (77)	0.38 (55)	0.53 (4)	0.58 (0)	0.38 (57)
March	0.24 (86)	0.33 (72)	0.48 (18)	0.53 (28)	0.36 (69)
April	0.22 (89)	0.29 (81)	0.43 (37)	0.49 (51)	0.34 (75)
May	0.18 (96)	0.26 (85)	0.39 (50)	0.46 (58)	0.32 (82)
June	0.17 (92)	0.25 (83)	0.38 (47)	0.45 (54)	0.31 (78)
July	0.13 (99)	0.27 (85)	0.38 (47)	0.49 (47)	0.30 (84)
August	0.14 (98)	0.25 (87)	0.37 (52)	0.46 (56)	0.30 (85)
September	0.18 (92)	0.24 (86)	0.37 (48)	0.44 (57)	0.32 (77)
October	0.20 (96)	0.28 (84)	0.41 (42)	0.48 (57)	0.33 (82)
November	0.27 (78)	0.36 (64)	0.50 (14)	0.55 (21)	0.38 (59)
December	0.27 (86)	0.37 (59)	0.52 (2)	0.57 (0)	0.38 (61)
ANNUAL					
Mean	0.22	0.31	0.44	0.51	0.34
Std Dev	0.09	0.11	0.16	0.24	0.10
SD/Mean	0.41	0.34	0.36	0.47	0.29
Median	0.21	0.29	0.42	0.41	0.32
% of hours < 0.35 h^{-1}	88	71	30	36	71
% of hours > 0.70 h^{-1}	0	0	11	34	0

TABLE 6.
Mean Monthly Ages of Air

ZONES	LR	DR	KFA	BR4	BR3	BR2	MBR	First Floor	Second Floor
Case #2									
January	2.7	2.6	2.8	3.7	4.0	3.8	3.9	2.7	3.8
February	3.0	2.8	3.0	4.1	4.5	4.2	4.3	2.9	4.3
March	3.1	3.3	3.4	4.6	5.2	4.8	5.0	3.3	4.9
April	3.6	3.7	3.9	5.4	6.2	5.6	5.8	3.7	5.8
May	4.5	4.7	4.7	6.4	7.5	6.6	6.8	4.6	6.8
June	5.1	5.6	5.2	6.7	8.0	6.8	7.4	5.2	7.6
July	6.6	7.5	6.4	6.7	8.7	7.4	7.7	6.7	7.6
August	6.7	6.8	6.1	6.9	8.7	7.6	8.5	6.5	8.1
September	5.4	5.6	5.1	6.4	7.7	7.0	7.5	5.3	7.2
October	4.0	4.1	3.9	5.4	6.4	5.9	6.1	4.0	6.0
November	2.9	2.9	3.0	4.3	4.8	4.5	4.6	3.0	4.6
December	2.9	2.8	2.9	4.3	4.6	4.3	4.4	2.9	4.4
Case #3									
January	1.6	1.8	2.2	2.7	2.8	2.7	2.6	1.9	2.7
February	1.6	1.9	2.3	2.9	3.1	3.0	2.8	2.0	2.9
March	1.7	2.2	2.5	3.2	3.5	3.4	3.1	2.2	3.2
April	1.8	2.5	2.9	3.6	3.9	3.7	3.4	2.4	3.6
May	2.2	2.9	3.4	4.1	4.5	4.0	3.8	2.9	4.1
June	2.4	3.3	3.7	4.1	4.5	4.0	3.8	3.2	4.0
July	3.5	4.5	4.4	4.0	4.5	4.2	4.2	4.1	4.2
August	3.2	3.9	4.1	3.9	4.4	4.3	4.3	3.8	4.2
September	2.6	3.3	3.6	3.8	4.2	4.3	4.0	3.2	4.0
October	2.1	2.7	2.9	3.5	3.9	4.1	3.6	2.6	3.7
November	1.6	2.0	2.3	3.1	3.3	3.3	2.9	2.0	3.1
December	1.7	1.9	2.3	2.9	3.1	3.1	2.8	2.0	3.0
Case #4									
January	2.2	2.1	2.2	2.8	3.0	2.9	3.0	2.2	2.9
February	2.3	2.2	2.4	3.1	3.4	3.2	3.3	2.3	3.3
March	2.6	2.6	2.7	3.5	3.9	3.6	3.8	2.7	3.8
April	2.9	3.0	3.2	4.1	4.6	4.2	4.4	3.1	4.3
May	3.6	3.7	3.8	4.8	5.5	4.9	5.1	3.7	5.1
June	3.9	4.1	3.9	4.9	5.7	4.8	5.3	4.0	5.2
July	4.8	5.3	4.5	4.8	6.1	5.2	5.5	4.8	5.4
August	4.6	4.7	4.4	4.9	5.8	5.0	5.6	4.5	5.4
September	4.1	4.2	3.9	4.7	5.5	5.0	5.4	4.0	5.2
October	3.2	3.2	3.1	4.1	4.8	4.5	4.6	3.2	4.5
November	2.4	2.4	2.5	3.3	3.6	3.5	3.5	2.4	3.5
December	2.4	2.2	2.4	3.2	3.4	3.3	3.3	2.3	3.3
Case #5									
January	2.2	2.2	2.6	4.0	4.7	4.1	2.9	2.4	3.7
February	2.8	2.3	2.7	4.4	5.4	4.5	3.1	2.5	4.0
March	2.4	2.5	3.0	5.0	6.4	4.9	3.2	2.6	4.5
April	2.5	2.5	3.2	5.3	7.1	5.3	3.4	2.8	4.8
May	2.8	2.8	3.6	5.8	7.8	5.0	3.8	3.1	5.2
June	3.1	3.3	4.0	5.7	7.5	4.9	3.9	3.5	5.1
July	4.2	4.3	5.1	4.9	5.9	4.3	4.3	4.6	4.7
August	3.9	3.8	4.6	4.9	6.5	4.8	4.4	4.2	4.9
September	3.3	3.2	3.9	5.0	6.9	5.0	3.8	3.5	4.8
October	2.7	2.7	3.3	5.0	7.0	5.7	3.6	2.9	4.9
November	2.3	2.3	2.8	4.4	5.6	4.7	3.1	2.5	4.1
December	2.3	2.3	2.7	4.2	5.2	4.6	3.1	2.5	4.0

TABLE 7.
Calculated Energy Consumption

	Heating	%*	Cooling	%*	Fans Forced-air	Kitchen	Bathrooms	Total	%*	TOTAL
Case #1	6750	99	50	1						6800
Case #2	9220	67	90	1	4280	160	40	4480	32	13790
Case #3	13060	72	110	1	4280	160	590	5030	28	18200
Case #4	14580	60	120	0	8740	160	590	9490	39	24190
Case #5	9740	63	100	1	4280	160	1210	5650	36	15490
Case #6	9430	99	110	1						9540

Energy in units of MJ.

	Heating	%*	Cooling	%*	Fans Forced-air	Kitchen	Bathrooms	Total	%*	TOTAL
Case #1	1880	99	10	1						1890
Case #2	2560	67	20	1	1190	50	10	1250	33	3830
Case #3	3630	72	30	1	1190	50	160	1400	28	5060
Case #4	4050	60	30	0	2430	50	160	2640	39	6720
Case #5	2700	63	30	1	1190	50	330	1570	37	4300
Case #6	2620	99	30	1						2650

Energy in units of kWh.

* Percentage of TOTAL energy consumption.

TABLE 8.
Concentration Summary for Case #2

MONTH	VOC, mg/m3	CO, mg/m3			NO_2, mg/m3			RH, %	Percent of	CO_2, mg/m3
	Living area	KFA	LR	Bedrooms	KFA	LR	Bedrooms	House	hours < 30%	Bedrooms
January	1.03	2.6	2.2	2.3	660	120	170	24	95	2500
February	1.13	2.7	2.2	2.3	690	120	170	28	80	2710
March	1.23	2.8	2.2	2.4	760	100	150	29	65	3000
April	1.37	3.0	2.2	2.4	780	90	120	35	0	3440
May	1.55	3.1	2.3	2.5	780	90	120	40	0	3730
June	1.65	3.2	2.4	2.6	780	80	120	37	1	3940
July	1.64	3.0	2.6	2.6	690	120	160	29	63	3400
August	1.72	3.1	2.5	2.6	750	110	150	31	32	3630
September	1.68	3.5	2.3	2.5	860	60	80	42	0	4400
October	1.47	3.0	2.3	2.4	780	90	120	43	0	3510
November	1.17	2.8	2.2	2.3	750	100	150	34	17	2900
December	1.14	2.7	2.2	2.3	690	120	170	31	48	2750
ANNUAL										
Mean	1.40	3.0	2.3	2.4	750	100	140	34	33	3330
Std Dev	0.31	1.9	0.8	0.9	50	20	30	7		610
SD/Mean	0.22	0.64	0.33	0.36	0.07	0.20	0.21	0.20		0.18

TABLE 9.
Concentration Summary for Case #3

MONTH	VOC, mg/m³ Living area	CO, mg/m³ KFA	CO, mg/m³ LR	CO, mg/m³ Bedrooms	NO_2, mg/m³ KFA	NO_2, mg/m³ LR	NO_2, mg/m³ Bedrooms	RH, % House	Percent of hours < 30%	CO_2, mg/m³ Bedrooms
January	0.75	2.4	1.9	2.1	660	110	160	22	99	2040
February	0.80	2.5	2.0	2.1	690	100	160	25	94	2210
March	0.86	2.6	1.9	2.1	760	100	150	26	82	2390
April	0.92	2.7	1.9	2.1	780	80	130	33	21	2710
May	1.02	2.7	2.0	2.2	780	80	130	38	2	2940
June	1.07	2.8	2.0	2.2	780	80	120	37	1	3120
July	1.16	2.7	2.2	2.3	680	120	150	32	28	2870
August	1.16	2.7	2.1	2.2	750	100	140	34	11	2970
September	1.06	3.0	1.9	2.1	860	60	100	40	0	3390
October	0.98	2.7	1.9	2.1	780	80	130	39	0	2750
November	0.82	2.5	1.9	2.1	750	100	150	31	33	2310
December	0.82	2.5	2.0	2.1	690	110	160	28	69	2230
ANNUAL										
Mean	0.95	2.6	2.0	2.1	750	90	140	32	36	2660
Std Dev	0.22	1.9	0.6	0.8	50	20	20	7		460
SD/Mean	0.23	0.70	0.31	0.36	0.07	0.17	0.14	0.21		0.17

TABLE 10.
Concentration Summary for Case #4

MONTH	VOC, mg/m3	CO, mg/m3			NO_2, mg/m3			RH, %	Percent of	CO_2, mg/m3
	Living area	KFA	LR	Bedrooms	KFA	LR	Bedrooms	House	hours < 30%	Bedrooms
January	0.77	2.4	2.0	2.0	670	120	150	22	99	2020
February	0.82	2.4	2.0	2.0	690	120	150	25	94	2170
March	0.89	2.4	2.0	2.1	760	120	140	26	83	2390
April	0.97	2.5	2.0	2.1	790	110	140	33	17	2720
May	1.04	2.5	2.0	2.1	780	110	140	38	2	2900
June	1.06	2.5	2.1	2.1	780	110	140	30	56	3060
July	1.01	2.5	2.1	2.1	690	130	150	27	91	2540
August	1.06	2.5	2.1	2.1	760	120	140	28	77	2750
September	1.10	2.6	2.0	2.1	860	100	120	39	1	3600
October	1.01	2.5	2.0	2.1	780	110	140	39	0	2760
November	0.86	2.4	2.0	2.0	760	120	140	31	33	2330
December	0.84	2.4	2.0	2.1	700	130	150	28	68	2190
ANNUAL										
Mean	0.95	2.5	2.0	2.1	750	120	140	30	52	2620
Std Dev	0.20	1.7	0.7	0.7	50	10	10	6		460
SD/Mean	0.21	0.68	0.32	0.32	0.07	0.08	0.07	0.21		0.18

TABLE 11.
Concentration Summary for Case #5

MONTH	VOC, mg/m3	CO, mg/m3			NO_2, mg/m3			RH, %	Percent of	CO_2, mg/m3
	Living area	KFA	LR	Bedrooms	KFA	LR	Bedrooms	House	hours < 30%	Bedrooms
January	0.90	3	2	2	660	140	190	24	96	2570
February	0.94	3	2	2	680	130	180	27	86	2710
March	1.00	3	2	2	750	120	170	28	74	2910
April	1.05	3	2	2	780	100	140	34	4	3220
May	1.13	3	2	2	780	100	140	39	0	3310
June	1.18	3	2	2	780	100	140	37	1	3400
July	1.28	3	2	3	680	140	170	31	38	3120
August	1.25	3	2	2	750	120	160	34	16	3220
September	1.17	3	2	2	860	70	100	41	0	3650
October	1.09	3	2	2	780	100	140	40	0	3260
November	0.95	3	2	2	750	120	160	33	29	2840
December	0.95	3	2	2	680	130	180	29	57	2740
ANNUAL										
Mean	1.08	2.8	2.2	2.4	750	110	160	31	33	3080
Std Dev	0.16	1.9	0.8	0.9	60	20	20	6		390
SD/Mean	0.15	0.67	0.35	0.39	0.08	0.18	0.16	0.19		0.13

TABLE 12.
Concentration Summary for Case #6

MONTH	VOC, mg/m³ Living area	CO, mg/m³ KFA	CO, mg/m³ LR	CO, mg/m³ Bedrooms	NO_2, mg/m³ KFA	NO_2, mg/m³ LR	NO_2, mg/m³ Bedrooms	RH, % House	Percent of hours < 30%	CO_2, mg/m³ Bedrooms
January	--	--	--	--	--	--	--	29	63	--
February	--	--	--	--	--	--	--	32	28	--
March	--	--	--	--	--	--	--	33	34	--
April	--	--	--	--	--	--	--	38	0	--
May	--	--	--	--	--	--	--	43	0	--
June	--	--	--	--	--	--	--	41	0	--
July	--	--	--	--	--	--	--	36	2	--
August	--	--	--	--	--	--	--	39	1	--
September	--	--	--	--	--	--	--	44	0	--
October	--	--	--	--	--	--	--	44	0	--
November	--	--	--	--	--	--	--	37	8	--
December	--	--	--	--	--	--	--	34	23	--
ANNUAL										
Mean	0.97	2.7	2.6	2.6	410	280	290	38	13	2240
Std Dev	0.04	1.5	1.3	1.3	0	0	0	7		100
SD/Mean	0.04	0.54	0.51	0.51	0.01	0.00	0.00	0.17		0.04

TABLE 13.
Summary of Annual Occupant Exposure

Case/Contaminant	Male	Female	Child #1	Child #2	Child #3	Mean
#2/ CO	2.8	2.9	2.9	2.9	3.0	2.9
NO_2	50	76	68	69	83	69
VOC	1.47	1.43	1.42	1.45	1.45	1.44
CO_2	3170	2900	2590	2860	2880	2890
#3/ CO	2.3	2.6	2.5	2.5	2.6	2.5
NO_2	50	77	68	69	83	70
VOC	0.98	0.95	1.00	1.02	1.04	1.00
CO_2	2470	2270	2060	2290	2350	2290
#4/ CO	2.3	2.5	2.4	2.5	2.6	2.4
NO_2	48	72	69	71	86	69
VOC	1.01	0.98	0.95	0.95	0.96	0.97
CO_2	2400	2180	1880	2050	2100	2120
#5/ CO	2.6	2.8	2.8	2.9	2.9	2.8
NO_2	52	78	70	71	86	71
VOC	1.09	1.07	1.15	1.20	1.17	1.13
CO_2	2600	2400	2430	2740	2720	2580
#6/ CO	2.8	2.9	2.7	2.9	2.9	2.8
NO_2	56	69	67	69	77	67
VOC	0.99	0.99	0.97	0.97	0.98	0.98
CO_2	2080	1990	1920	1980	2000	1990

All exposures in units of mg/m^3 except for NO_2 which is in units of $\mu g/m^3$.

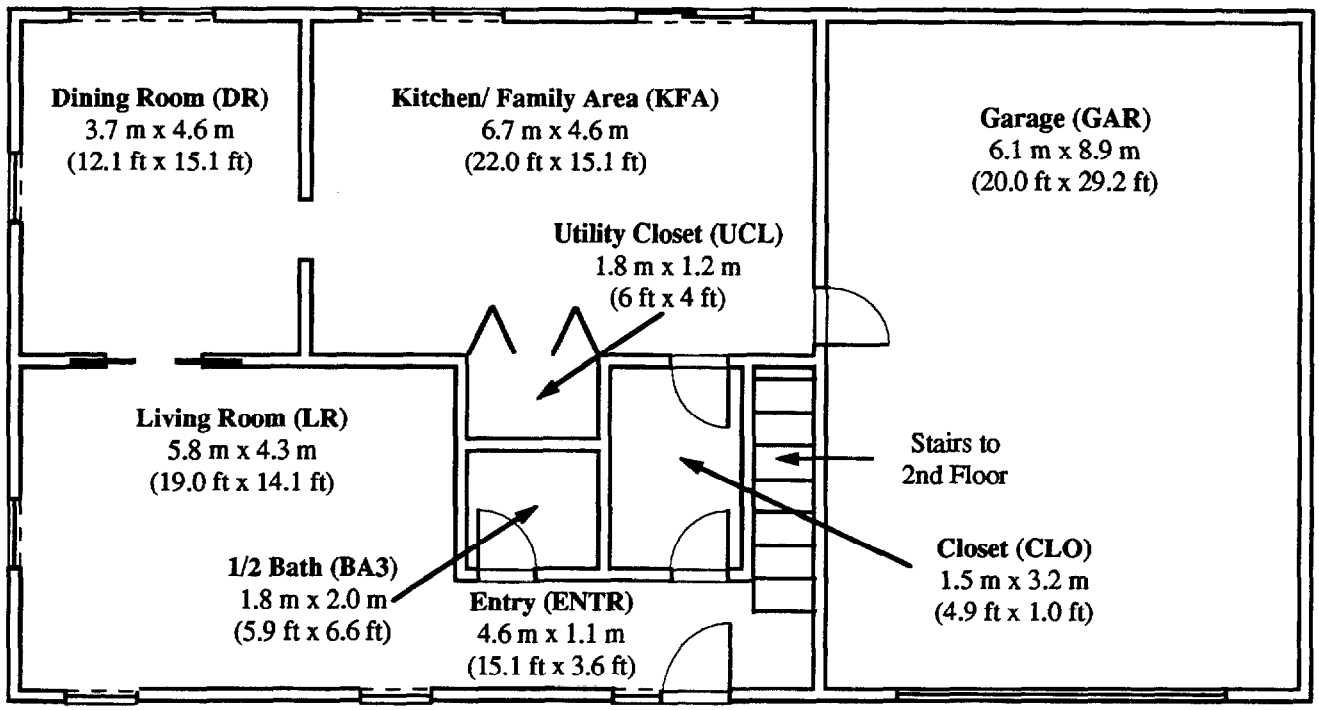

First Floor

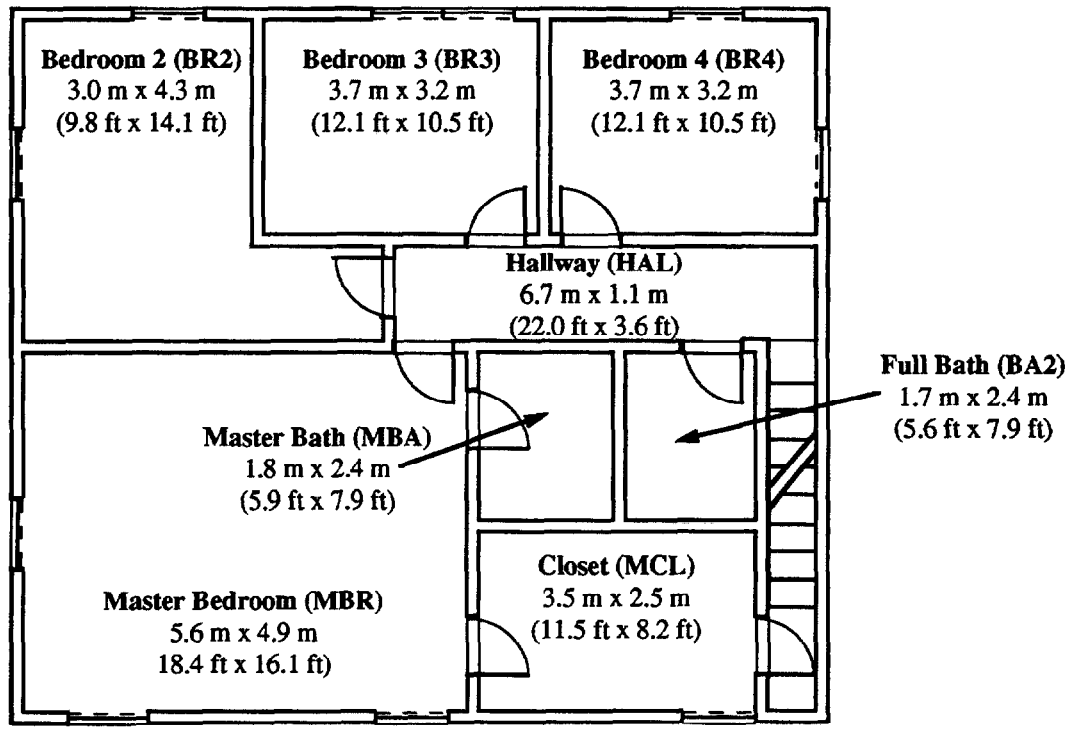

Second Floor

Figure 1 Layout of Living Space

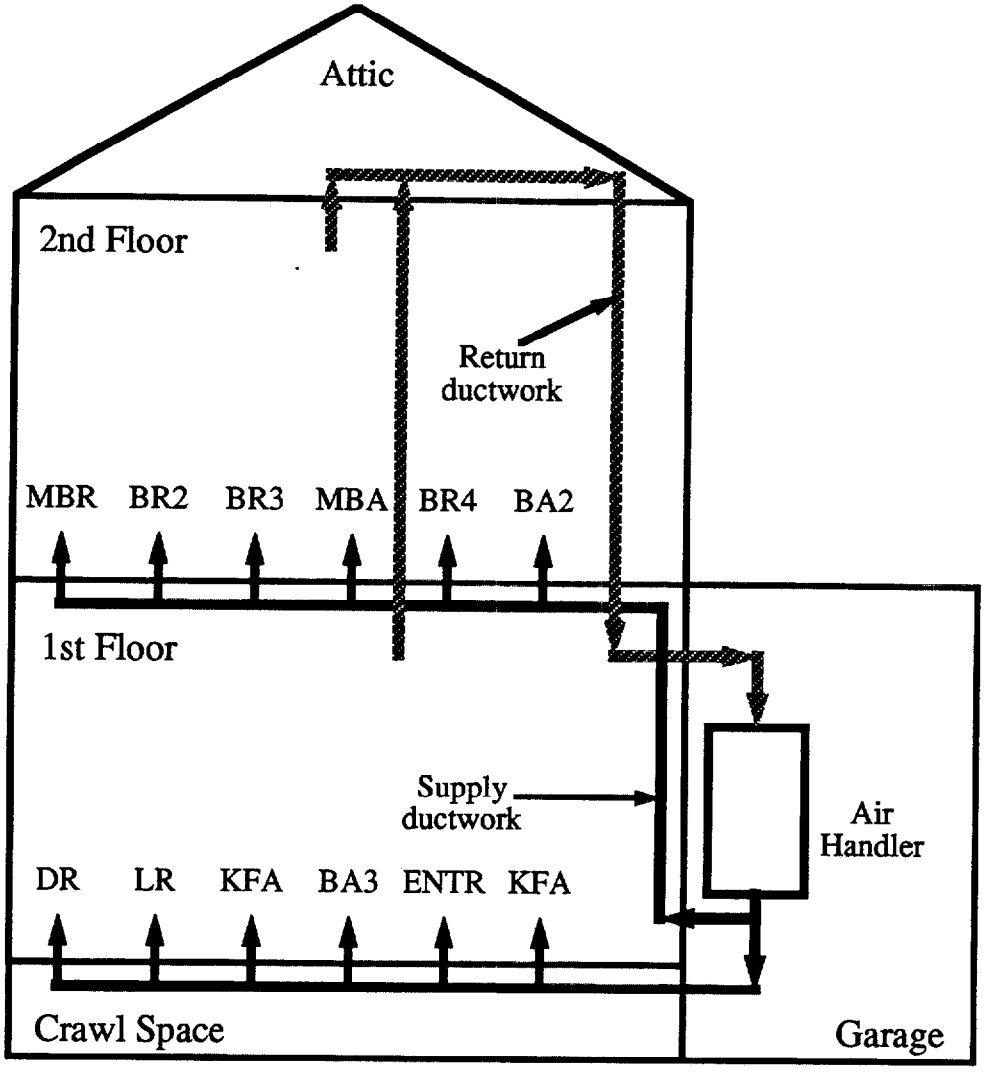

Figure 2 Schematic of Air Distribution Ductwork

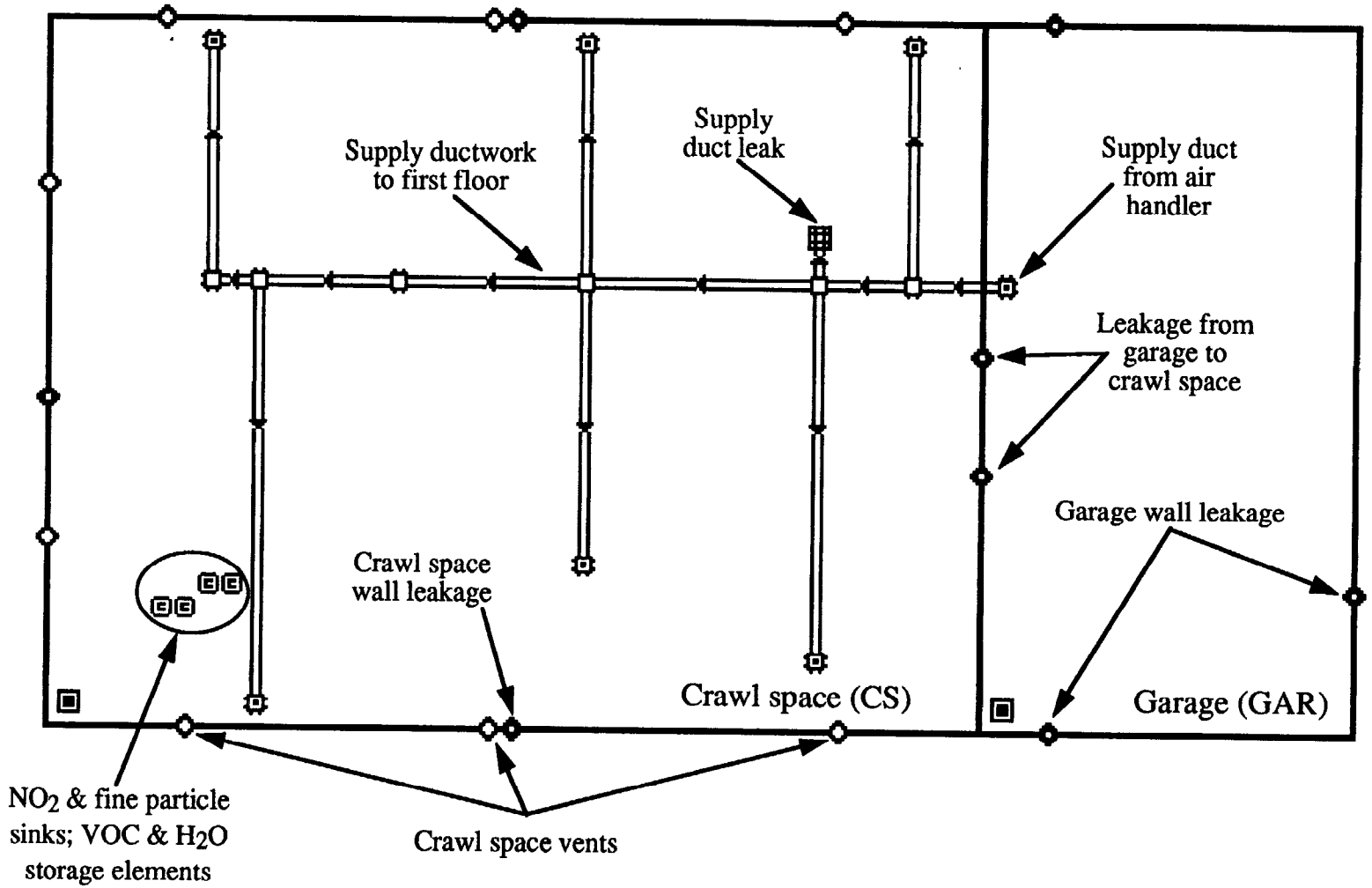

Figure 3 CONTAM Sketchpad of Ground Level

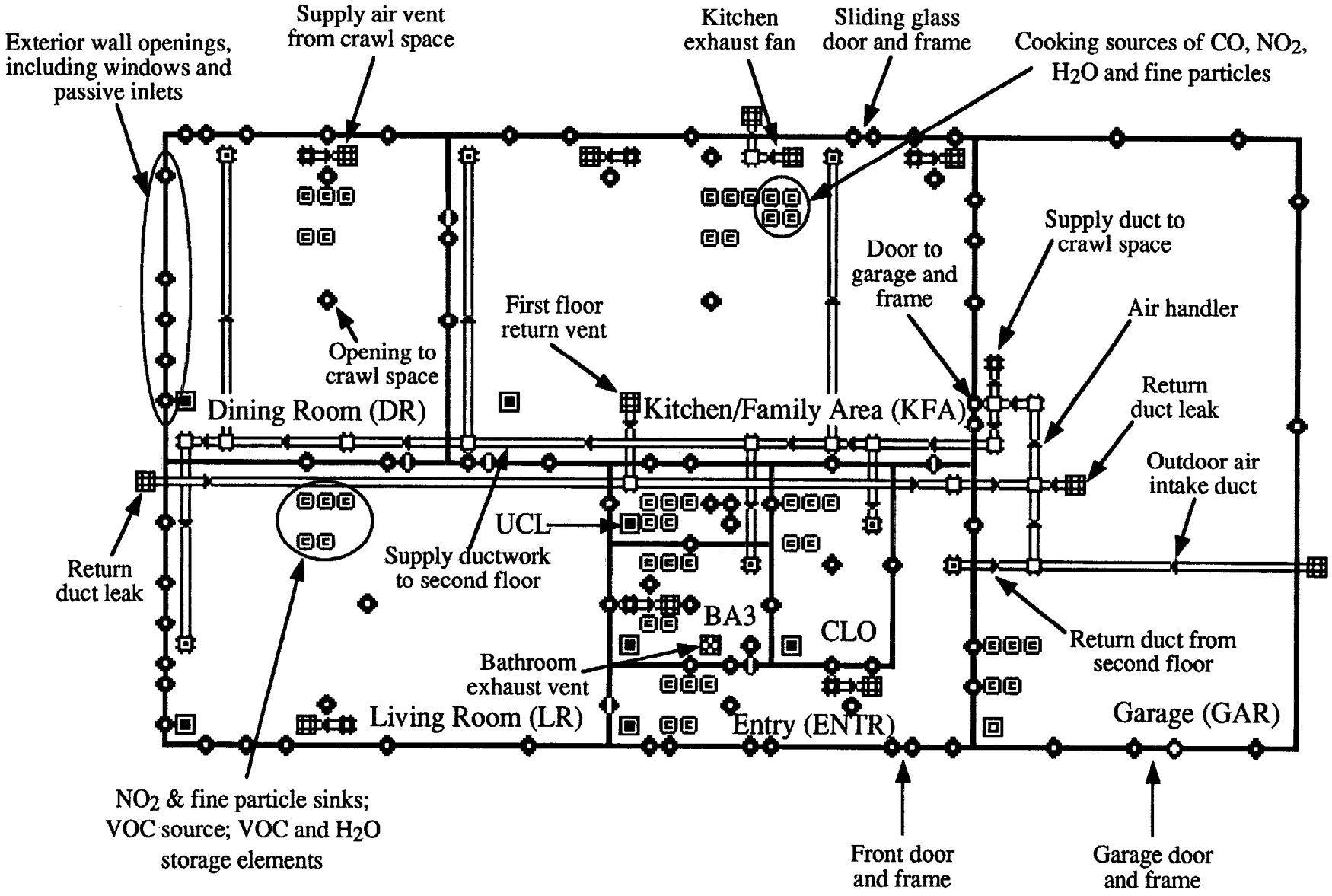

Figure 4 CONTAM Sketchpad of First Floor

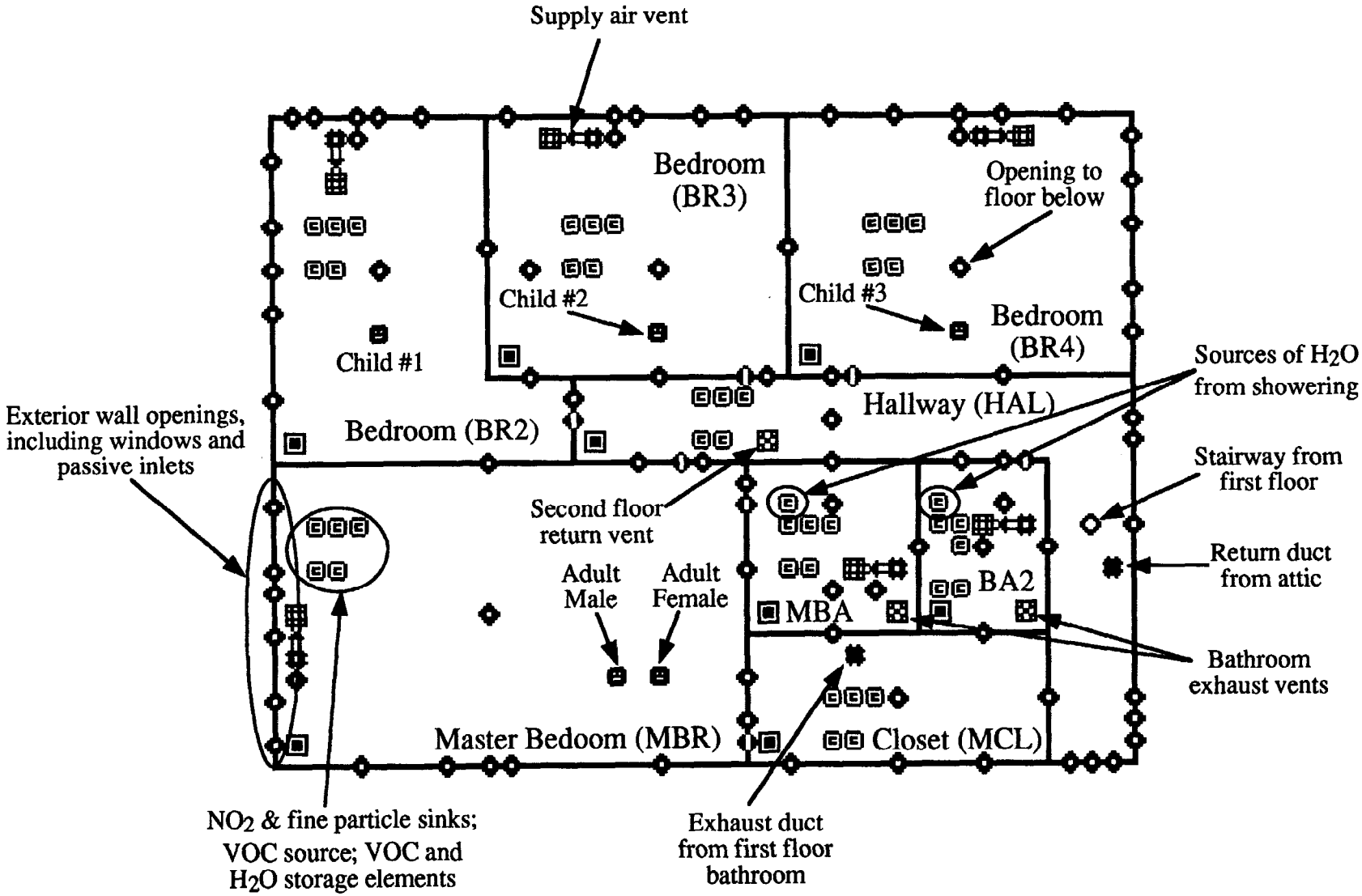

Figure 5 CONTAM Sketchpad of Second Floor

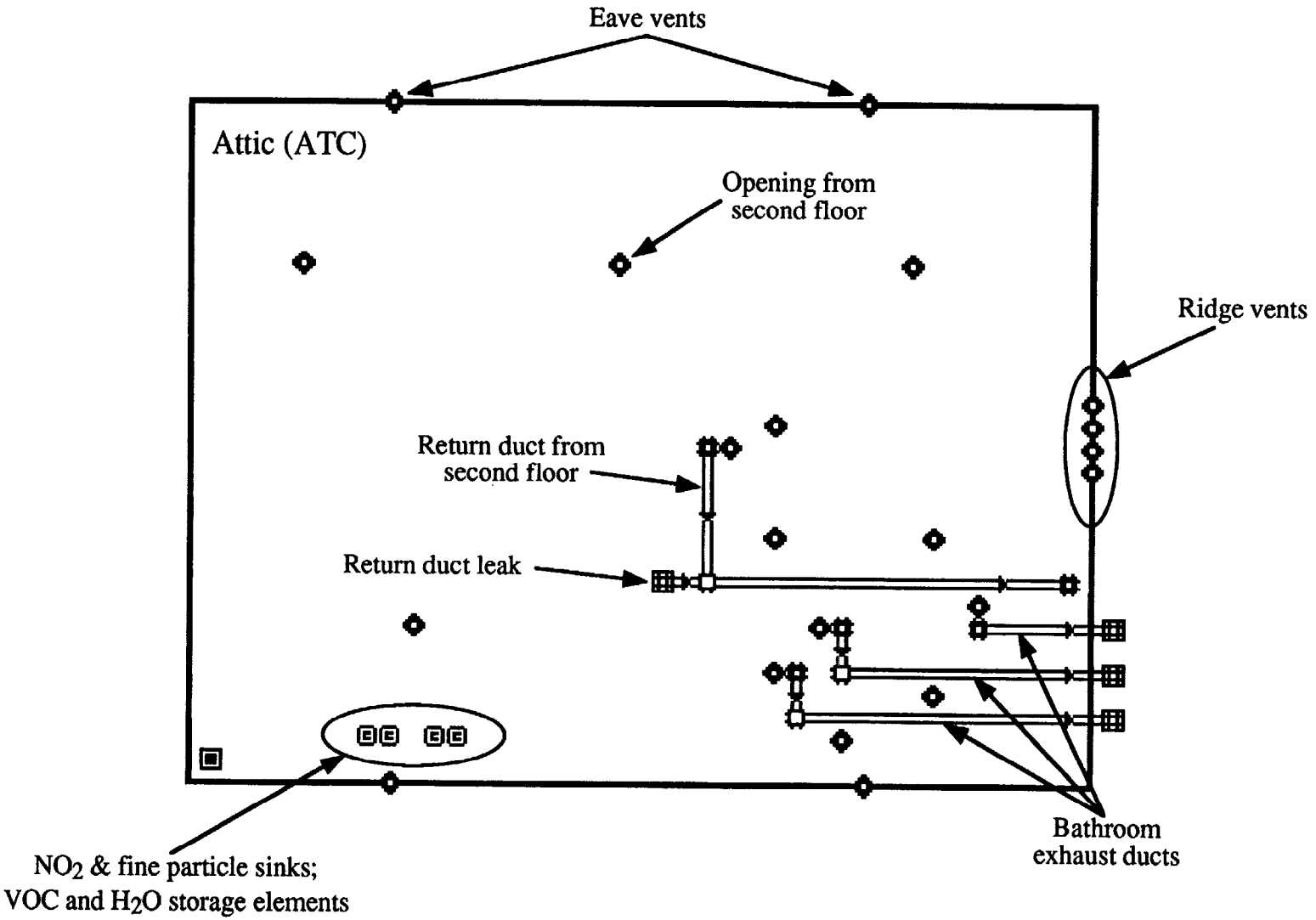

Figure 6 CONTAM Sketchpad of Attic

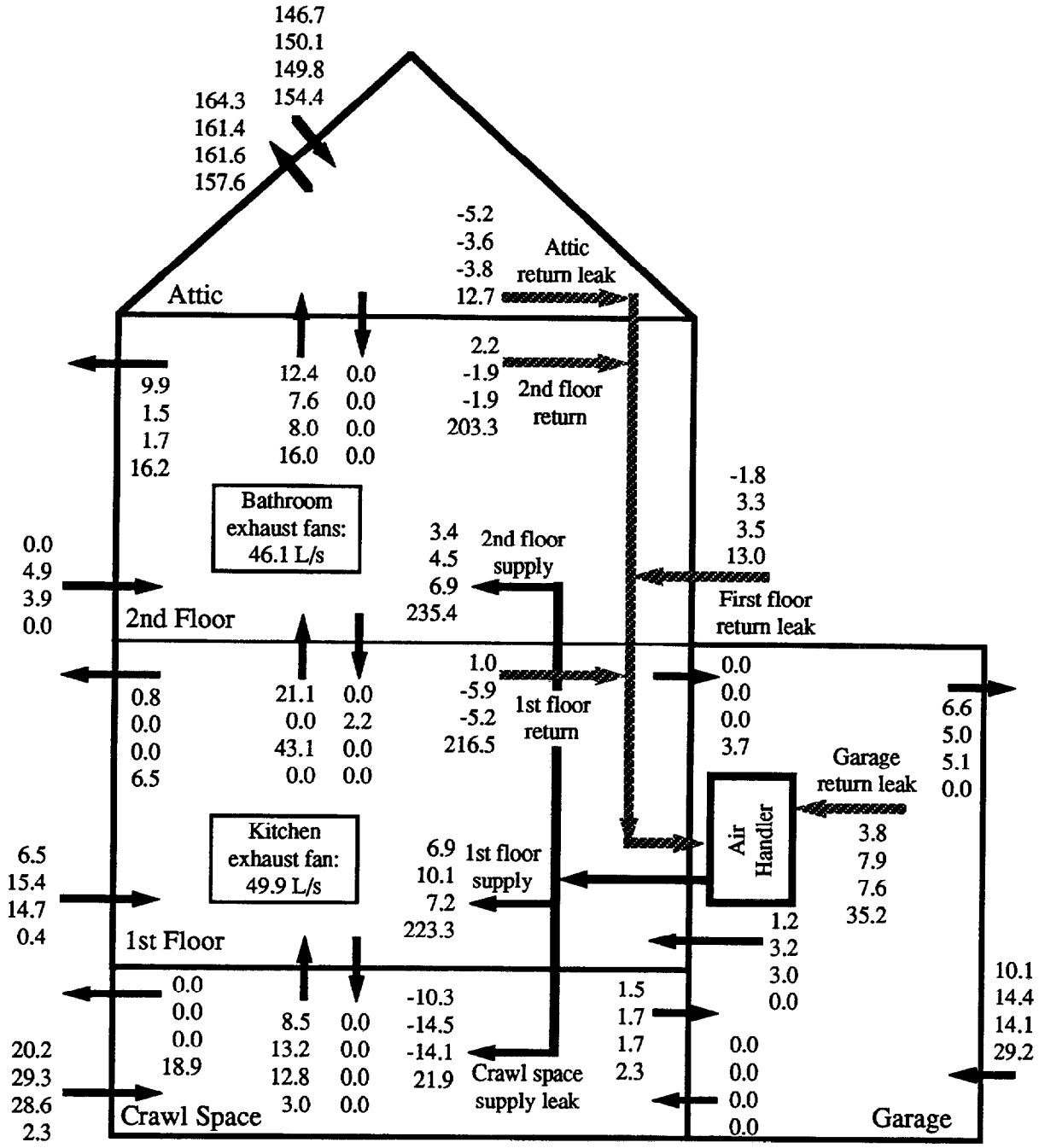

Cases
All fans off, all interior doors open.
Kitchen exhaust fan on.
Upstairs bathroom exhaust fans on; upstairs bathroom doors closed.
Forced-air fan on; all interior doors open.

All flows in standard L/s; multiply by 2.12 to obtain cfm.
Minus sign indicates that air flows in opposite direction of arrow.

Figure 7 Impacts of Fans on Interzone Airflow Patterns

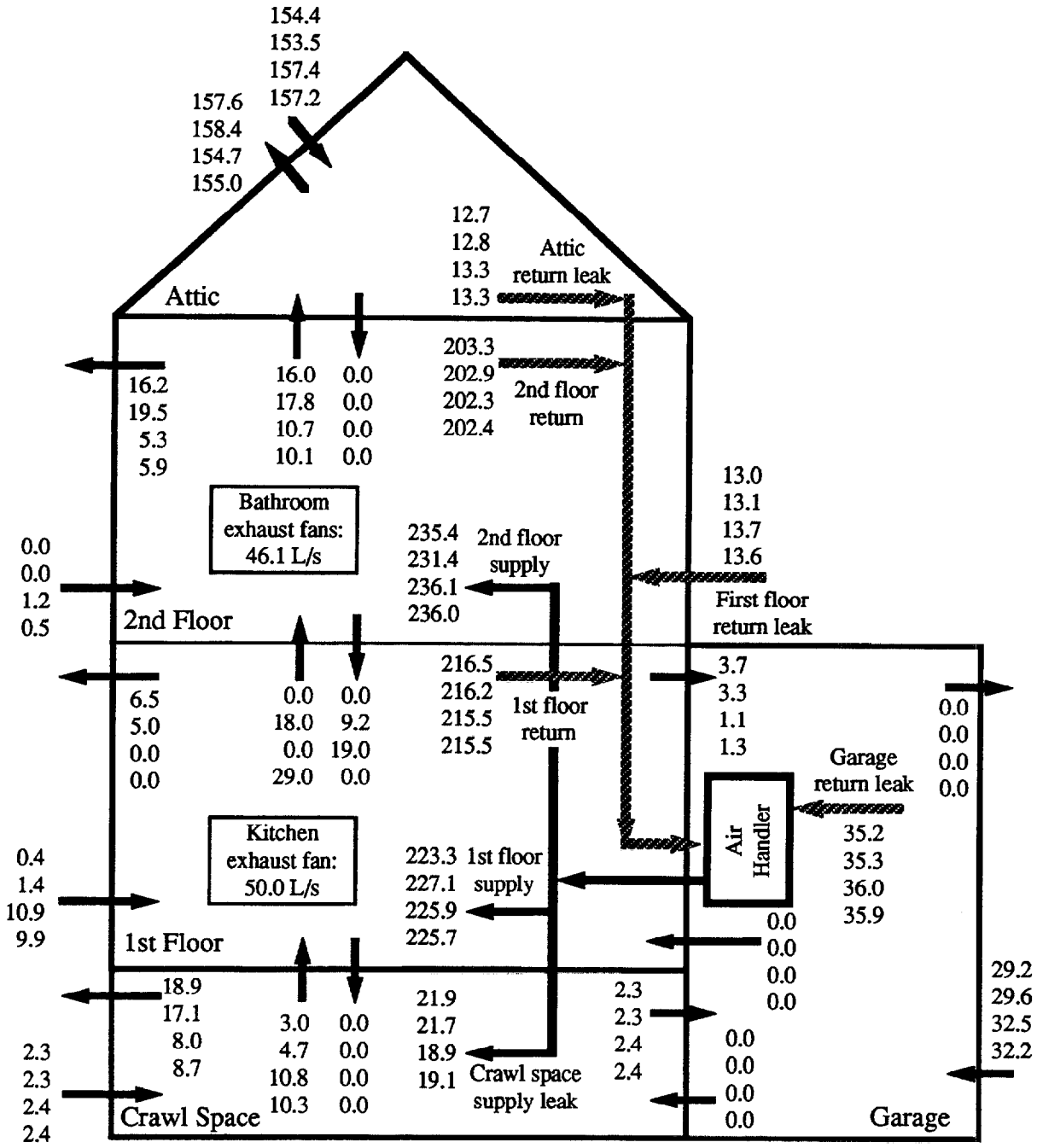

Cases
Forced-air fan on; all interior doors open.
Forced-air fan on; bedroom doors closed.
Kitchen exhaust fan on.
Upstairs bathroom exhaust fans on; upstairs bathroom doors closed.

All flows in standard L/s; multiply by 2.12 to obtain cfm.

Figure 8 Interzone Airflow Patterns with Forced-Air Fan On

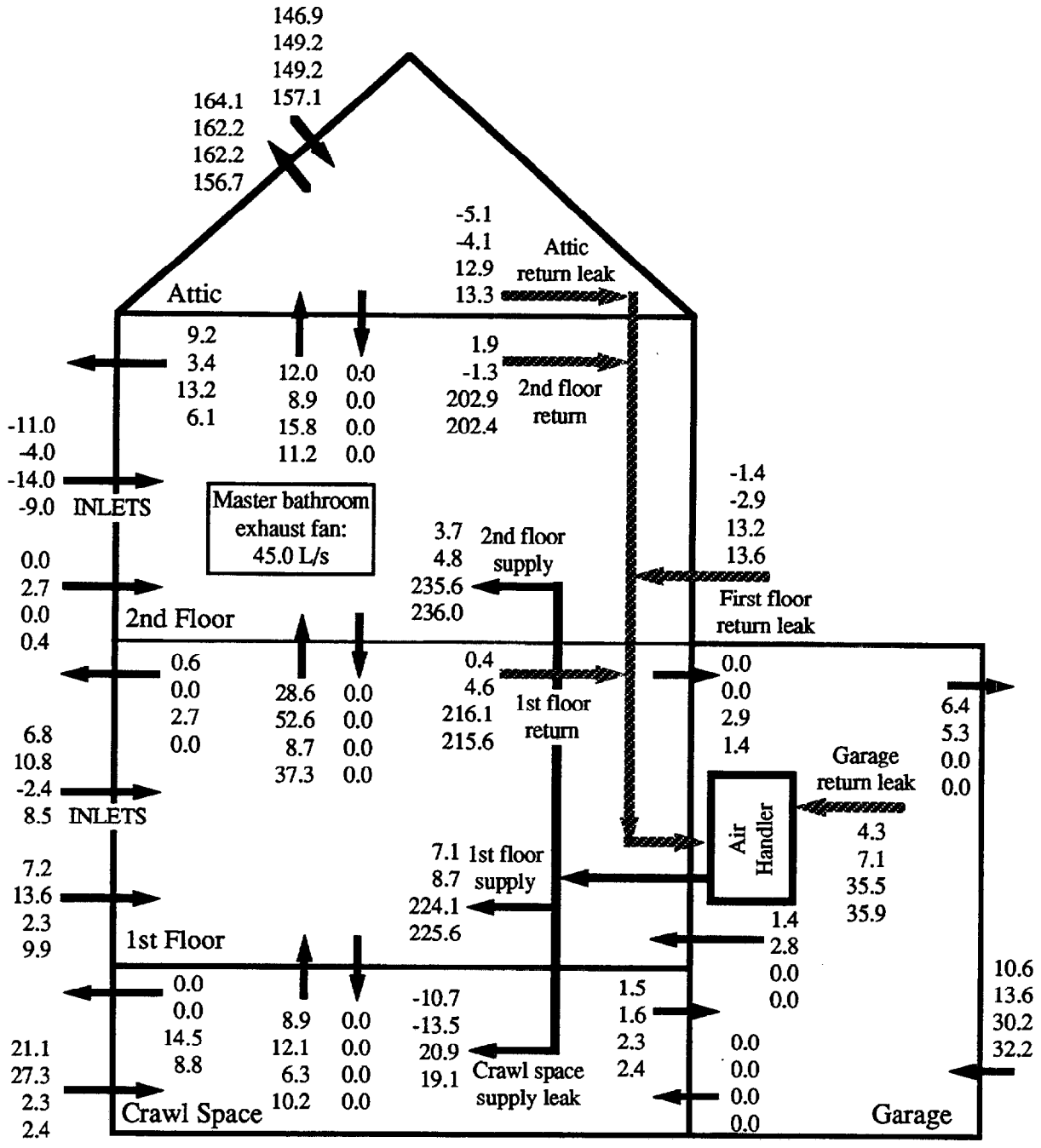

Cases
Forced-air fan off; all interior doors open.
Forced-air fan off; master bathroom exhaust fan on.
Forced-air fan on; all interior doors open.
Forced-air fan on; master bathroom exhaust fan on.

All flows in standard L/s; multiply by 2.12 to obtain cfm.
Minus sign indicates that air flows in opposite direction of arrow.

Figure 9 Interzone Airflow Patterns with Inlets Open

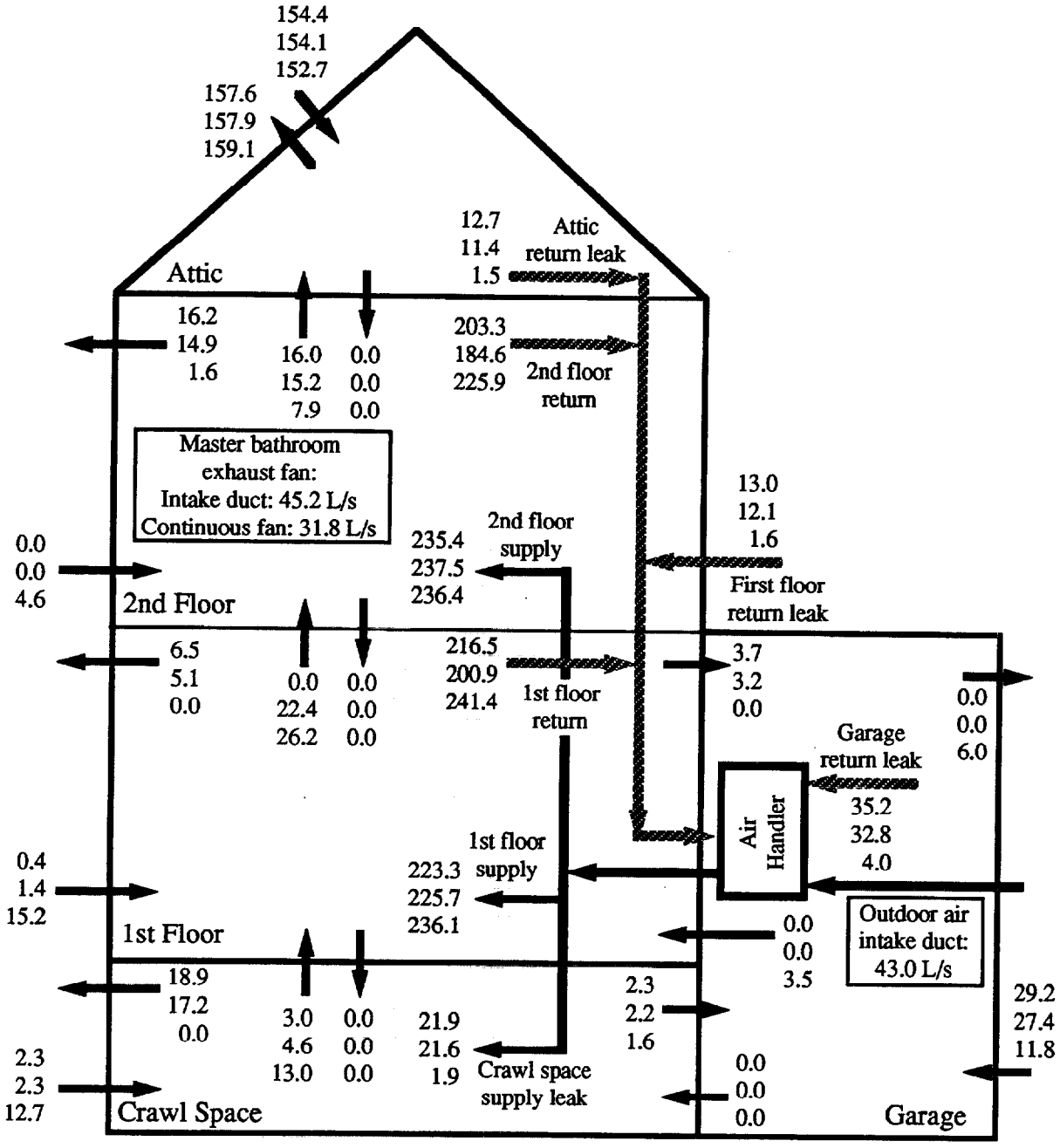

Cases
Forced-air fan on; all interior doors open.
Forced-air fan on; intake duct on furnace return.
Forced-air fan on; reduced duct leakage; continuous fan in master bathroom.

All flows in standard L/s; multiply by 2.12 to obtain cfm.
Minus sign indicates that air flows in opposite direction of arrow.

Figure 10 Interzone Airflow Patterns with Mechanical Ventilation

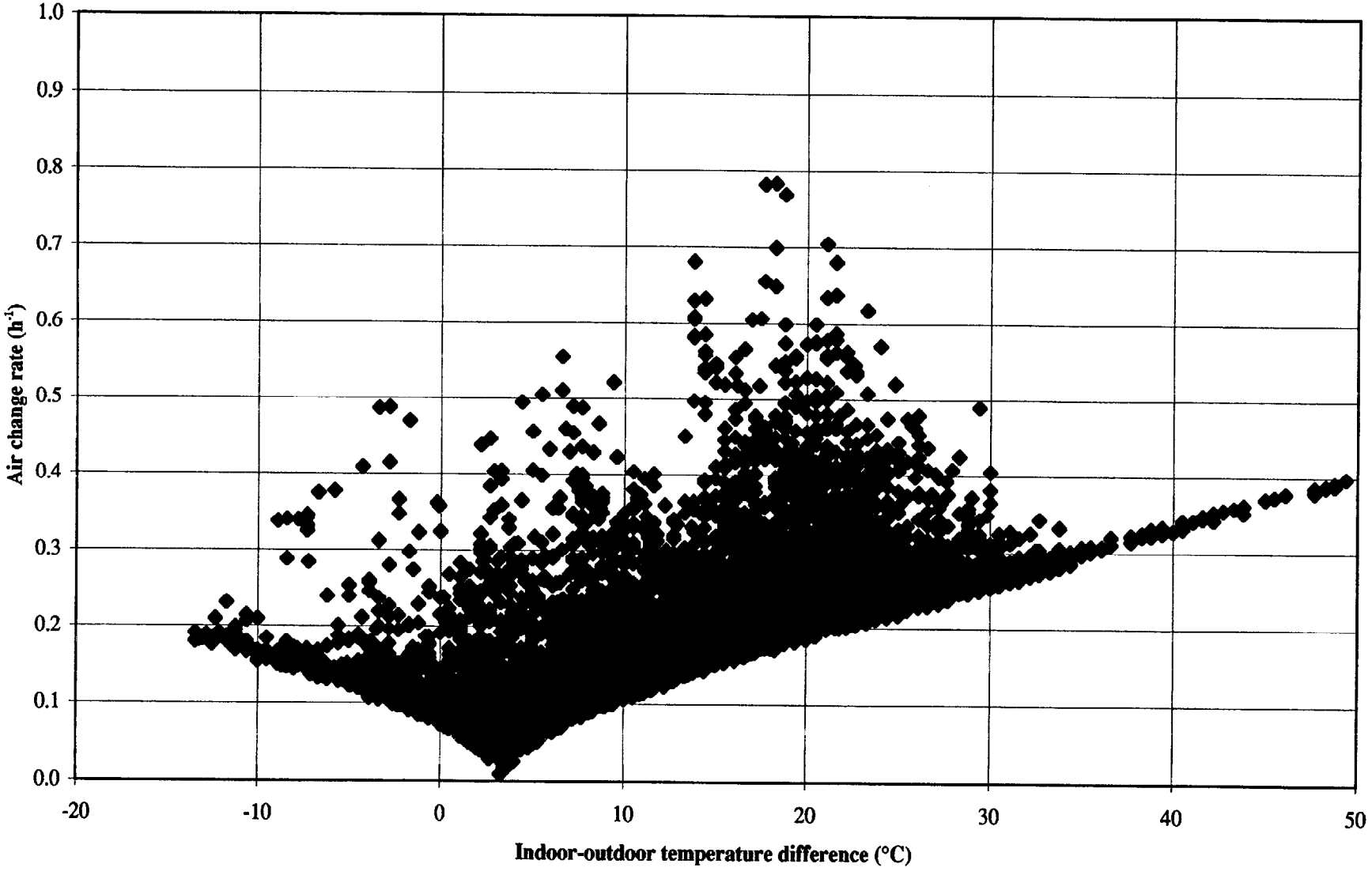

Figure 11 Case #1 Hourly Mean Air Change Rates, All Data Points

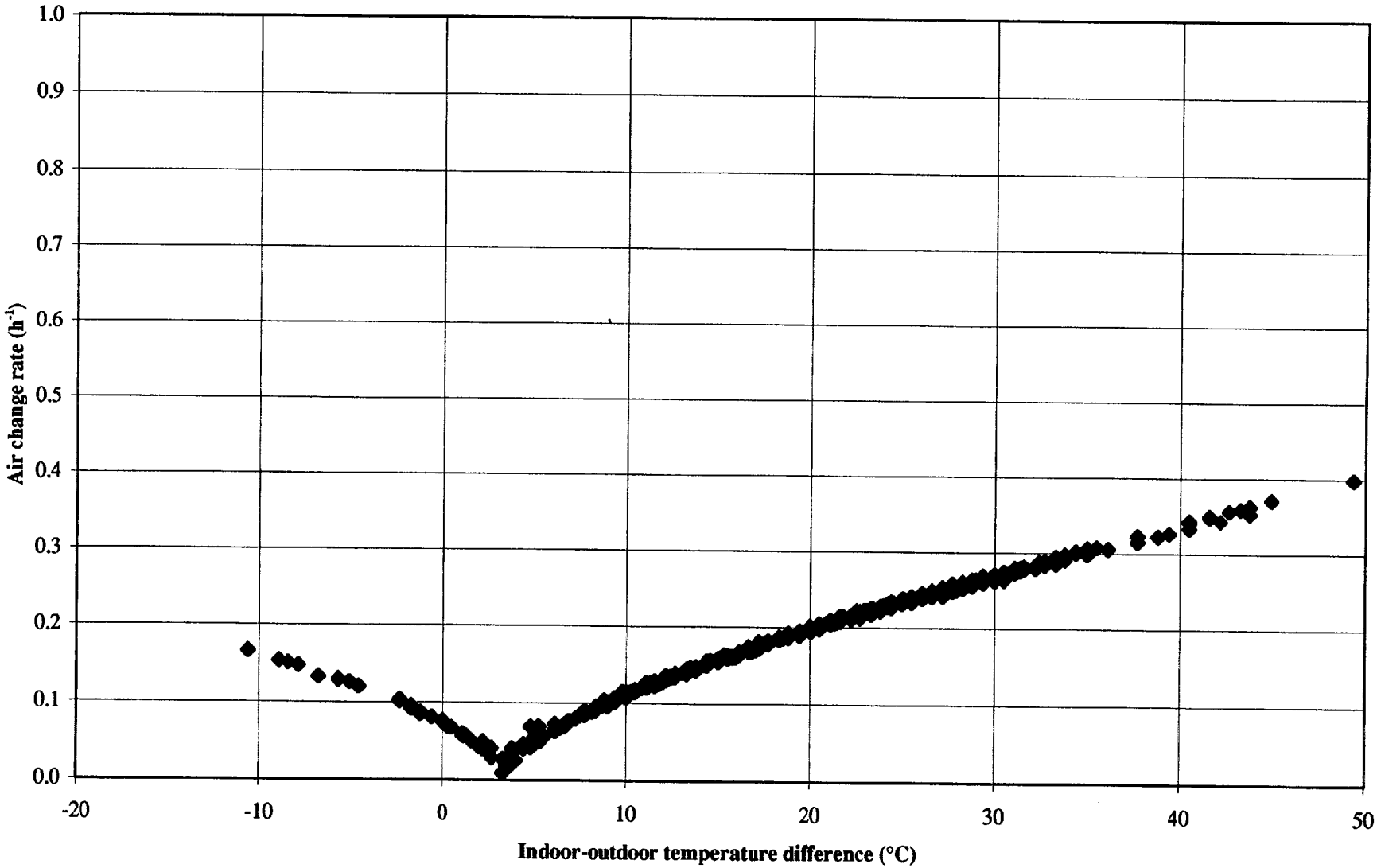

Figure 12 Case #1 Hourly Mean Air Changes Rates, Wind Speed < 2 m/s

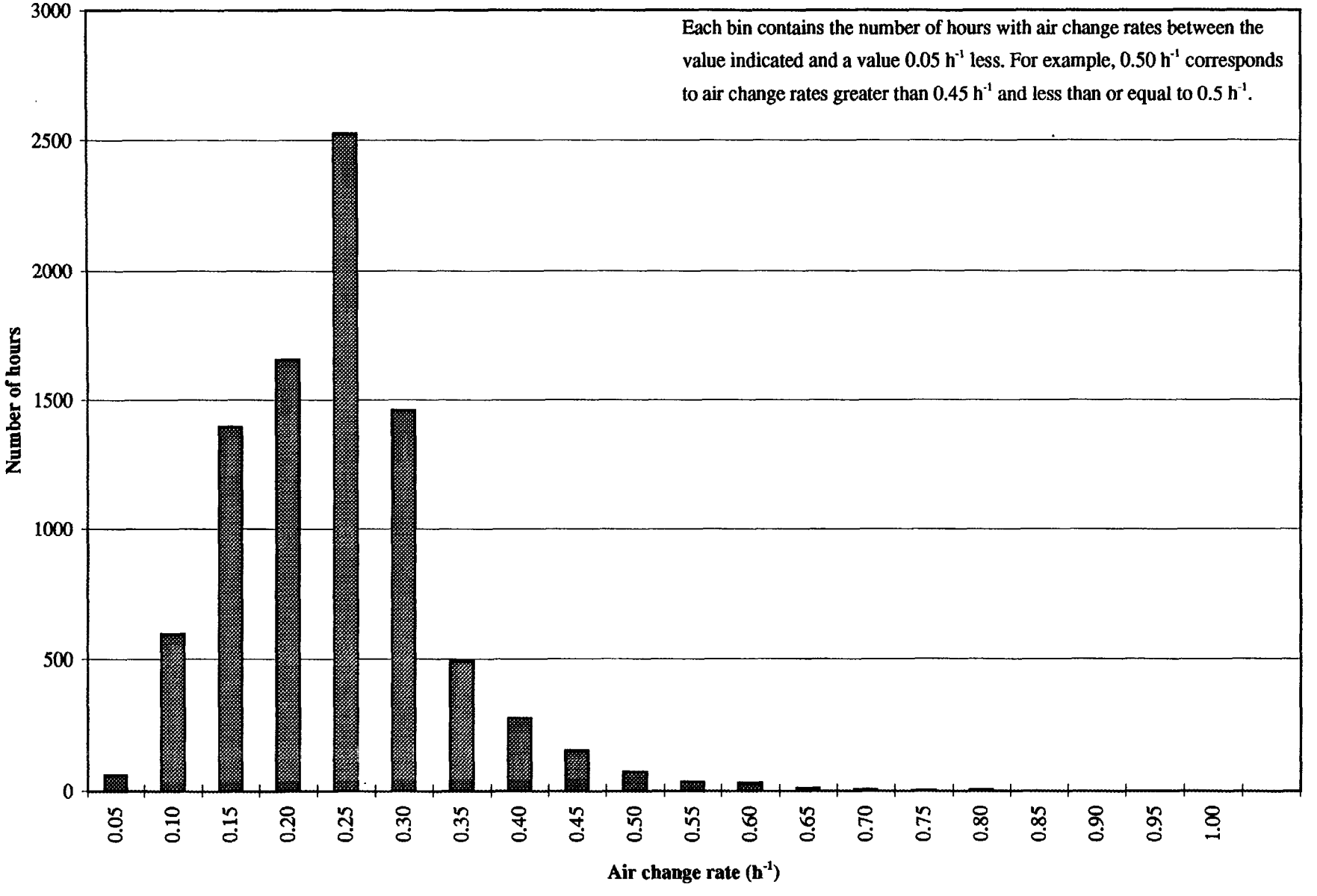

Figure 13 Frequency Distribution of Air Change Rates for Case #1

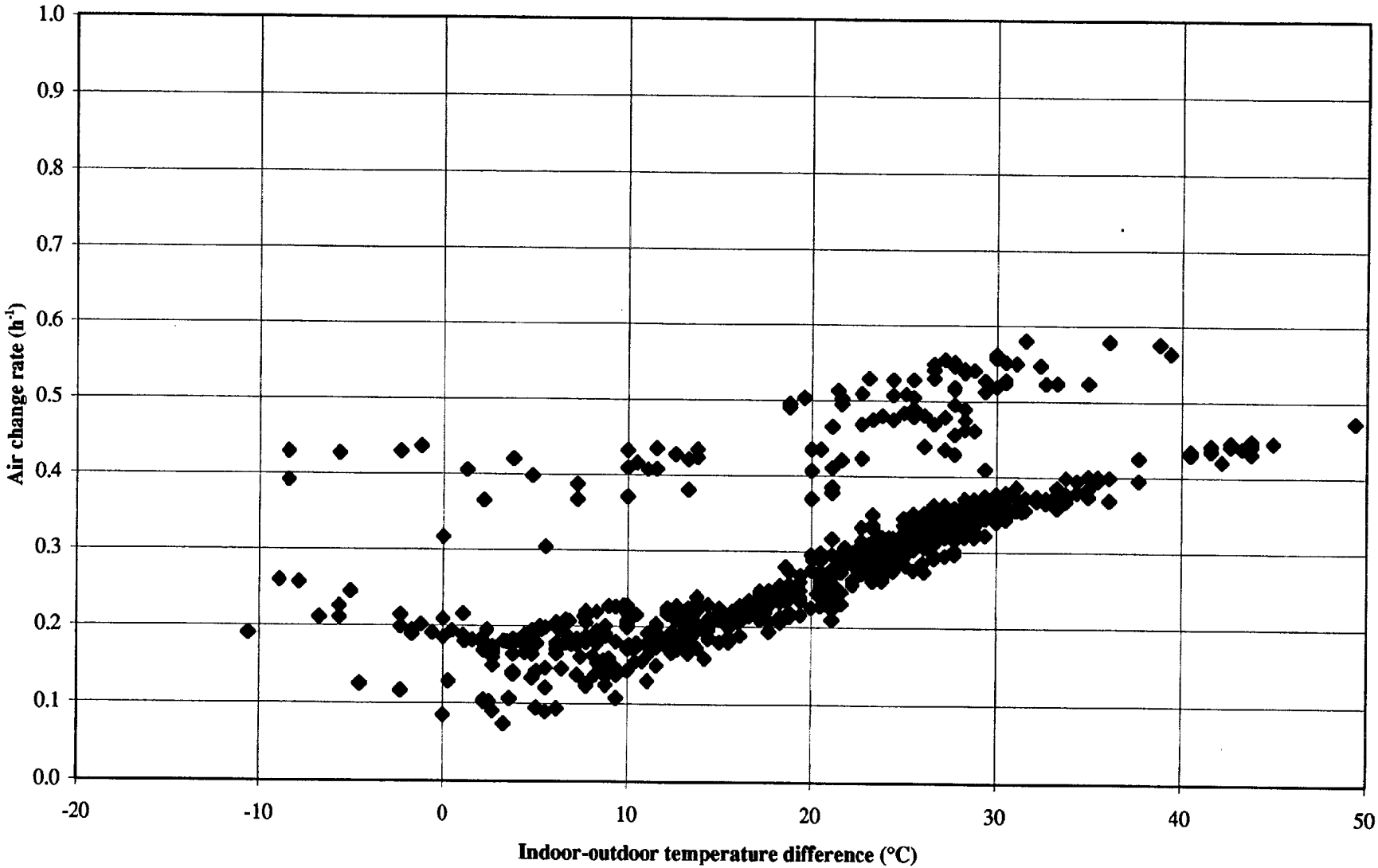

Figure 14 Case #2 Hourly Mean Air Change Rates, Wind Speed < 2 m/s

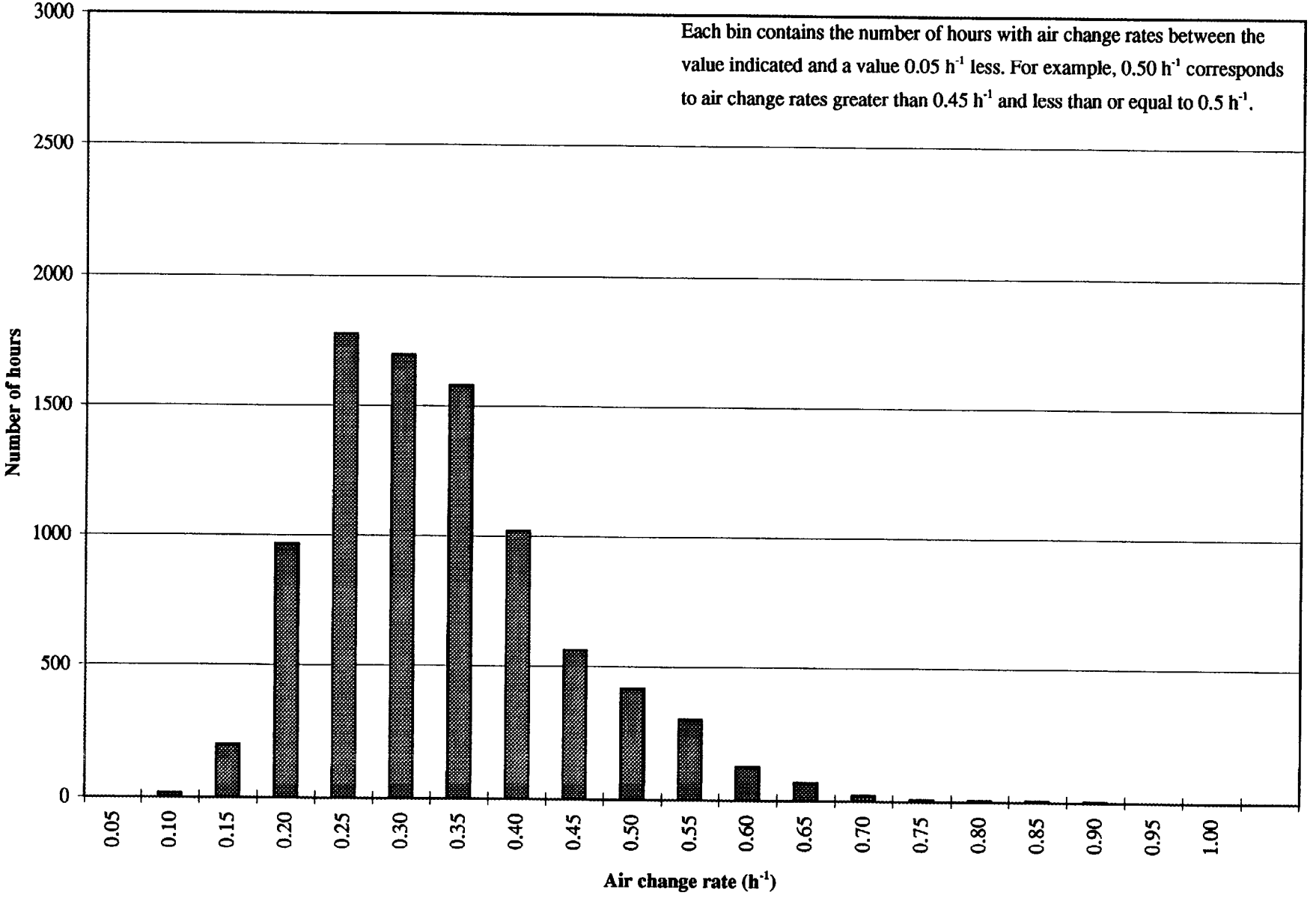

Figure 15 Frequency Distribution of Air Change Rates for Case #2

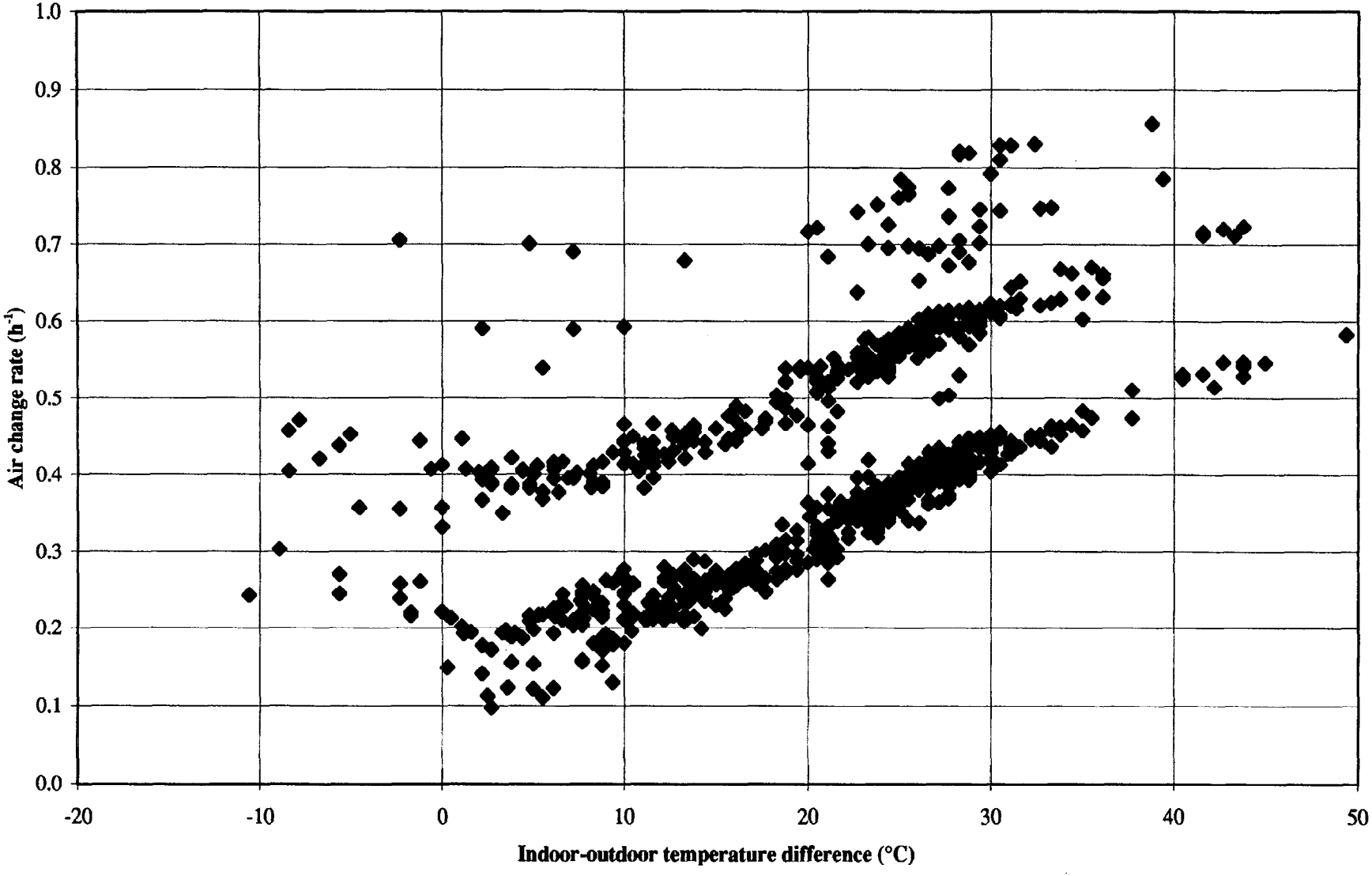

Figure 16 Case #3 Hourly Mean Air Change Rates, Wind Speed < 2 m/s

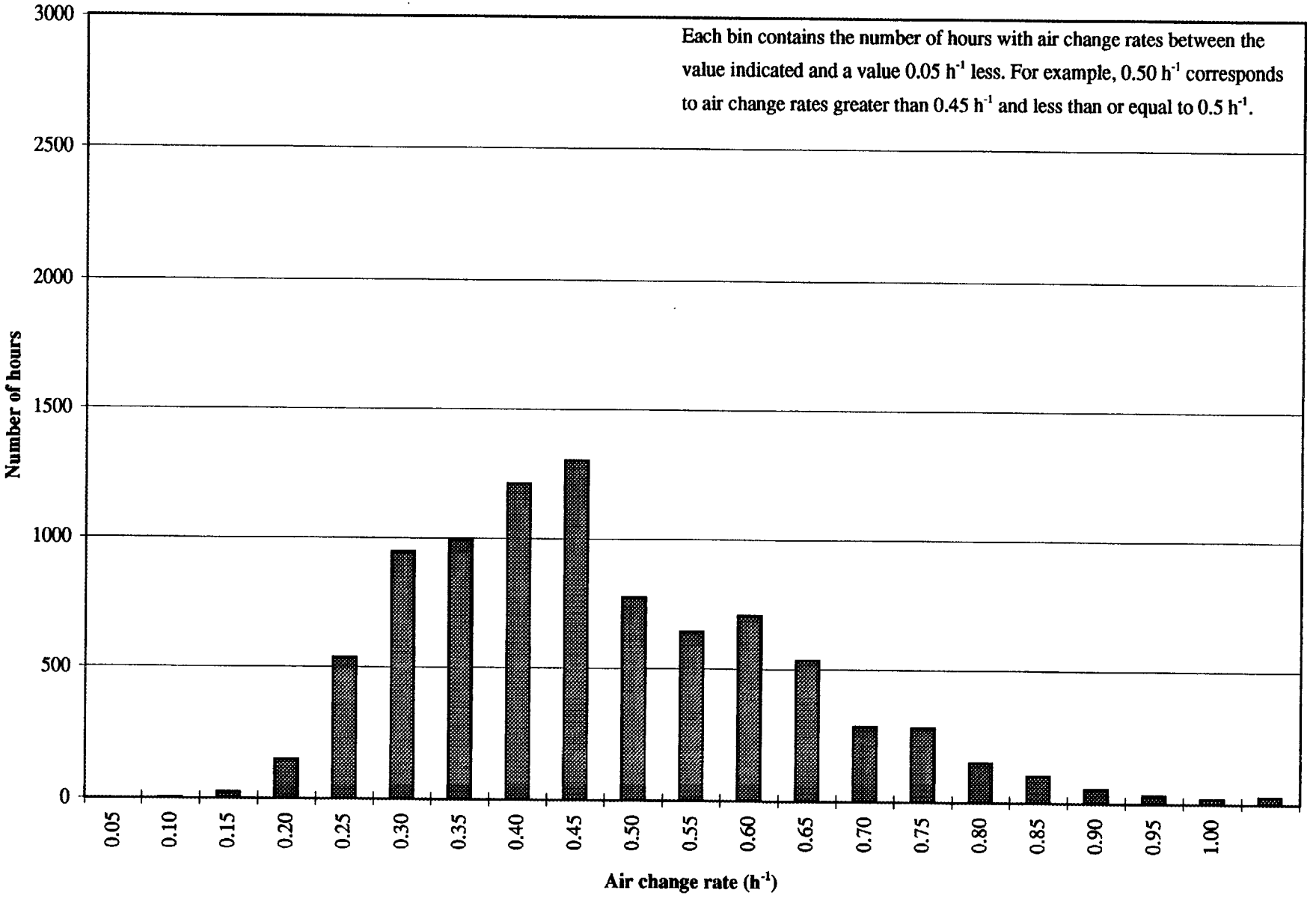

Figure 17 Frequency Distribution of Air Change Rates for Case #3

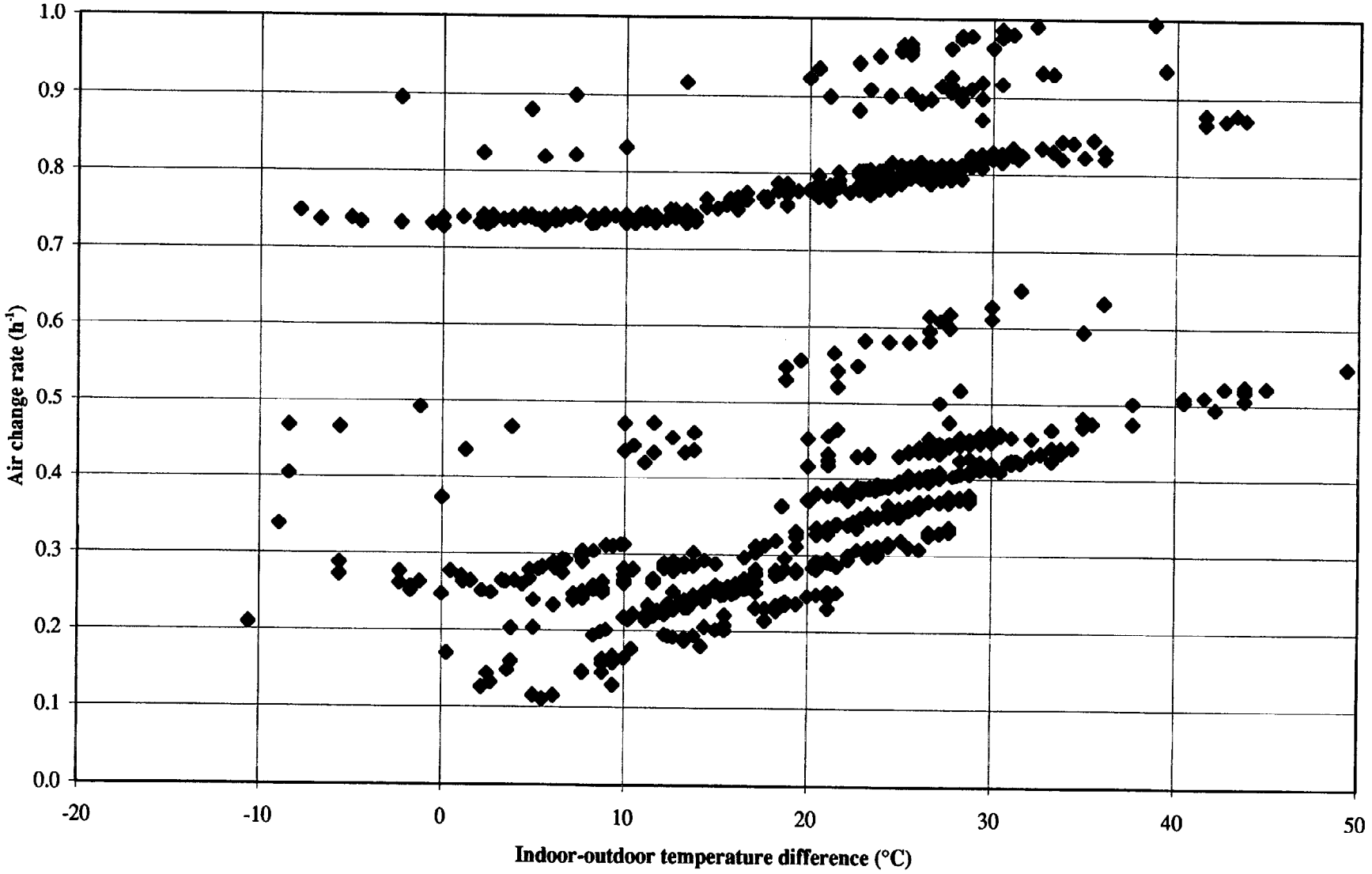

Figure 18 Case #4 Hourly Mean Air Change Rates, Wind Speed < 2 m/s

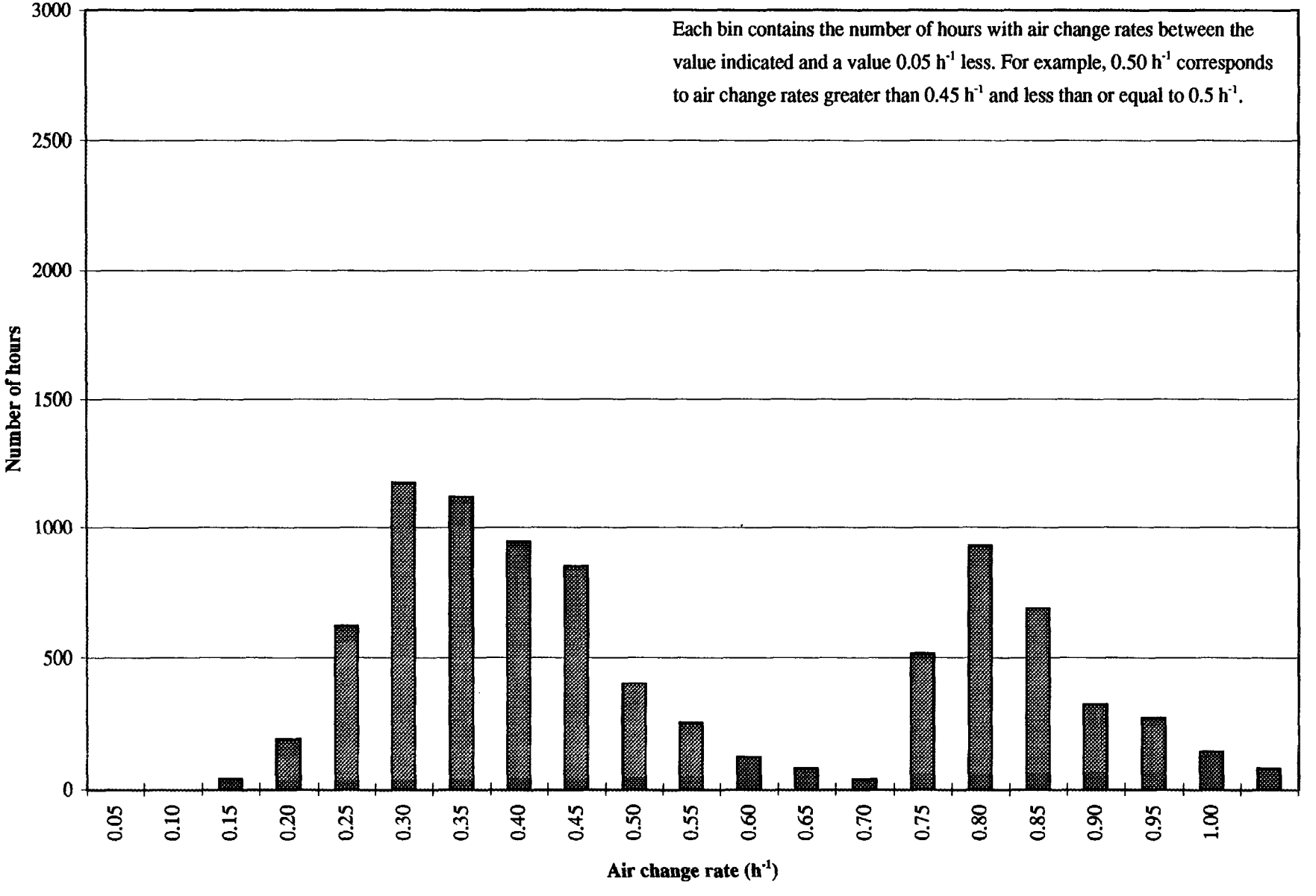

Figure 19 Frequency Distribution of Air Change Rates for Case #4

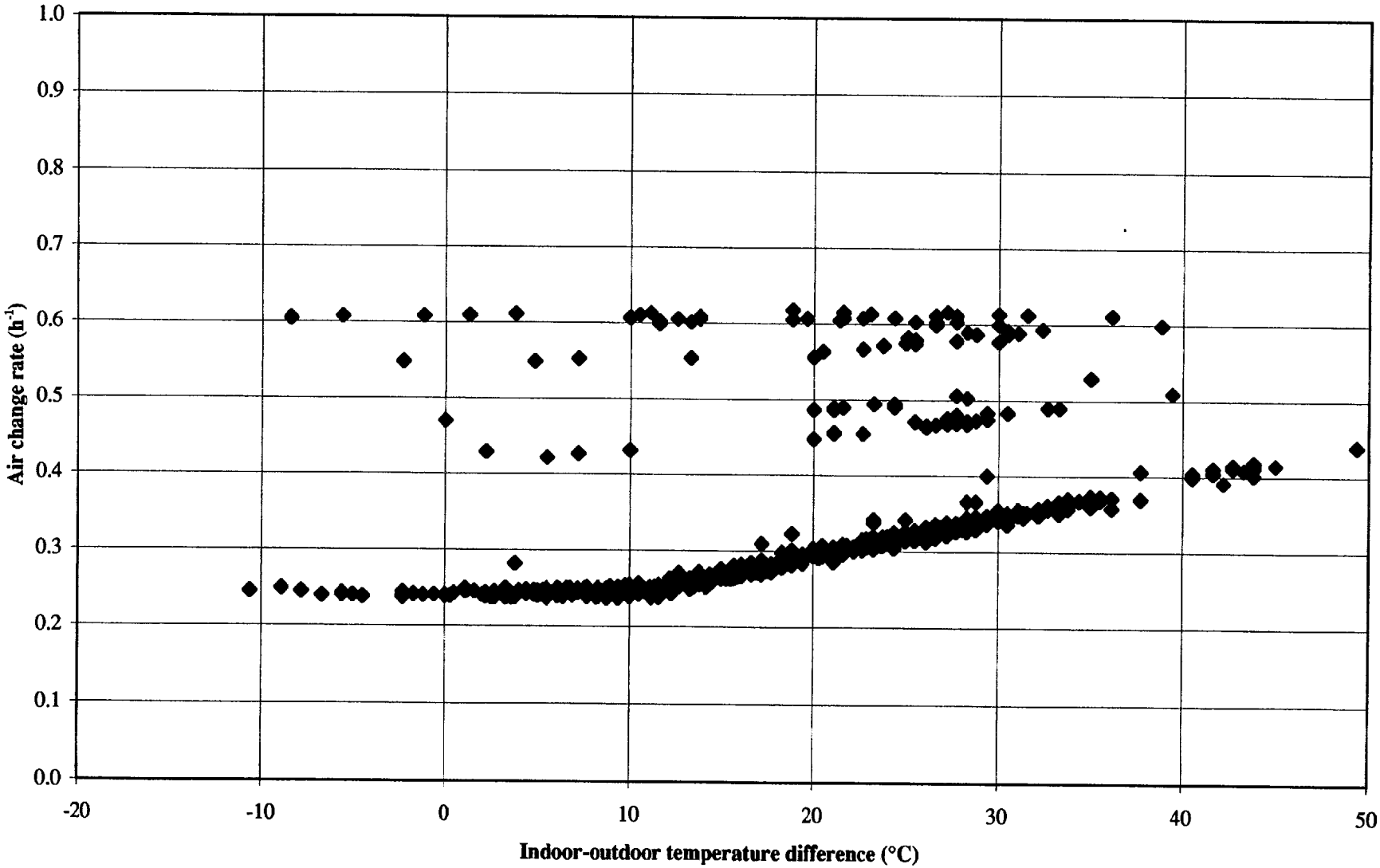

Figure 20 Case #5 Hourly Mean Air Change Rates, Wind Speed < 2 m/s

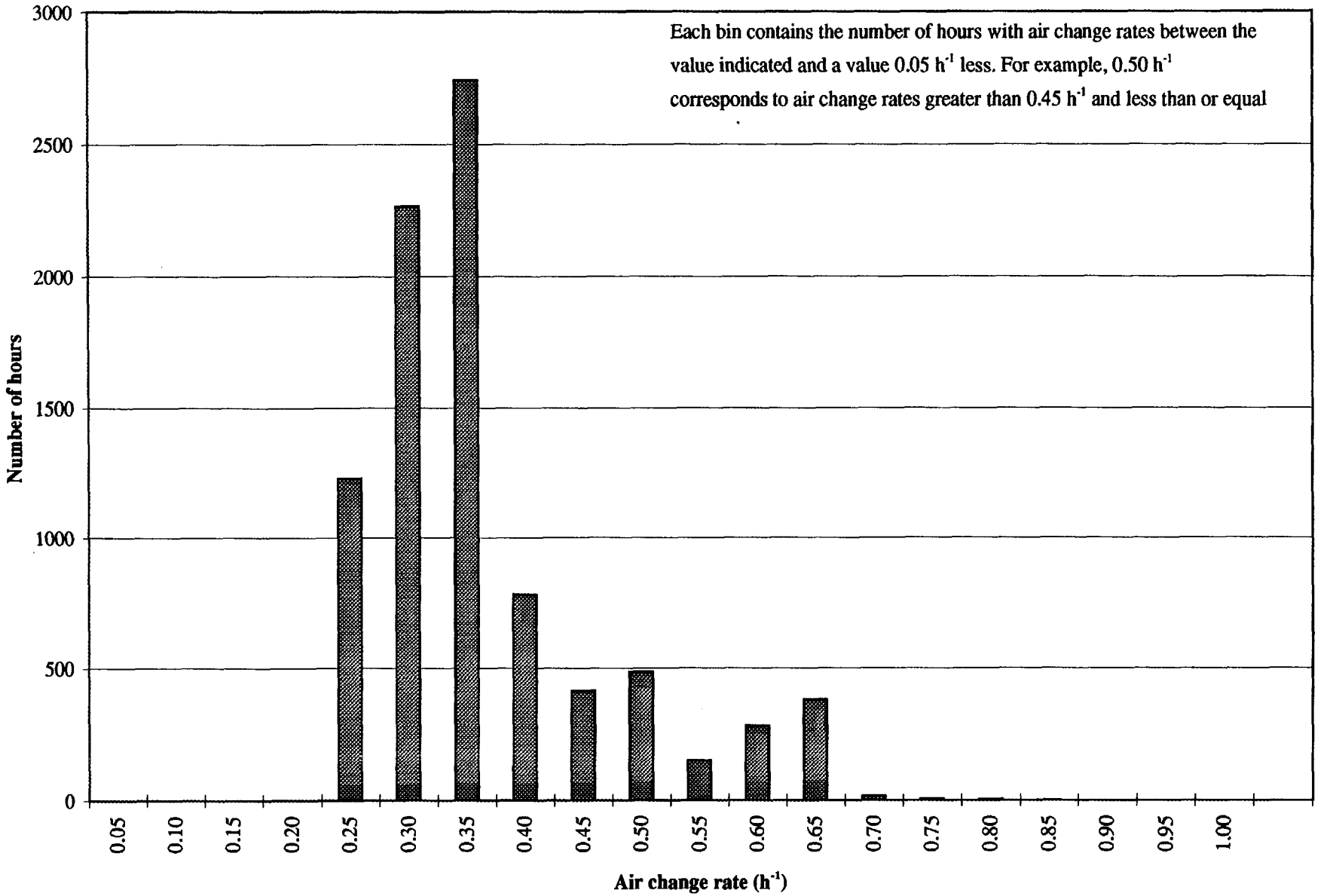

Figure 21 Frequency Distribution of Air Change Rates for Case #5

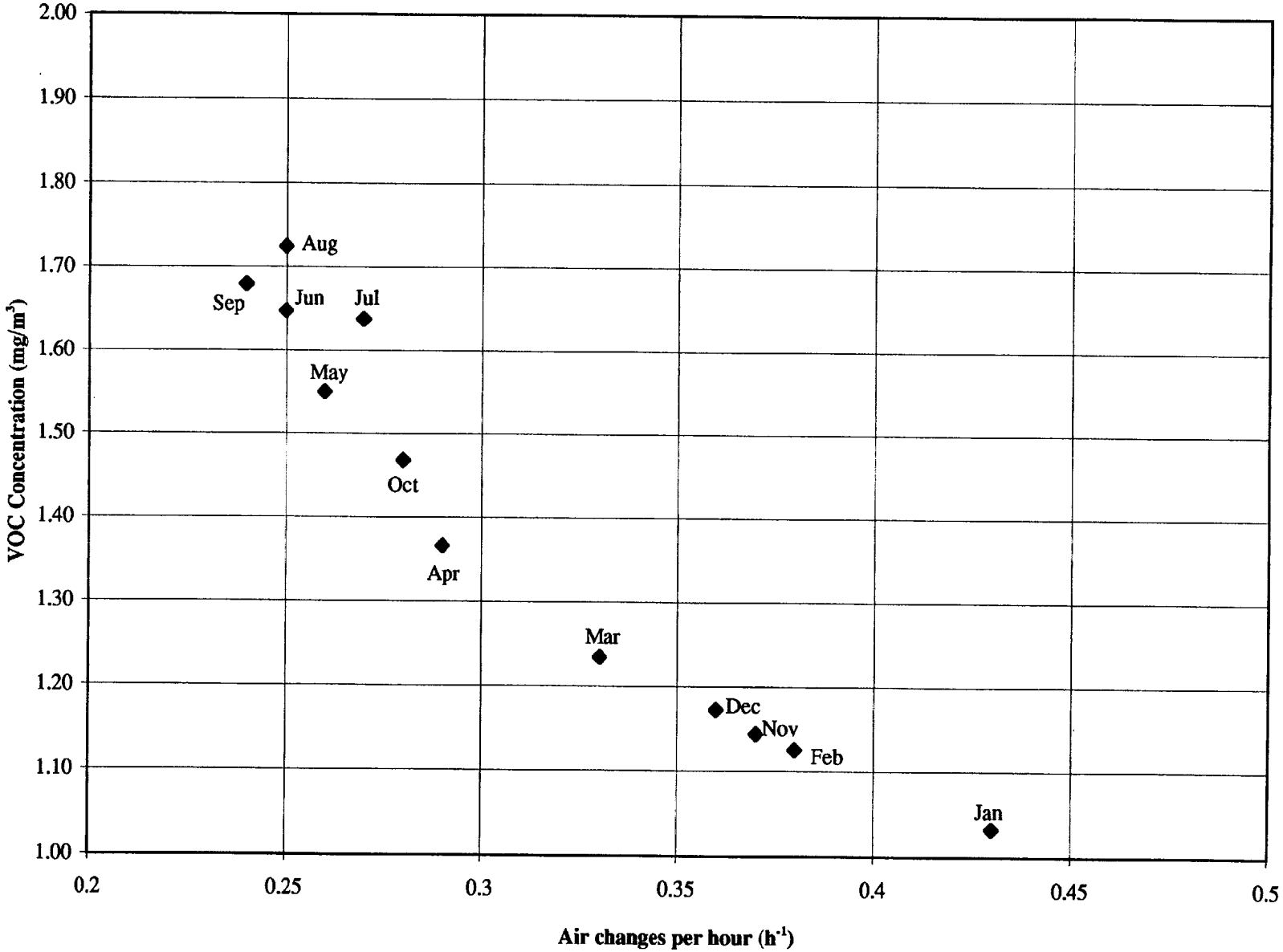

Figure 22 Monthly Mean VOC Concentrations versus Air Change Rates for Case #2

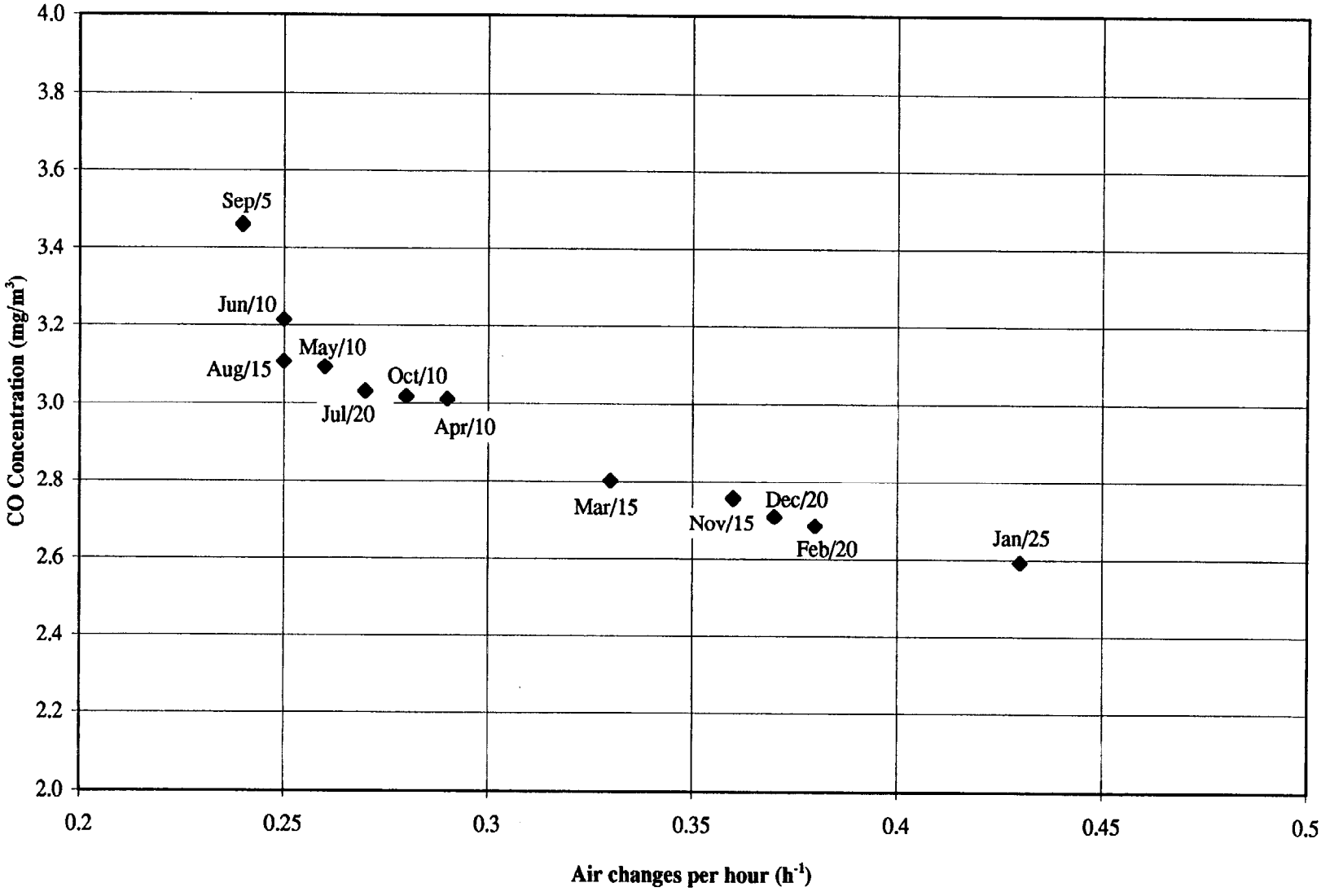

Figure 23 Monthly Mean Carbon Monoxide Concentrations versus Air Change Rates for Case #2

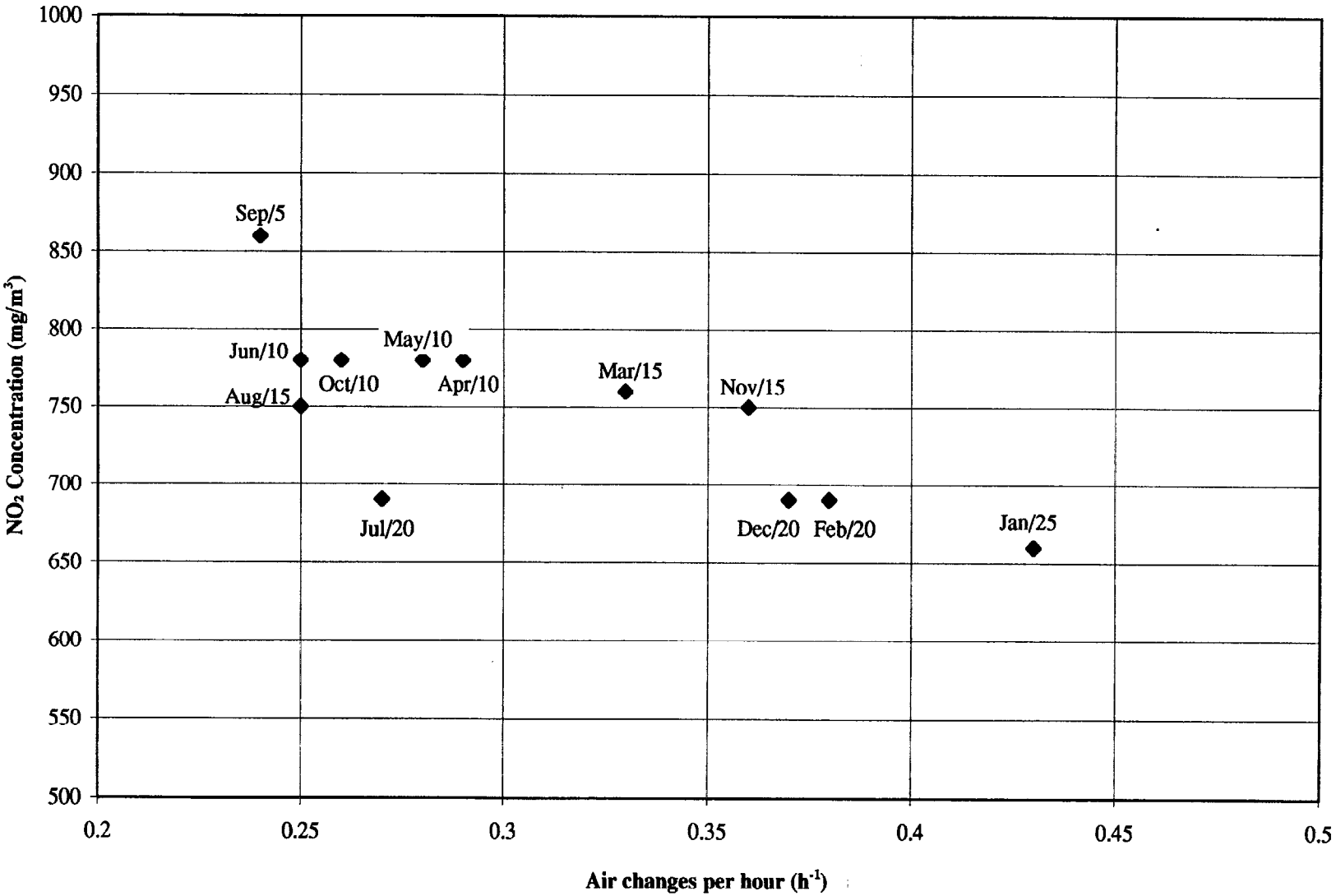

Figure 24 Monthly Mean Nitrogen Dioxide Concentrations versus Air Change Rates for Case #2

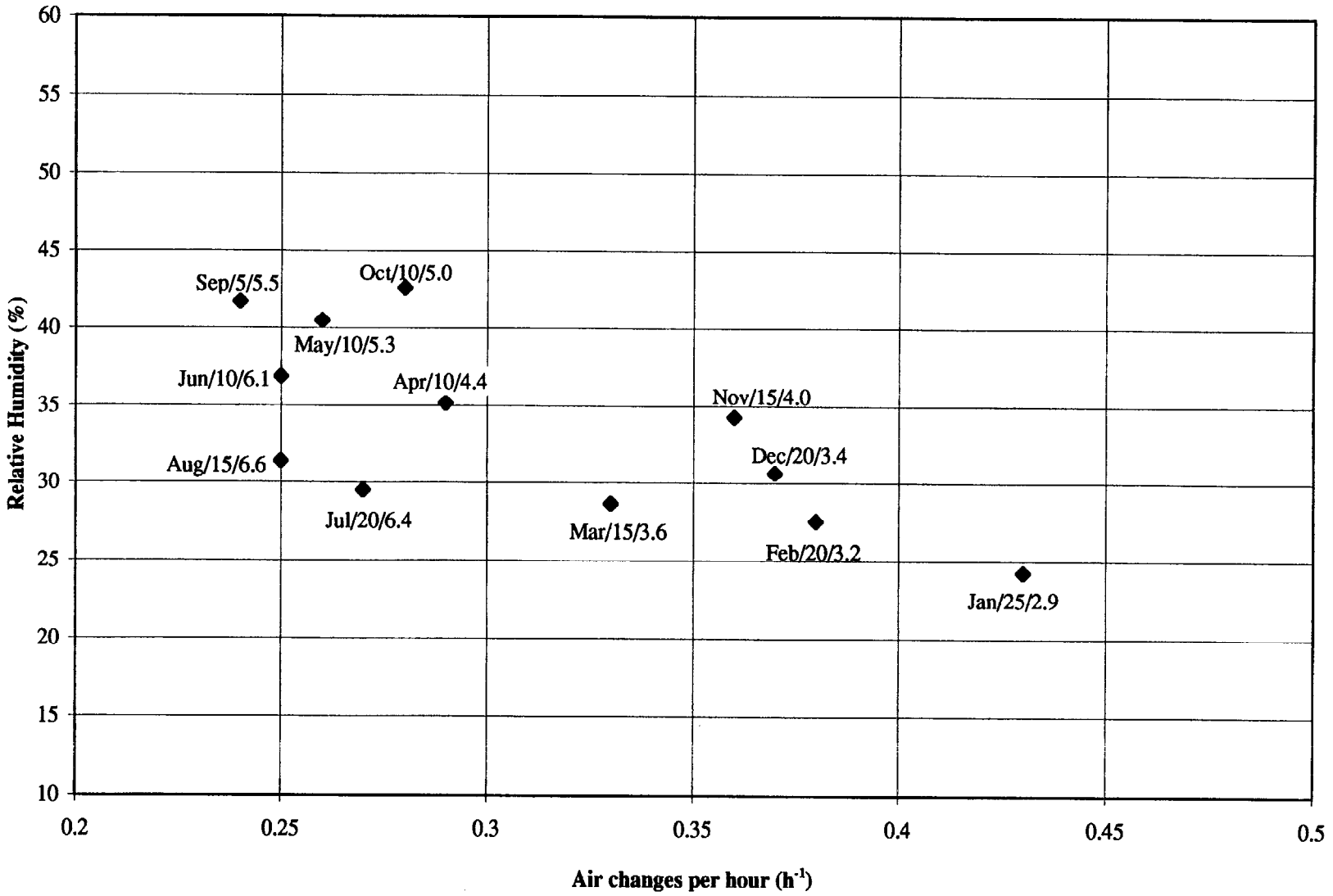

Figure 25 Monthly Mean Relative Humidity versus Air Change Rates for Case #2

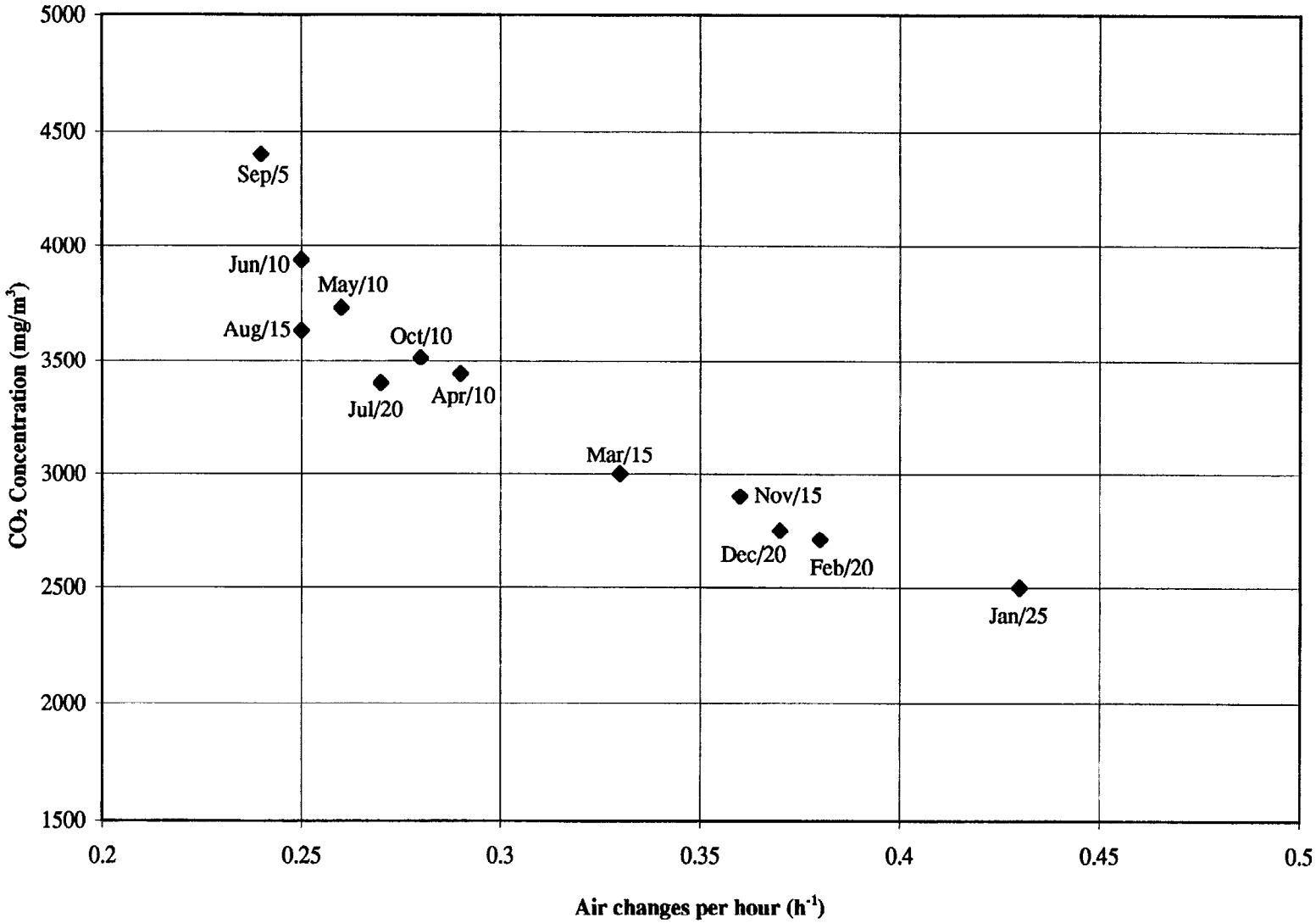

Figure 26 Mean Monthly Carbon Dioxide Concentrations versus Air Change Rates for Case #2

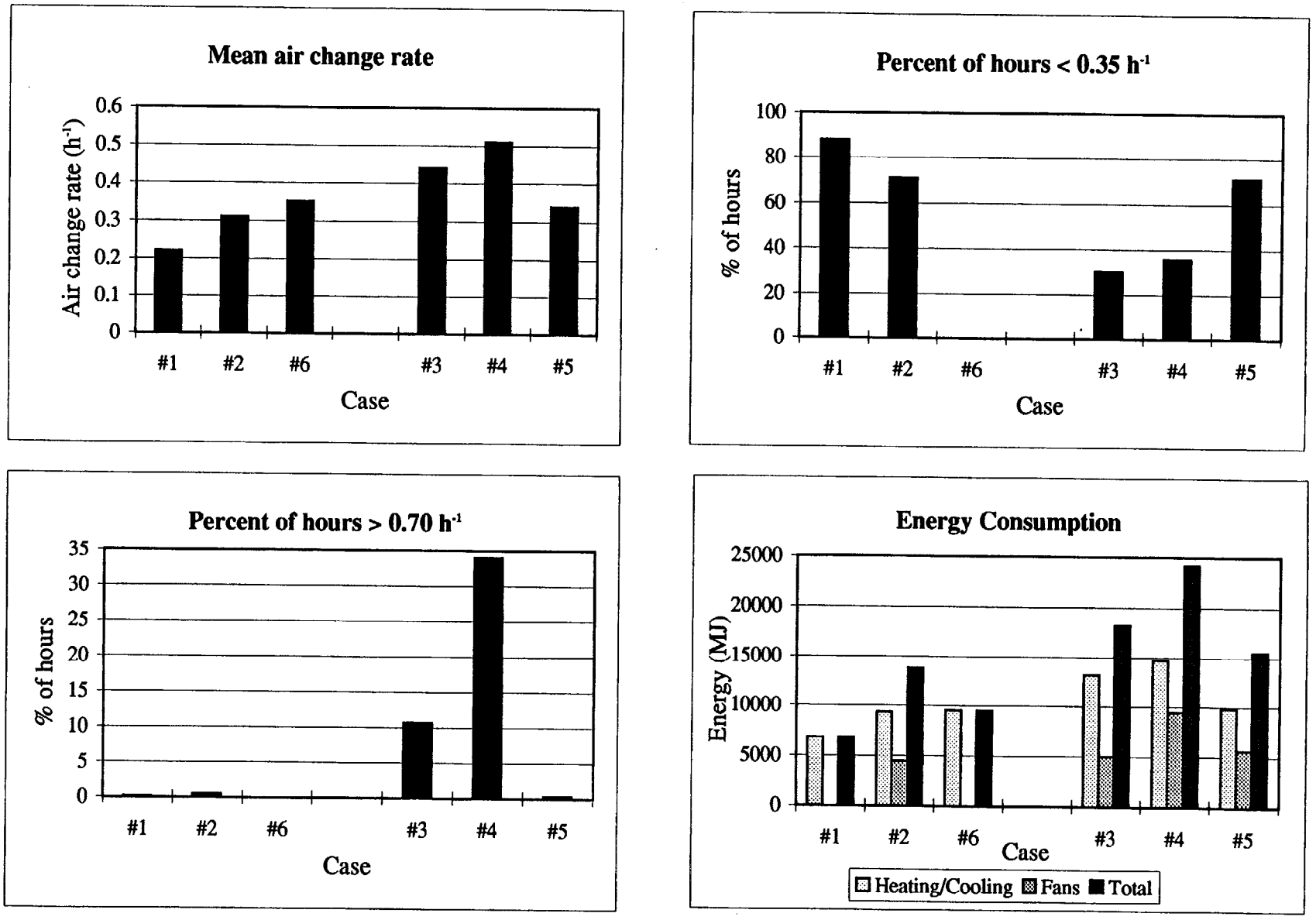

Figure 27 Summary of Air Change Rate and Energy Consumption Results

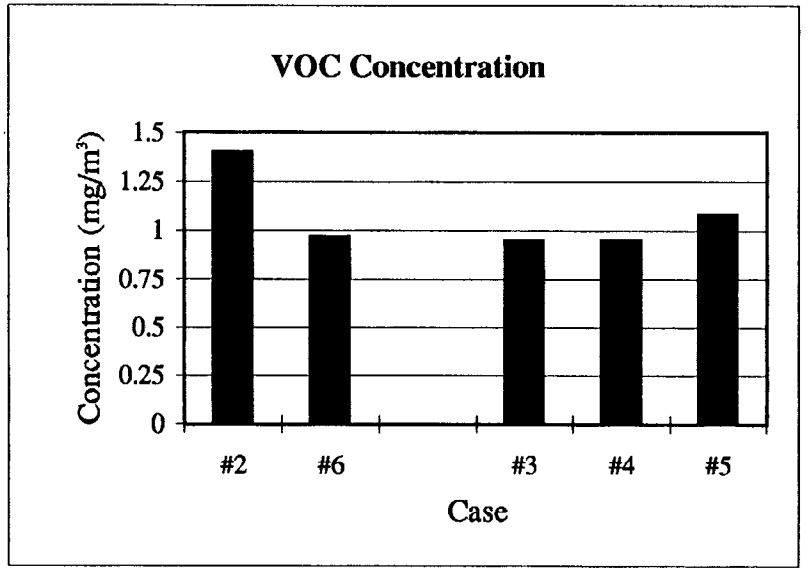

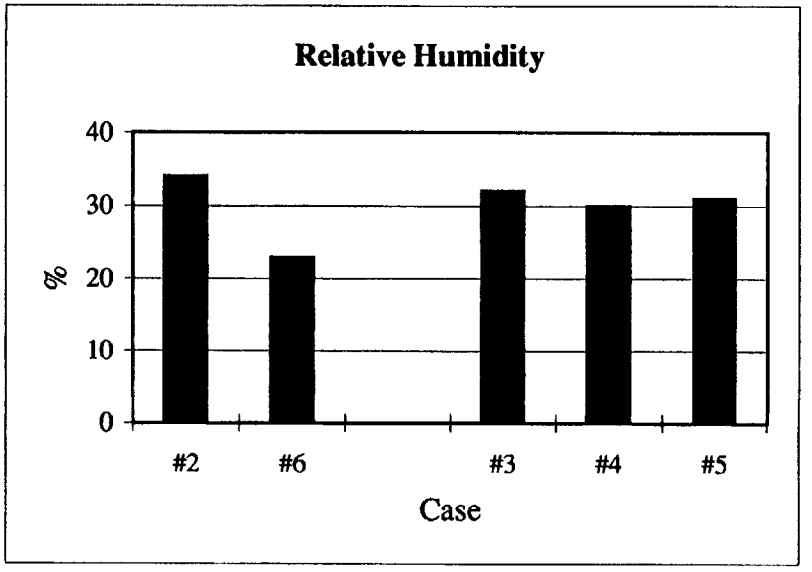

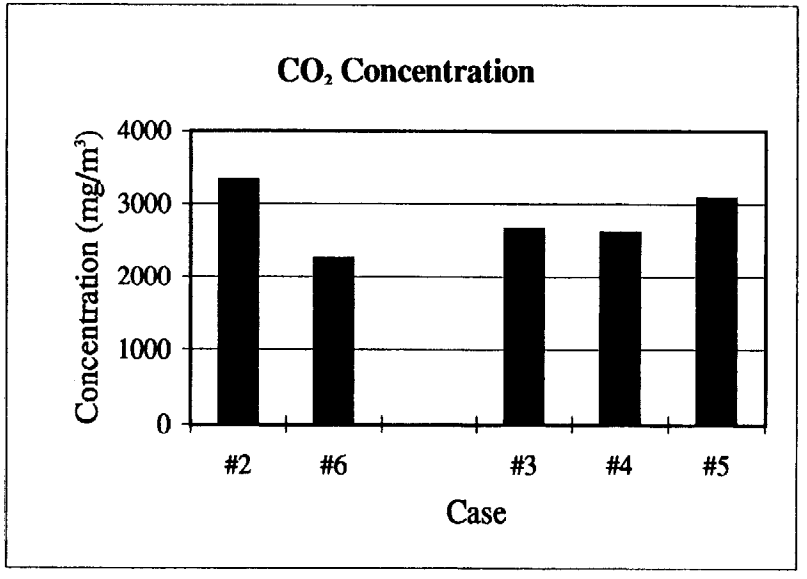

Figure 28 Summary of Contaminant Concentration Results

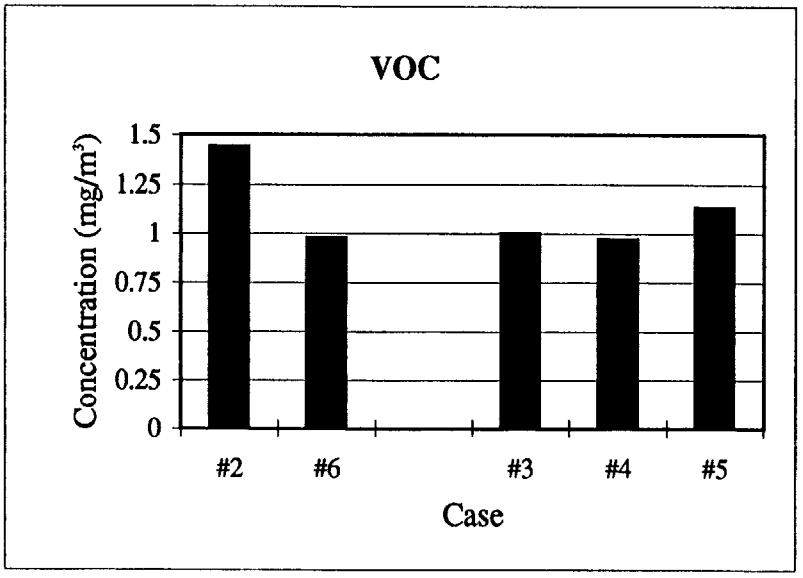

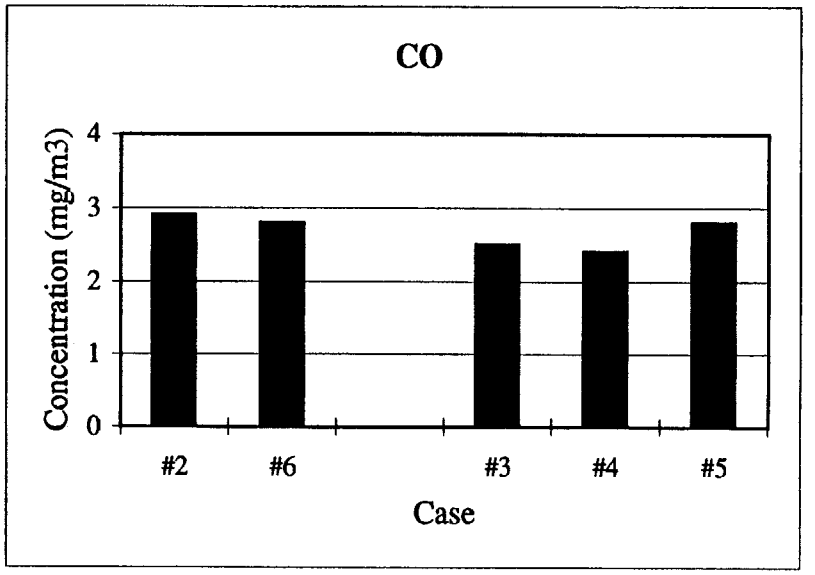

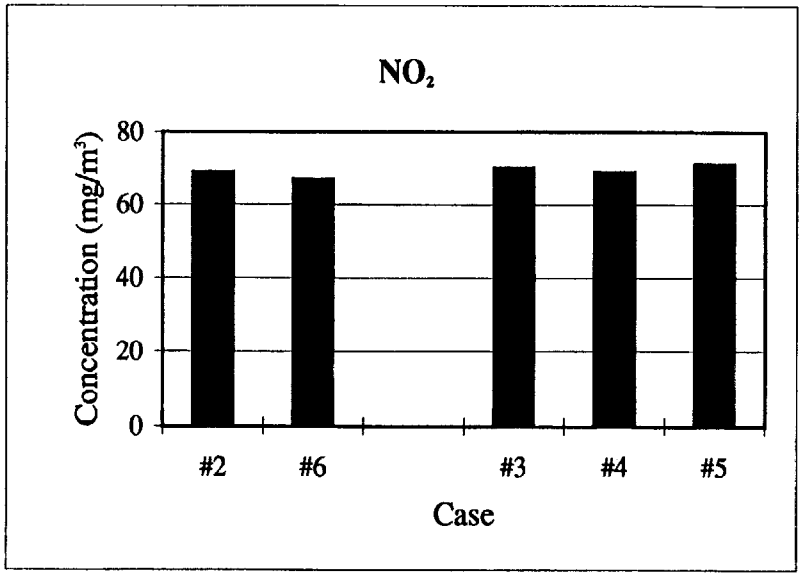

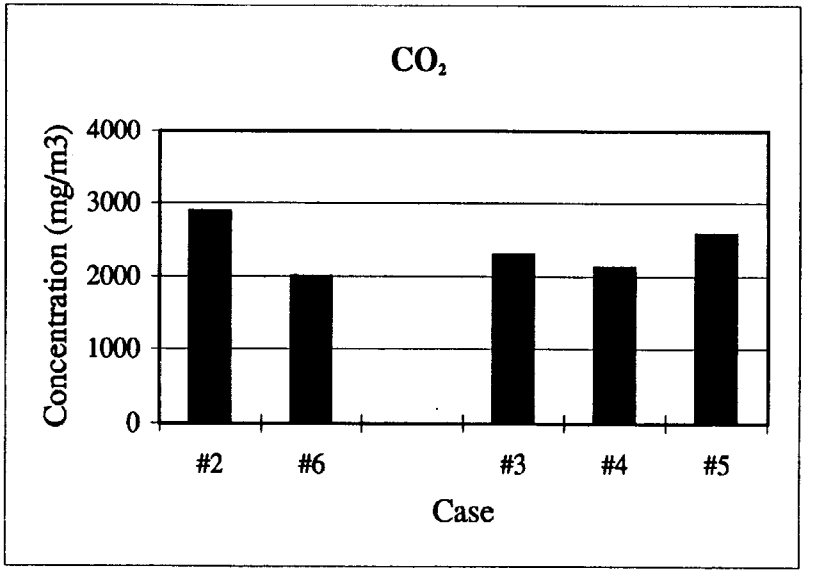

Figure 29 Summary of Exposure Results